OCT 9 1966
635

MASTER

WT-1488

AEC Category · HEALTH AND SAFETY
Military Category · 26

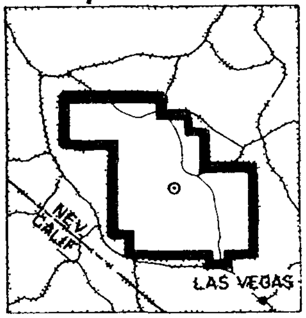

NEVADA TEST SITE
MAY - OCTOBER 1957

OPERATION PLUMBBOB

Projects 37.1, 37.2, 37.2a, 37.3 and 37.6

DISTRIBUTION, CHARACTERISTICS, AND BIOTIC AVAILABILITY OF FALLOUT, OPERATION PLUMBBOB

Issuance Date : July 26, 1966

RELEASED FOR ANNOUNCEMENT
IN NUCLEAR SCIENCE ABSTRACTS

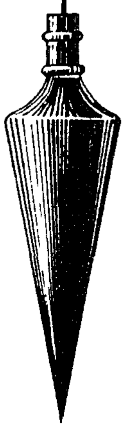

CIVIL EFFECTS TEST GROUP

LEGAL NOTICE

This report was prepared as an account of Government sponsored work. Neither the United States, nor the Commission, nor any person acting on behalf of the Commission:

A. Makes any warranty or representation, expressed or implied, with respect to the accuracy, completeness, or usefulness of the information contained in this report, or that the use of any information, apparatus, method, or process disclosed in this report may not infringe privately owned rights; or

B. Assumes any liabilities with respect to the use of, or for damages resulting from the use of any information, apparatus, method, or process disclosed in this report.

As used in the above, "person acting on behalf of the Commission" includes any employee or contractor of the Commission, or employee of such contractor, to the extent that such employee or contractor of the Commission, or employee of such contractor prepares, disseminates, or provides access to, any information pursuant to his employment or contract with the Commission, or his employment with such contractor.

H.C. $3.00 1.50

RELEASED FOR ANNOUNCEMENT
IN NUCLEAR SCIENCE ABSTRACTS

Report to the Test Director

DISTRIBUTION, CHARACTERISTICS, AND BIOTIC AVAILABILITY OF FALLOUT, OPERATION PLUMBBOB

By:

K. H. Larson, J. W. Neel, H. A. Hawthrone,
H. M. Mork, R. H. Rowland, L. Baurmash,
R. G. Lindberg, J. H. Olafson, B. W. Kowalewsky

Approved by: K. H. LARSON
Director
Program 37

Approved by: L. J. DEAL
Chief
Civil Effects Branch

Laboratory of Nuclear Medicine and Radiation Biology
The University of California at Los Angeles
900 Veteran Avenue
Los Angeles, California 90024

CHAPTER 2

THE DELINEATION AND DISTRIBUTION OF FALLOUT

2. 1 INTRODUCTION

The delineation and distribution of fallout debris deposited in an area is the first essential phase of environmental assessment studies. This provides the basis for identification and definition of those physical, chemical, radiological and biological parameters which jointly comprise fallout phenomenology. This first phase is concerned primarily with: (1) documenting the geographical distribution and radiation level of contamination in the biosphere of the path of fallout deposition; and (2) measuring the time-of-arrival of fallout or radiation along the path of deposition. Data and their evaluation are presented for seven tower mounted and four balloon mounted shots.

2. 2 PROCEDURE

Detailed description is given in Appendix A, Sections A. 2. 1, A. 2. 2, and A. 2. 3 of the methods and equipment used in this phase of study. It should be noted that the aerial radiometric survey techniques used by the U. S. Geological Survey (USGS) were adapted to monitoring fallout patterns on a routine basis for the first ime during this test series by this program.

2. 3 RESULTS

Table 2. 1 gives the total yield, type of device support, and the mean see level elevations of cloud top and base of each above-surface shot documented by Projects 37. 2a and 37. 2. Isodose-rate contours, the time-of-arrival of fallout, and an estimate of the predominant particle size fraction are shown below on maps of each fallout pattern.

TABLE 2 1 Project 37 2a and 37. 2 Shot Participation, Device Support, Yield, and Cloud Height.

MSL, Mean Sea Level

Series No.	Shot Name	Date	H Hour, PDT	Type of Device Support	Height of Detonation, ft	Total Yield, kt[a]	Cloud Height, MSL, ft[a] Top	Base	Tropopause[a] MSL, ft
1	Boltzmann	28 May	0455	Tower	500	12	33,000	23,000	41,000
4	Wilson	18 June	0445	Balloon	500	10	35,000	25,000	40,000
5	Priscilla	24 June	0630	Balloon	700	37	43,000	24,000	49,000
6	Hood	5 July	0440	Balloon	1500	74	48,000	35,000	53,000
7	Diablo	15 July	0430	Tower	500	17	32,000	20,000	43,000
13	Shasta	18 Aug	0500	Tower	500	17	32,000	16,000	50,000
16	Smoky	31 Aug	0530	Tower	700	44	38,000	(20,000 Est)	35,000
17	Galileo	2 Sept	0540	Tower	500	11	37,000	17,000	39,000
21	Fizeau	14 Sept	0945	Tower	500	11	40,000	27,000	43,000
22	Newton	16 Sept	0550	Balloon	1500	12	32,000	19,000	52,000
23	Rainier	19 Sept	1000	Underground	-790	1 7	no cloud or venting		---
24	Whitney	23 Sept	0530	Tower	500	19	30,000	18,000	53,000

(a) From "Fallout Program Quarterly Summary Report," Report No. HASL-142, January 1, 1964, page 227, USAEC, Health and Safety Laboratory, New York.

2.3.1 Fallout Patterns

Isodose-rate contours at H + 12 hours and time-of-arrival of fallout and/or radiation are shown in Figures 2.1 to 2.12 for seven tower mounted and four balloom mounted detonations. The dose-rate values were measured during station recovery, from H + 24 to H + 30 hours, and corrected to H + 12 hours by data shown in Table A.2 and the Plumbbob Composite Decay Curve (Figure 4.11).

Boltzmann Fallout Pattern (Figure 2.1): This pattern is based upon Program 37 ground and aerial survey data and Off-Site Rad-safe ground survey results. The isodose-rate contours shown from ground zero to Arc I (approximately 35 miles) are estimated because of rough terrain and inaccessibility. The time-of-arrival of fallout after H + 5 hours is estimated on the basis of a few measured values and calculated cloud trajectories from the Fallout Prediction Unit (FOPU), Test Manager's Organization. Only aerial survey data were available at times-of-arrival of fallout greater than H + 9 hours.

The 100 mr/hr contour which defines the hot spot west of Warm Springs, Nevada, (approximately 76 miles from ground zero) is of particular interest. This area was characterized by having approximately 75 percent of the total activity associated with less than 44 micron material in the area of maximum dose rates (see Appendix C). There is the suggestion that the northern portion of a mountain ridge may have contributed to this deposition of the observed hot spot. There were no rain clouds observed in this immediate area by personnel of the radio-relay communication aircraft at H-40 minutes. The only rain clouds observed were approximately 20 miles to the west.

Wilson Fallout Pattern (Figure 2.2): This Shot was not originally scheduled for documentation, and Program 37 fallout measurements were obtained only by aerial survey. The pattern is based on these and Off-Site Rad-Safe ground survey data. There is some doubt as to the magnitude of fallout in the southwest portion of the pattern. Fallout time-of-arrival is based on cloud trajectory estimates by FOPU.

Priscilla Fallout Pattern (Figure 2.3): Dose-rate contours of this pattern are based on Program 37 ground and aerial survey data and some Off-Site Rad-Safe results. However, the isodose-rate contours between Arc I (Indian Springs Road) and ground zero are estimated. The time-of-arrival of fallout is based on measured values. The occurrence of isolated hot-spots and the predominance of less than 44 micron fallout material on all sampling arcs is of special interest. There was excellent agreement on the magnitude and location of the midline, the occurrence and location of the hot spots, and the dose-rate contours of the southern half of the pattern. However, there was only good agreement as to the location of the northern boundary of this pattern.

Hood Fallout Pattern (Figure 2.4): This pattern is based on Program 37 ground and aerial survey data. Some of the isodose-rate contours are estimated on the basis of the contamination levels measured in the fallout collectors (see Table 2.3 for conversion factors). The pattern is north of previous Plumbob contamination; therefore, the dose-rate values are reliable even though of low intensity. The pattern is characterized by hot spots and a predominance of less than 44 micron material, as in the case of Shot Priscilla.

Diablo Fallout Pattern (Figure 2.5): Program 37 ground and aerial survey and Off-Site Rad-Safe ground survey data were used to develop this pattern with good agreement beyond 100 miles. The isodose-rate contours on the western edge of the fallout pattern are estimates and may be located too far west. The lack of roads in this area precluded the collection of survey data. The time-of-arrival of fallout after H + 6 hours is estimated on the basis of the measured times and calculated cloud trajectories. The Diablo pattern shows a large hot spot east of Lund, Nevada. It was well documented.

Shasta Fallout Pattern (Figure 2.6): This pattern is based on On-Site Rad-Safe data pertinent to Shasta fallout in Yucca Flat, and Program 37 ground and aerial survey data for the area beyond NTS. Off-Site Rad-Safe data were not used. The isodose-rate contours shown are the net result after the appropriate deduction of residual contamination from Shot Diablo, especially on the eastern portion. Cloud trajectories were used to calculate the estimated time-of-arrival of fallout after H + 5 hours.

Smoky Fallout Pattern (Figures 2.7a, 2.7b, 2.8): Figures 2.7a and b present the detailed fallout pattern developed from Program 37 ground and aerial survey data from ground zero to northeastern Utah. Figure 2.8 shows the complete pattern from ground zero to Casper, Wyoming. The pattern is based on aerial survey data only, from Panguitch, Utah to the northeast. The pattern was still readily detectable at 700 miles from ground zero at D + 5 days. The fact that the time-of-arrival isopleths parallel the major axis of the pattern to a large extent is of particular interest and is probably the result of vertical shear. There were at least two hot spots delineated.

Galileo Fallout Pattern (Figure 2.9): Program 37 ground and aerial survey data are the basis for this pattern south of Highway 6. Off-Site Rad-Safe data were used north of Highway 6. The lack of complete monitoring data necessitated the estimation of the shape of the western edge and the close-in portion of this pattern.

Fizeau Fallout Pattern (Figure 2.10): This pattern is based on On-Site Rad-Safe data pertinent to the fallout in Yucca Flat and Program 37 ground and aerial survey data and Off-Site Rad-Safe data beyond NTS. The fallout time-of-arrival contours, both measured and estimated, compare favorably with FOPU calculated cloud trajectories.

Newton Fallout Pattern (Figure 2.11): Detected fallout levels were of very low intensity and are not reliable, therefore, this pattern is only an estimate. Where possible, dose rates were calculated from the granular fallout collectors. No measurements of time-of-arrival of fallout were obtained.

Whitney Fallout Pattern (Figure 2.12): This pattern is based on Program 37 ground and aerial survey data with the exception of the northernmost portion, above Mina, Nevada (east of Walker Lake), which is based on aerial data alone. No information relative to the radiation levels in Yucca Flat and adjacent terrain was obtained: therefore, this portion is an estimate.

All seven tower mounted shots produced areas beyond NTS with dose rates in excess of 100 mr/hr at H + 12 hours and, with the exception of Shots Boltzmann and Galileo, small areas in excess of 1000 mr/hr at H + 12 hours. In contrast, balloon mounted Shots Wilson, Hood, and Newton, having a range in total yield from 10 to 74 kt, resulted in dose rates of less than 10 mr/hr at H + 12 hours at all locations of measurement. Shot Priscilla, a balloon mounted device whose fireball nearly intersected its ground zero ground surface, resulted in dose rates ranging from 10 to 100 mr/hr at H + 12 hours. Table 2.2 presents a summary comparing the areas within selected isodose-rate contours of fallout patterns from balloon and tower mounted shots. There are no apparent relationships; additional analysis and interpretation of basic data of meteorological observations, environmental factors, particle size distributions, and dose-rate measurements are required.

TABLE 2.2 Areas Within Selected Isodose-Rate Contours of Fallout Patterns From Balloon and Tower Mounted Detonations

Dose rate measurements made H + 24 to H + 30 hours and corrected to H + 12 hours EM, estimated and measure values, NC, not closed, ND not determined

Shot	Isodose-Rate Contours at H + 12 Hours						
	> 100	50-100	10-50	5-10	1-5	0.5-1	0.5-0.1
	Square Miles						
Balloon-Mounted							
Wilson, 500 ft (10 kt)	--	--	--	40 EM	704	2,940 NC	ND
Priscilla, 700 ft (37 kt)	--	60 EM	368	540	4,380 NC	ND	ND
Hood, 1500 ft (74 kt)	--	--	--	--	410 EM	2,315	11,915 NC
Newton, 1500 ft (12 kt)	--	--	--	--	--	125 EM	7,770 NC
Tower-Mounted							
Boltzmann, 500 ft (12 kt)	190 EM	390	1,348	1,510	8,310 NC	ND	ND
Biablo, 500 ft (17 kt)	400 EM	233	1,810	3,765	5,030 NC	ND	ND
Shasta, 500 ft (17 kt)	300 EM	162	727	1,421	6,830 NC	ND	ND
Smoky, 700 ft (44 kt)	470	283	2,267	1,645	4,230 NC	ND	ND
Galileo, 500 ft (11 kt)	104 EM	66 EM	525 EM	576 EM	3,110 NC	ND	ND
Fizeau, 500 ft (11 kt)	45 EM	46 EM	330 EM	635 EM	3,580 EM	ND	ND
Whitney, 500 ft (19 kt)	230 EM	120	854	1,308	7,950 EM	ND	ND

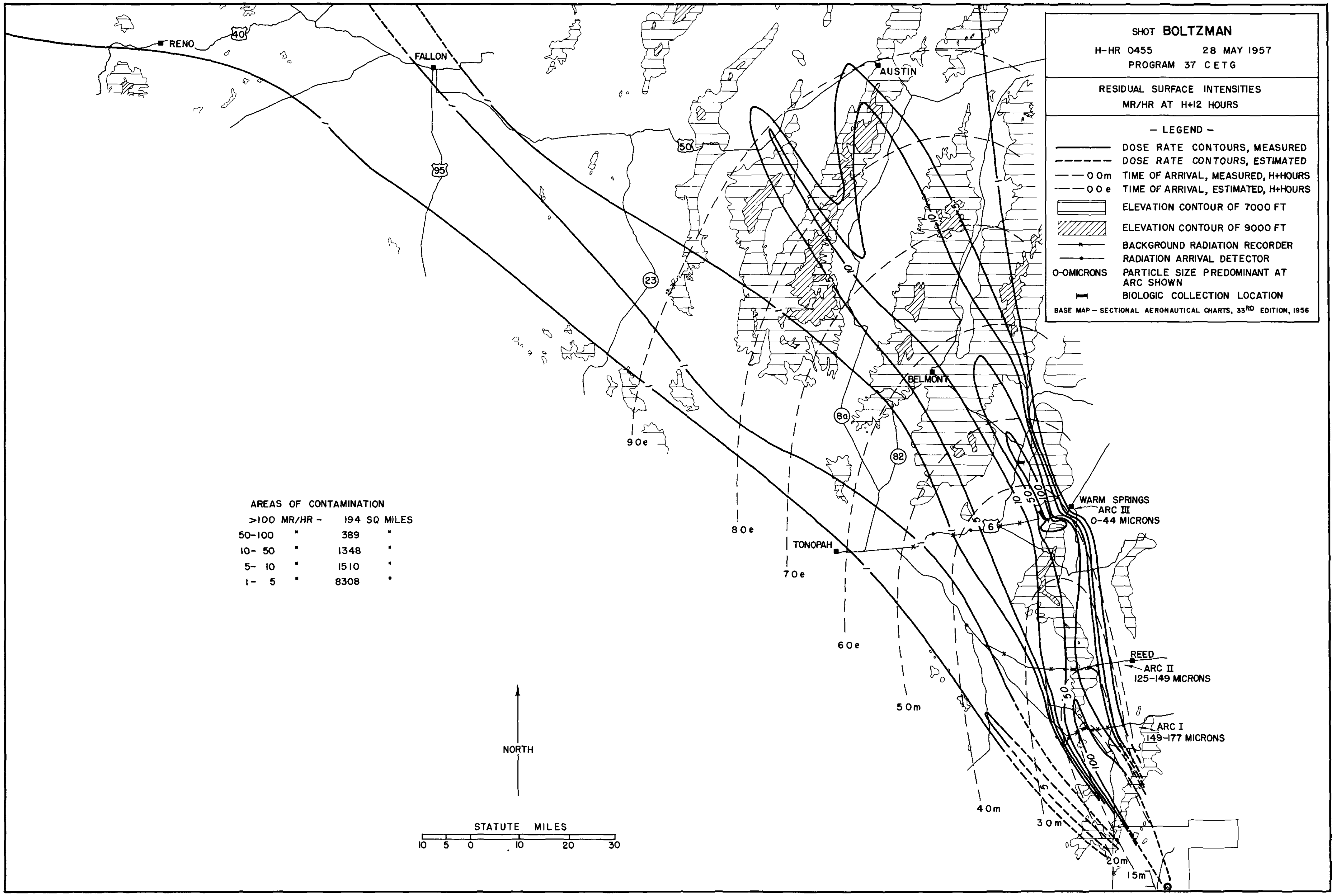
SHOT BOLTZMAN
H-HR 0455 28 MAY 1957
PROGRAM 37 CETG
RESIDUAL SURFACE INTENSITIES
MR/HR AT H+12 HOURS
- LEGEND -
DOSE RATE CONTOURS, MEASURED
DOSE RATE CONTOURS, ESTIMATED
0 0m TIME OF ARRIVAL, MEASURED, H+HOURS
0 0 e TIME OF ARRIVAL, ESTIMATED, H+HOURS
ELEVATION CONTOUR OF 7000 FT
ELEVATION CONTOUR OF 9000 FT
BACKGROUND RADIATION RECORDER
RADIATION ARRIVAL DETECTOR
O-OMICRONS PARTICLE SIZE PREDOMINANT AT ARC SHOWN
BIOLOGIC COLLECTION LOCATION
BASE MAP – SECTIONAL AERONAUTICAL CHARTS, 33RD EDITION, 1956
AREAS OF CONTAMINATION
>100 MR/HR - 194 SQ MILES
50-100 " 389 "
10- 50 " 1348 "
5- 10 " 1510 "
1- 5 " 8308 "
RENO
40
FALLON
50
95
23
AUSTIN
BELMONT
8a
82
6
TONOPAH
WARM SPRINGS
ARC III
0-44 MICRONS
REED
ARC II
125-149 MICRONS
ARC I
149-177 MICRONS
90e
80e
70e
60e
50m
40m
30m
20m
15m
10
5
50
100
NORTH
STATUTE MILES
10 5 0 10 20 30

FIGURE 2.1 Boltzmann Fallout Pattern

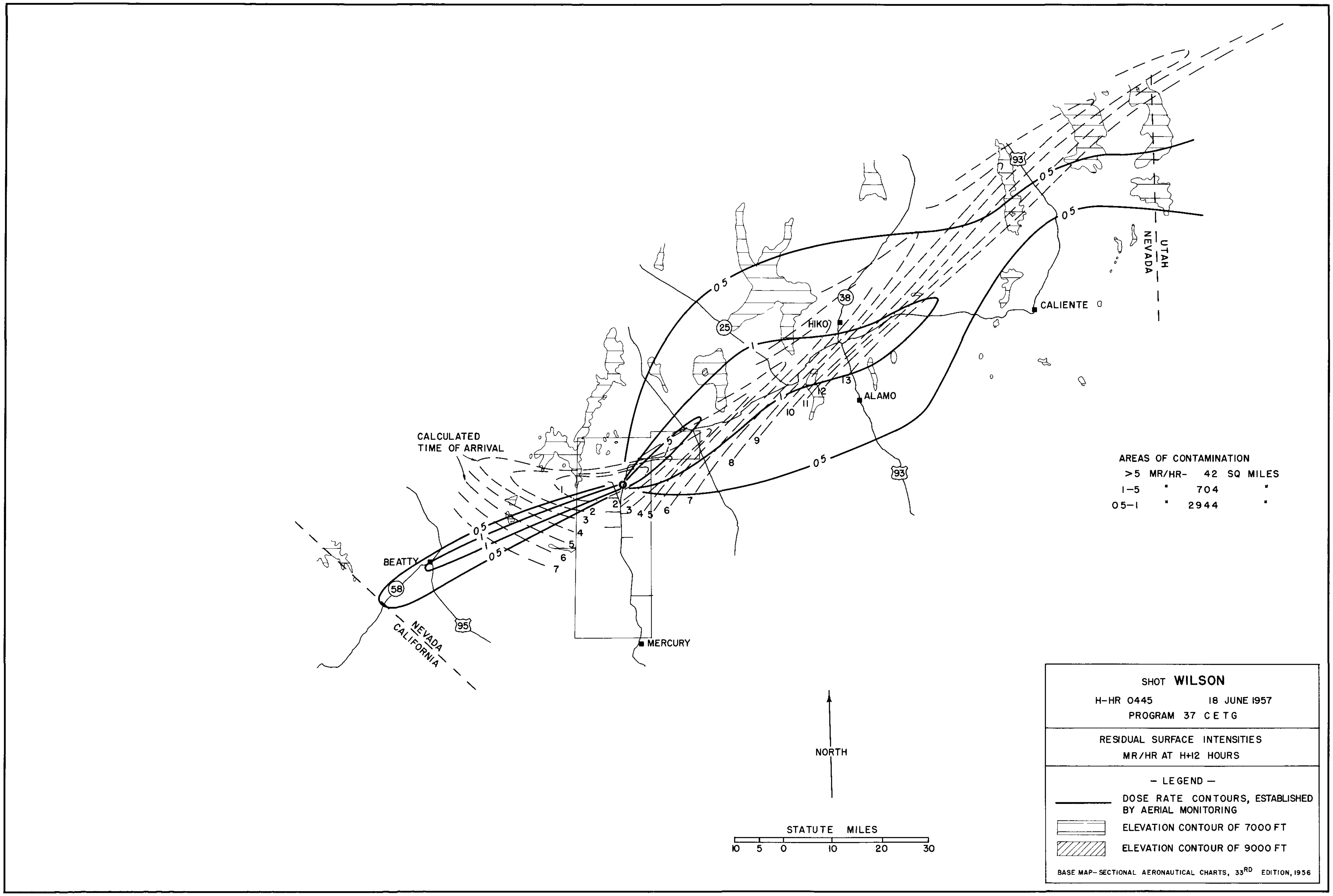

FIGURE 2 2 Wilson Fallout Pattern

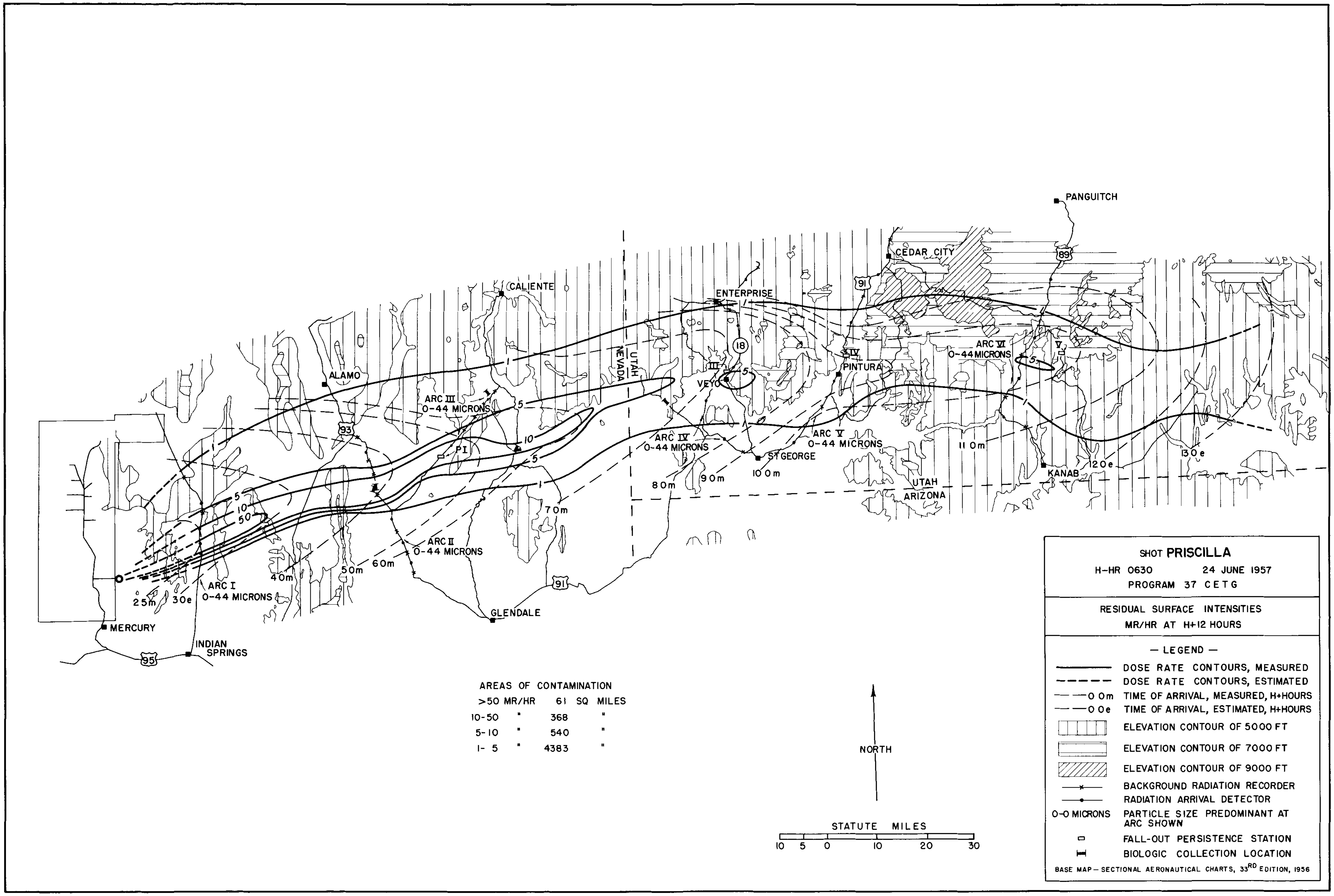

FIGURE 2.3 Priscilla Fallout Pattern

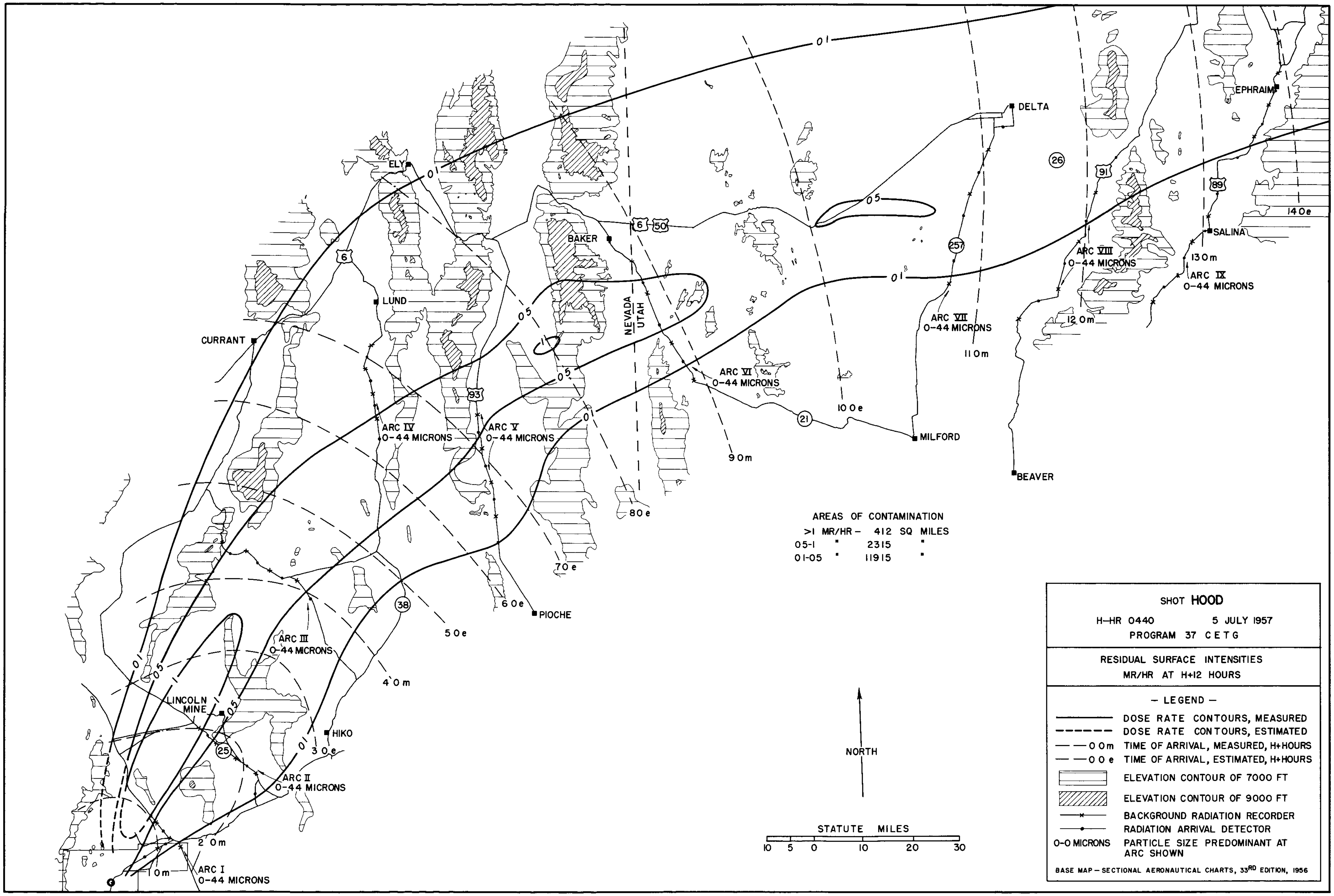

FIGURE 2.4 Hood Fallout Pattern

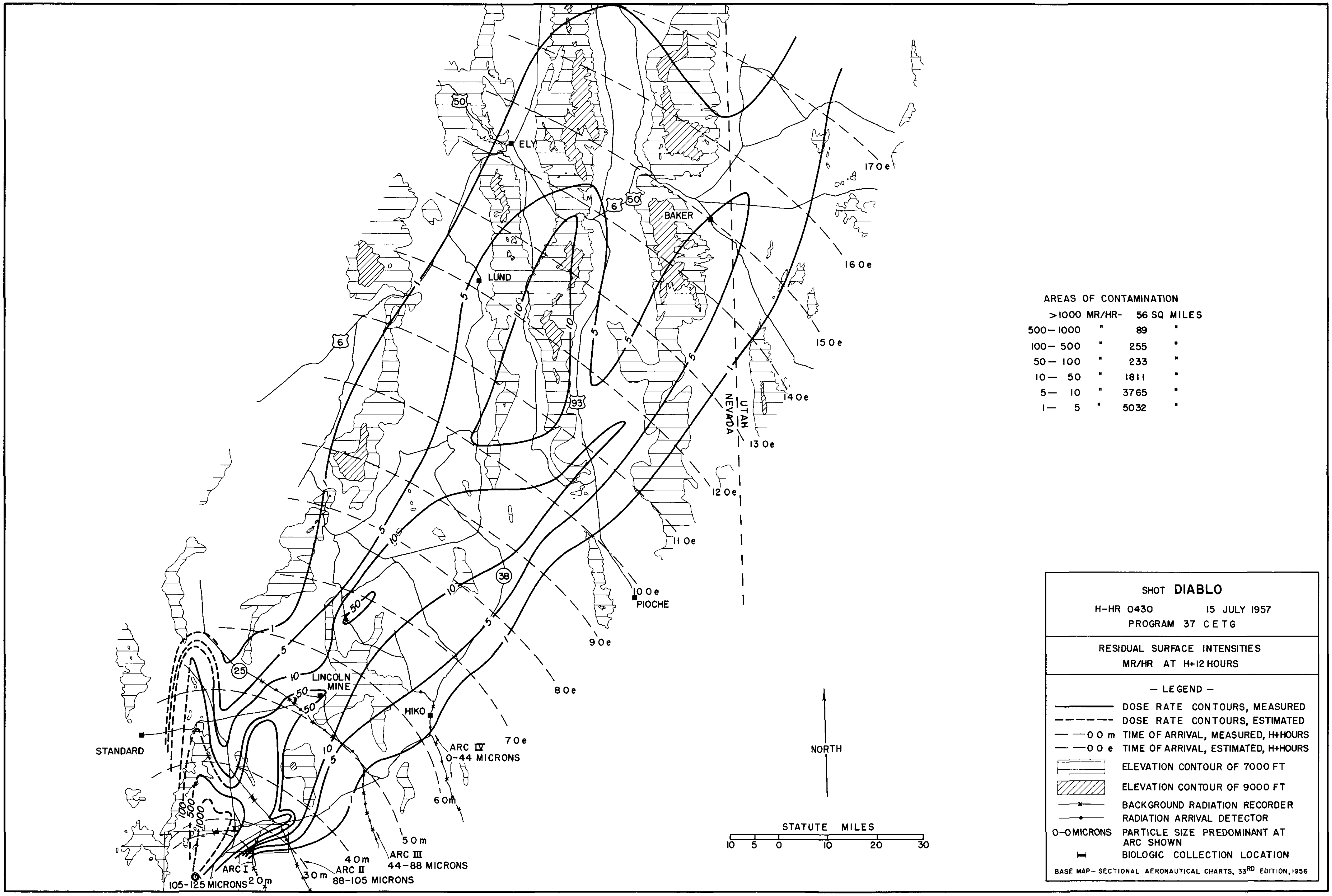

FIGURE 2.5 Diablo Fallout Pattern

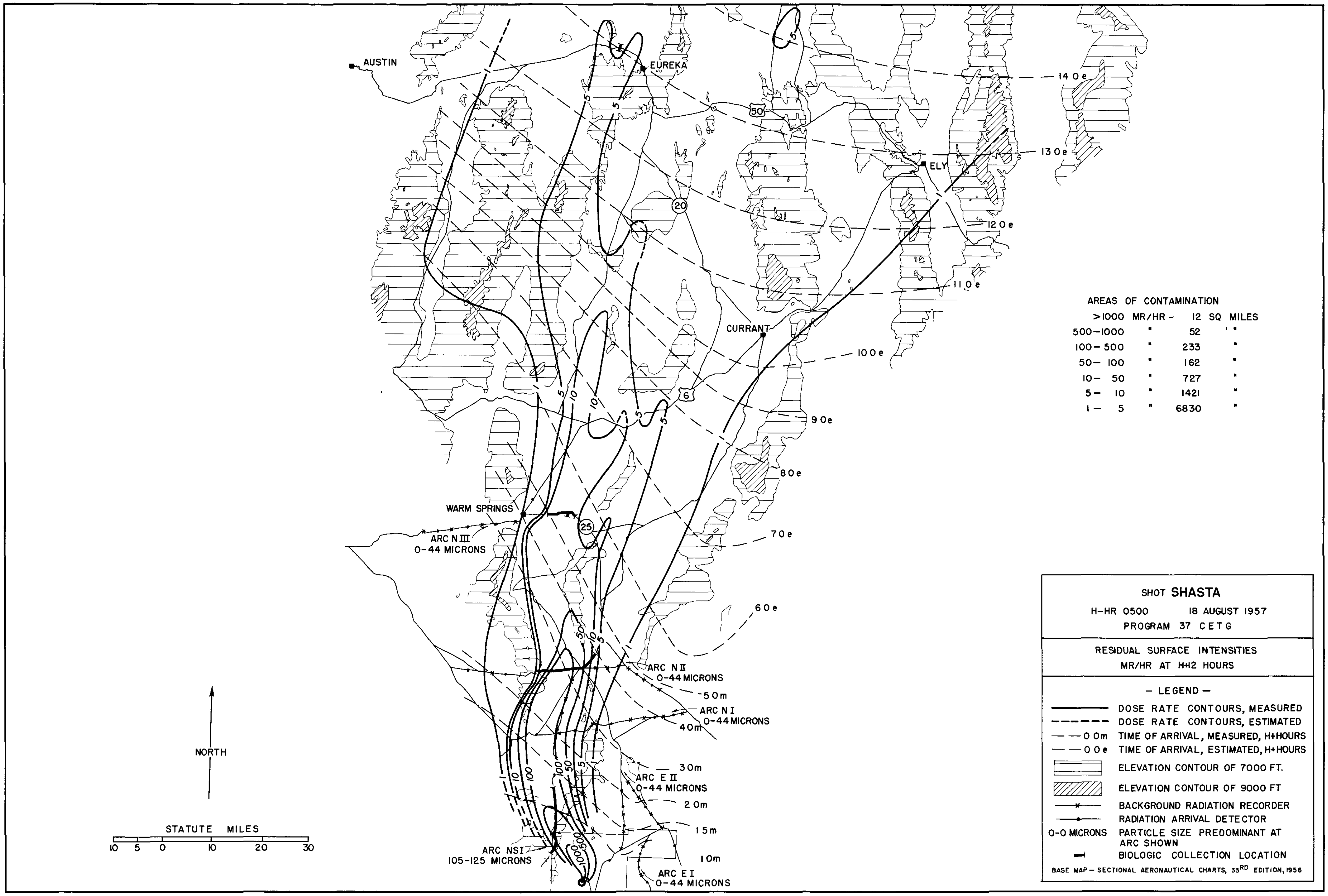

AREAS OF CONTAMINATION

>1000 MR/HR -	12	SQ MILES
500-1000 "	52	"
100-500 "	233	"
50-100 "	162	"
10-50 "	727	"
5-10 "	1421	"
1-5 "	6830	"

SHOT **SHASTA**
H-HR 0500 18 AUGUST 1957
PROGRAM 37 C E T G

RESIDUAL SURFACE INTENSITIES
MR/HR AT H+12 HOURS

– LEGEND –

———	DOSE RATE CONTOURS, MEASURED
– – – –	DOSE RATE CONTOURS, ESTIMATED
— — 0 0m	TIME OF ARRIVAL, MEASURED, H+HOURS
— — 0 0e	TIME OF ARRIVAL, ESTIMATED, H+HOURS
▤	ELEVATION CONTOUR OF 7000 FT.
▨	ELEVATION CONTOUR OF 9000 FT
—×—	BACKGROUND RADIATION RECORDER
—•—	RADIATION ARRIVAL DETECTOR
0-0 MICRONS	PARTICLE SIZE PREDOMINANT AT ARC SHOWN
⊢	BIOLOGIC COLLECTION LOCATION

BASE MAP – SECTIONAL AERONAUTICAL CHARTS, 33RD EDITION, 1956

FIGURE 2.6 Shasta Fallout Pattern

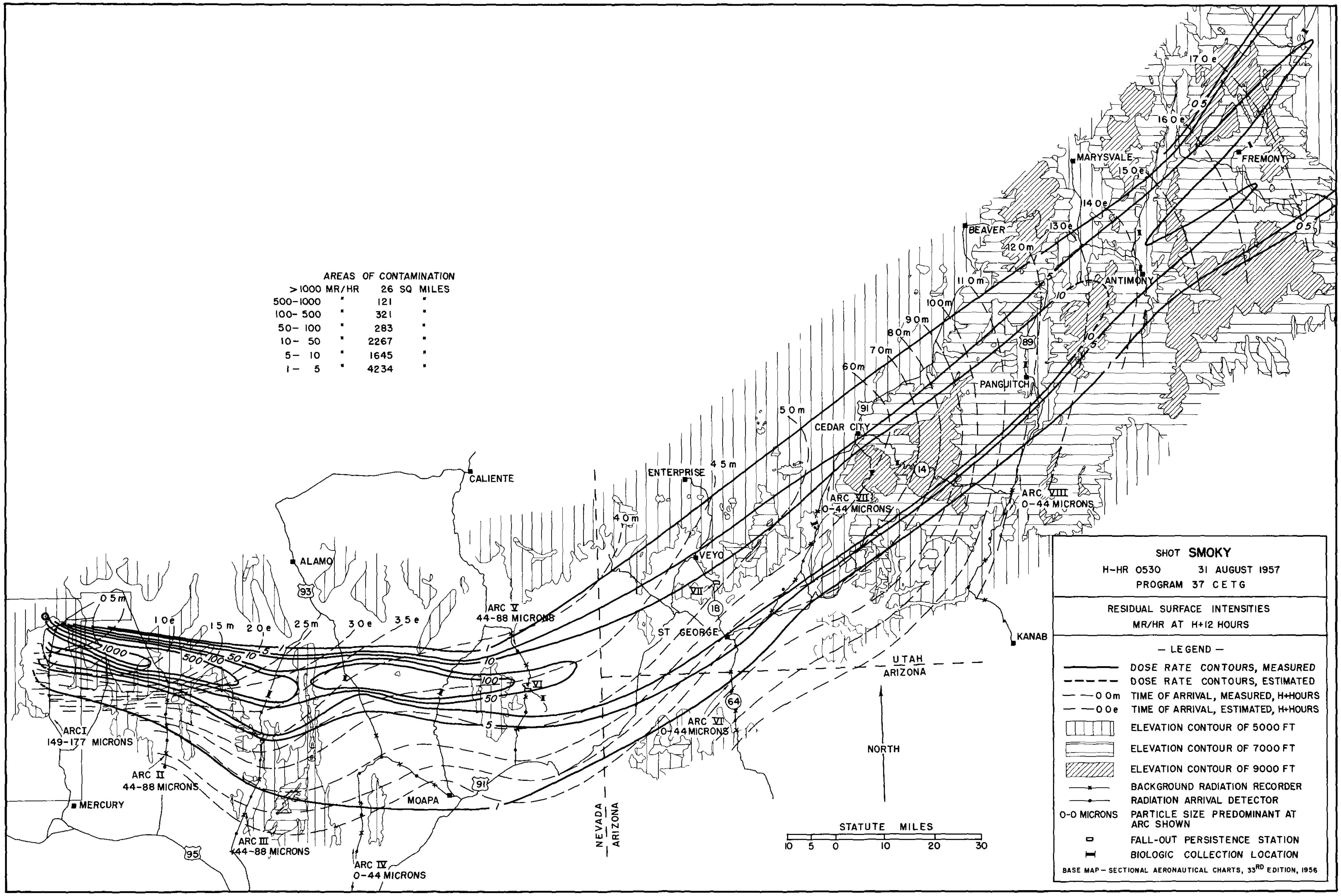

FIGURE 2.7a Smoky Fallout Pattern

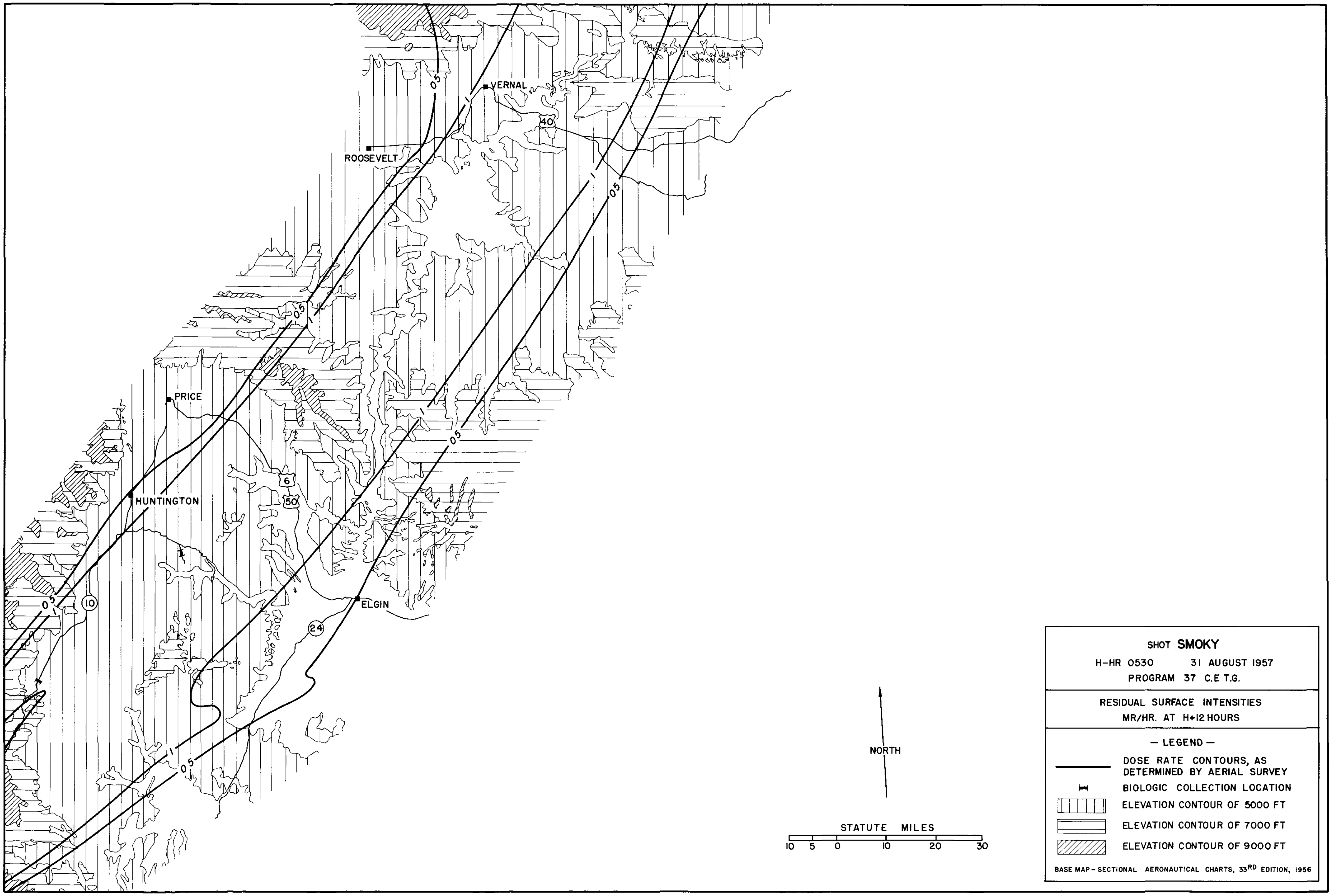
VERNAL
ROOSEVELT
PRICE
HUNTINGTON
ELGIN
40
6
50
10
24
05
1
NORTH
STATUTE MILES
10 5 0 10 20 30
SHOT SMOKY
H-HR 0530 31 AUGUST 1957
PROGRAM 37 C.E T.G.
RESIDUAL SURFACE INTENSITIES
MR/HR. AT H+12 HOURS
— LEGEND —
DOSE RATE CONTOURS, AS DETERMINED BY AERIAL SURVEY
BIOLOGIC COLLECTION LOCATION
ELEVATION CONTOUR OF 5000 FT
ELEVATION CONTOUR OF 7000 FT
ELEVATION CONTOUR OF 9000 FT
BASE MAP - SECTIONAL AERONAUTICAL CHARTS, 33RD EDITION, 1956

FIGURE 2.7b Smoky Fallout Pattern

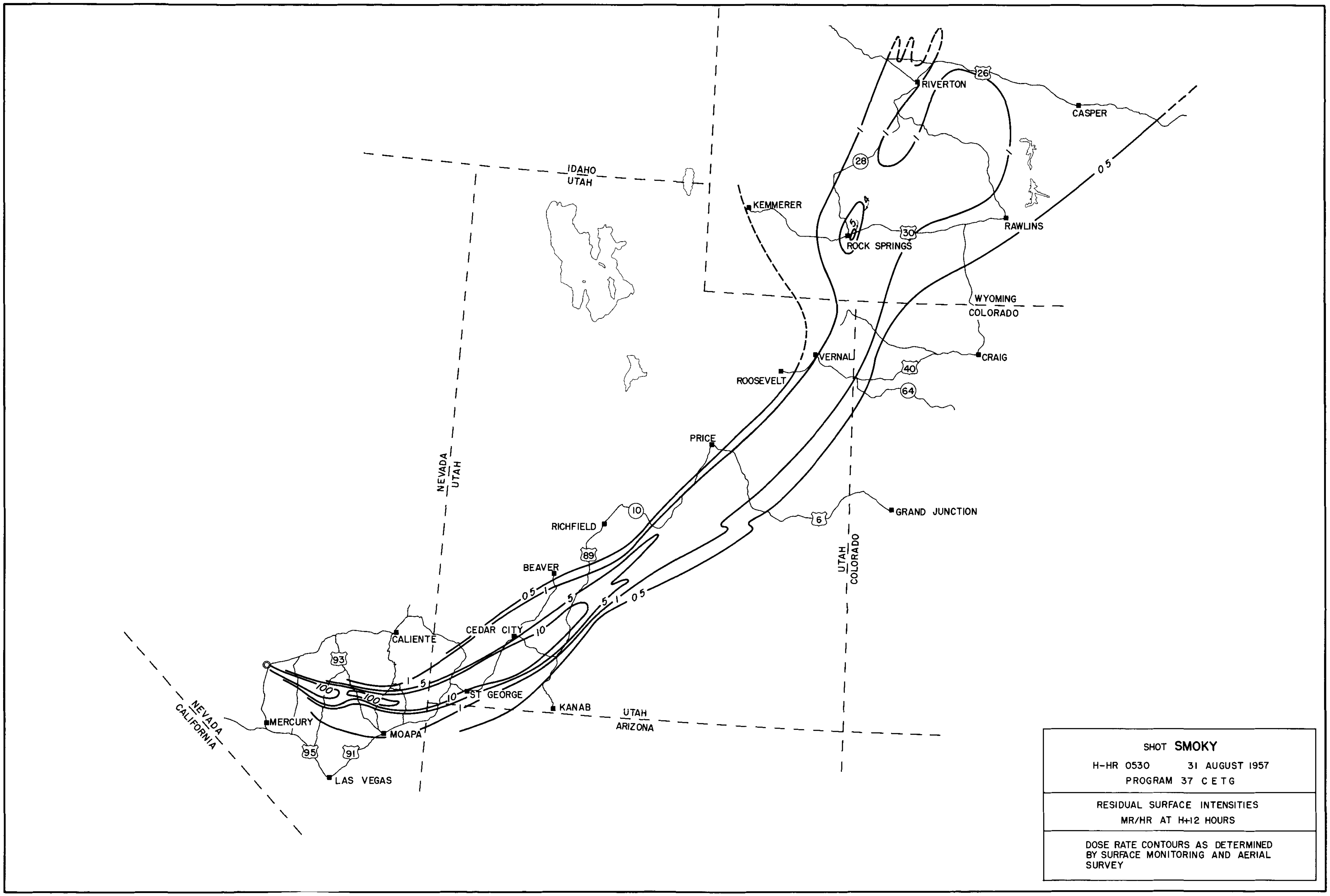

FIGURE 2.8 Smoky Extended Fallout Pattern

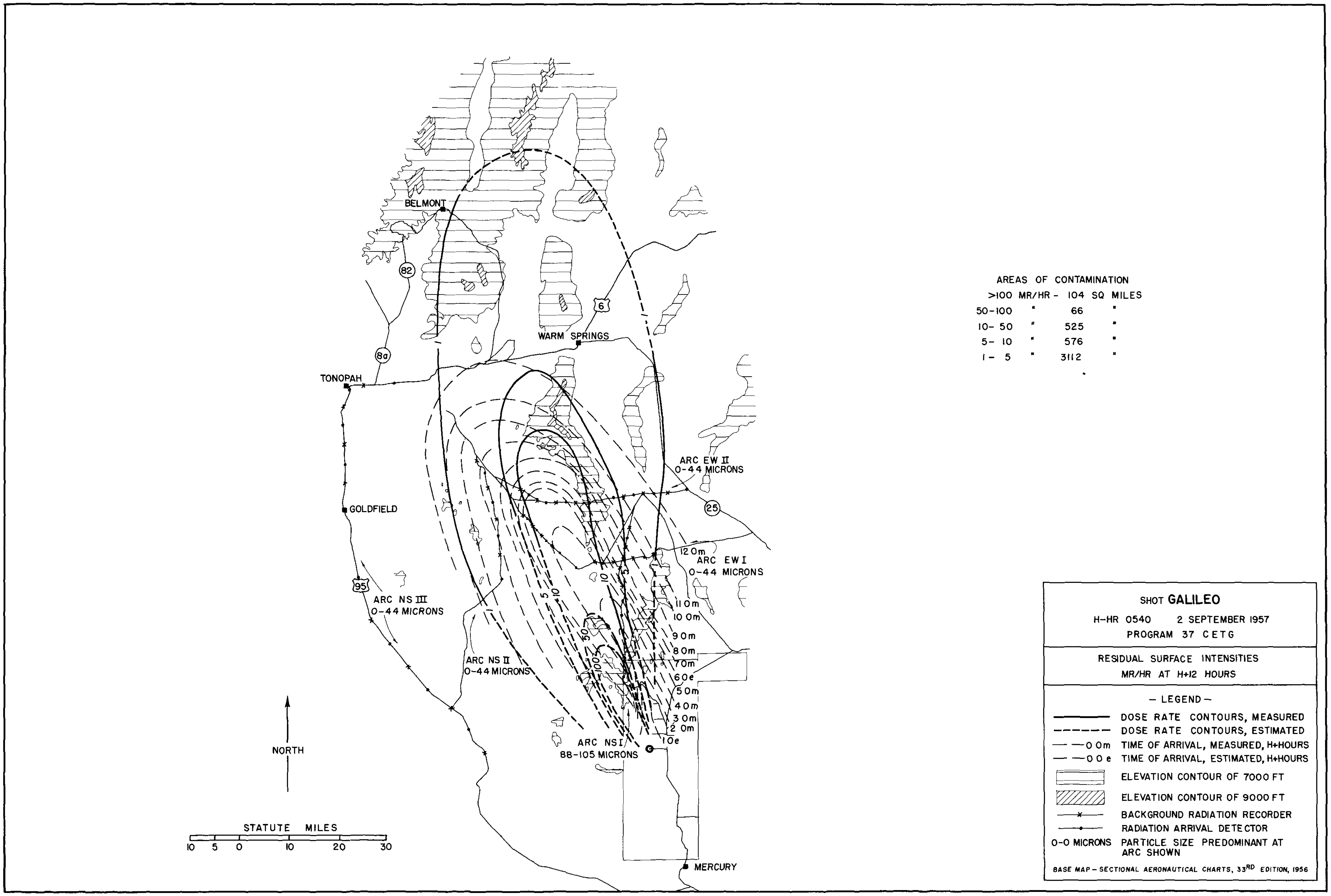
AREAS OF CONTAMINATION
>100 MR/HR - 104 SQ MILES
50-100 " 66 "
10-50 " 525 "
5-10 " 576 "
1-5 " 3112 "
SHOT GALILEO
H-HR 0540 2 SEPTEMBER 1957
PROGRAM 37 CETG
RESIDUAL SURFACE INTENSITIES
MR/HR AT H+12 HOURS
- LEGEND -
DOSE RATE CONTOURS, MEASURED
DOSE RATE CONTOURS, ESTIMATED
0 0m TIME OF ARRIVAL, MEASURED, H+HOURS
0 0 e TIME OF ARRIVAL, ESTIMATED, H+HOURS
ELEVATION CONTOUR OF 7000 FT
ELEVATION CONTOUR OF 9000 FT
BACKGROUND RADIATION RECORDER
RADIATION ARRIVAL DETECTOR
0-0 MICRONS PARTICLE SIZE PREDOMINANT AT ARC SHOWN
BASE MAP - SECTIONAL AERONAUTICAL CHARTS, 33RD EDITION, 1956
BELMONT
82
6
WARM SPRINGS
8a
TONOPAH
GOLDFIELD
95
ARC NS III
0-44 MICRONS
ARC NS II
0-44 MICRONS
ARC NS I
88-105 MICRONS
ARC EW II
0-44 MICRONS
25
12 0m
ARC EW I
0-44 MICRONS
11 0m
10 0m
9 0m
8 0m
7 0m
6 0e
5 0m
4 0m
3 0m
2 0m
1 0e
5
10
10
5
50
100
NORTH
STATUTE MILES
10 5 0 10 20 30
MERCURY

FIGURE 2.9 Galileo Fallout Pattern

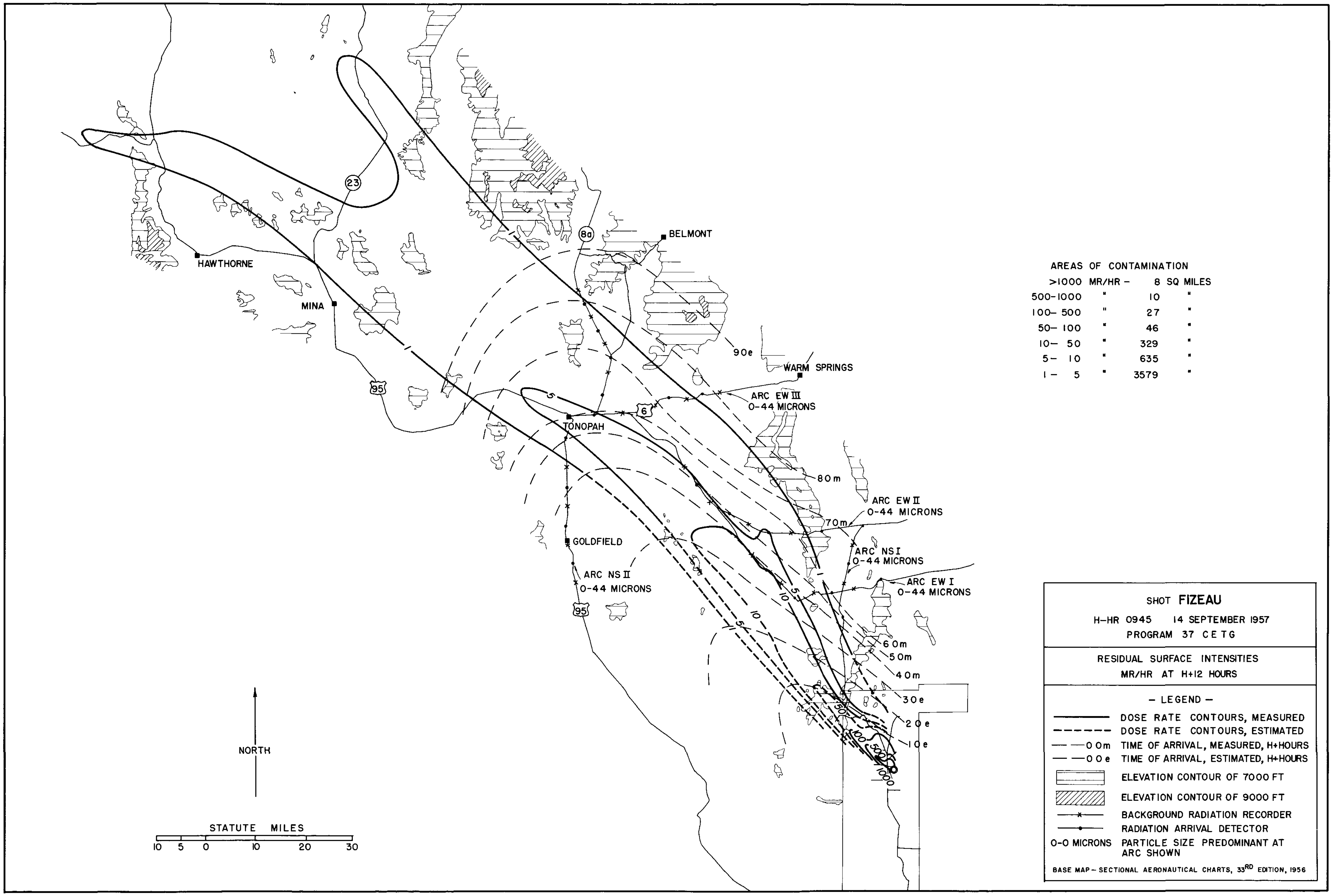

FIGURE 2.10 Fizeau Fallout Pattern

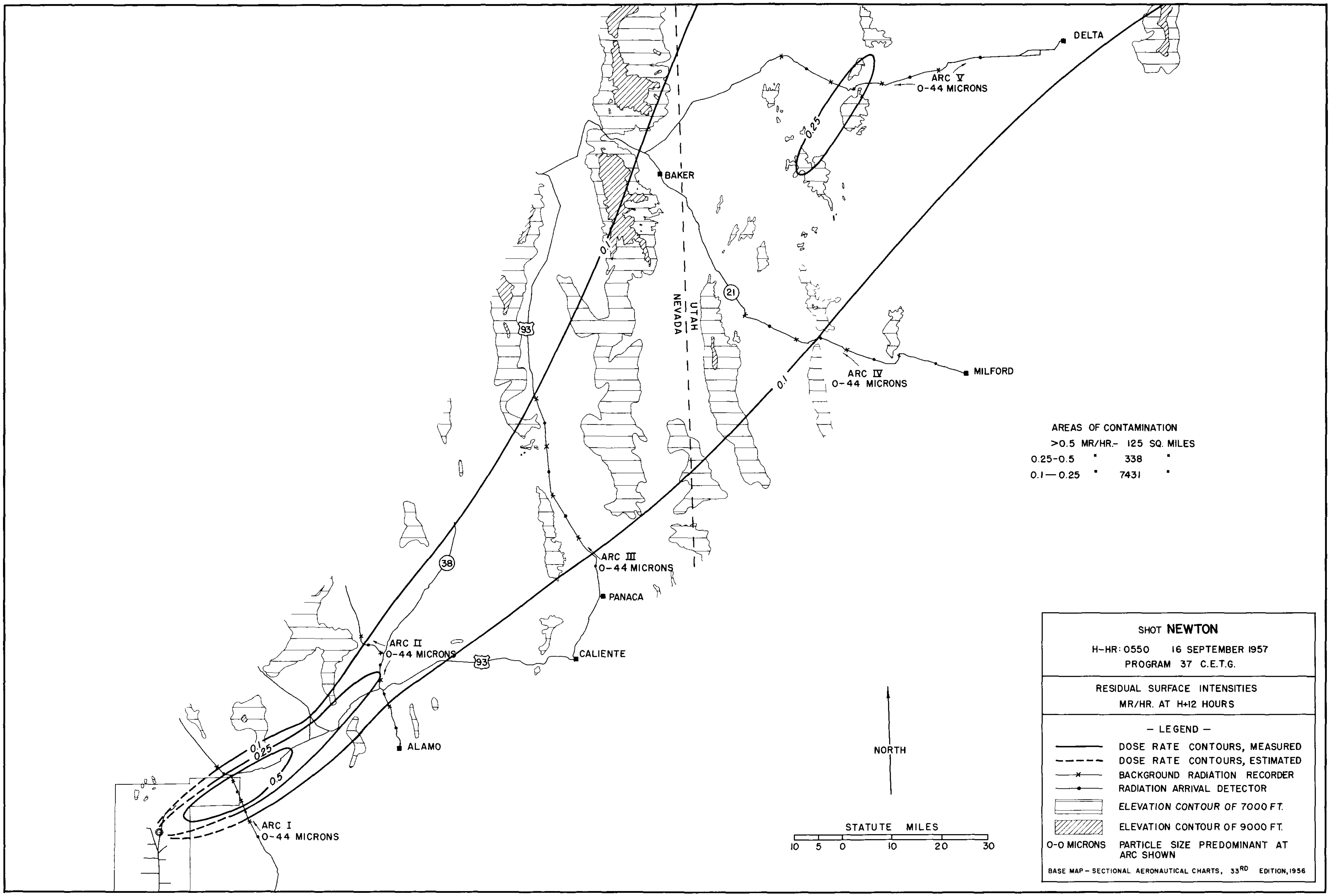
DELTA
ARC V
0-44 MICRONS
0.25
BAKER
0.1
UTAH
NEVADA
21
93
MILFORD
ARC IV
0-44 MICRONS
0.1
AREAS OF CONTAMINATION
>0.5 MR/HR.- 125 SQ. MILES
0.25-0.5 " 338 "
0.1—0.25 " 7431 "
38
ARC III
0-44 MICRONS
PANACA
ARC II
0-44 MICRONS
93
CALIENTE
ALAMO
0.1
0.25
0.5
ARC I
0-44 MICRONS
NORTH
STATUTE MILES
10 5 0 10 20 30
SHOT NEWTON
H-HR: 0550 16 SEPTEMBER 1957
PROGRAM 37 C.E.T.G.
RESIDUAL SURFACE INTENSITIES
MR/HR. AT H+12 HOURS
— LEGEND —
DOSE RATE CONTOURS, MEASURED
DOSE RATE CONTOURS, ESTIMATED
BACKGROUND RADIATION RECORDER
RADIATION ARRIVAL DETECTOR
ELEVATION CONTOUR OF 7000 FT.
ELEVATION CONTOUR OF 9000 FT.
0-0 MICRONS PARTICLE SIZE PREDOMINANT AT ARC SHOWN
BASE MAP – SECTIONAL AERONAUTICAL CHARTS, 33RD EDITION, 1956

FIGURE 2.11 Newton Fallout Pattern

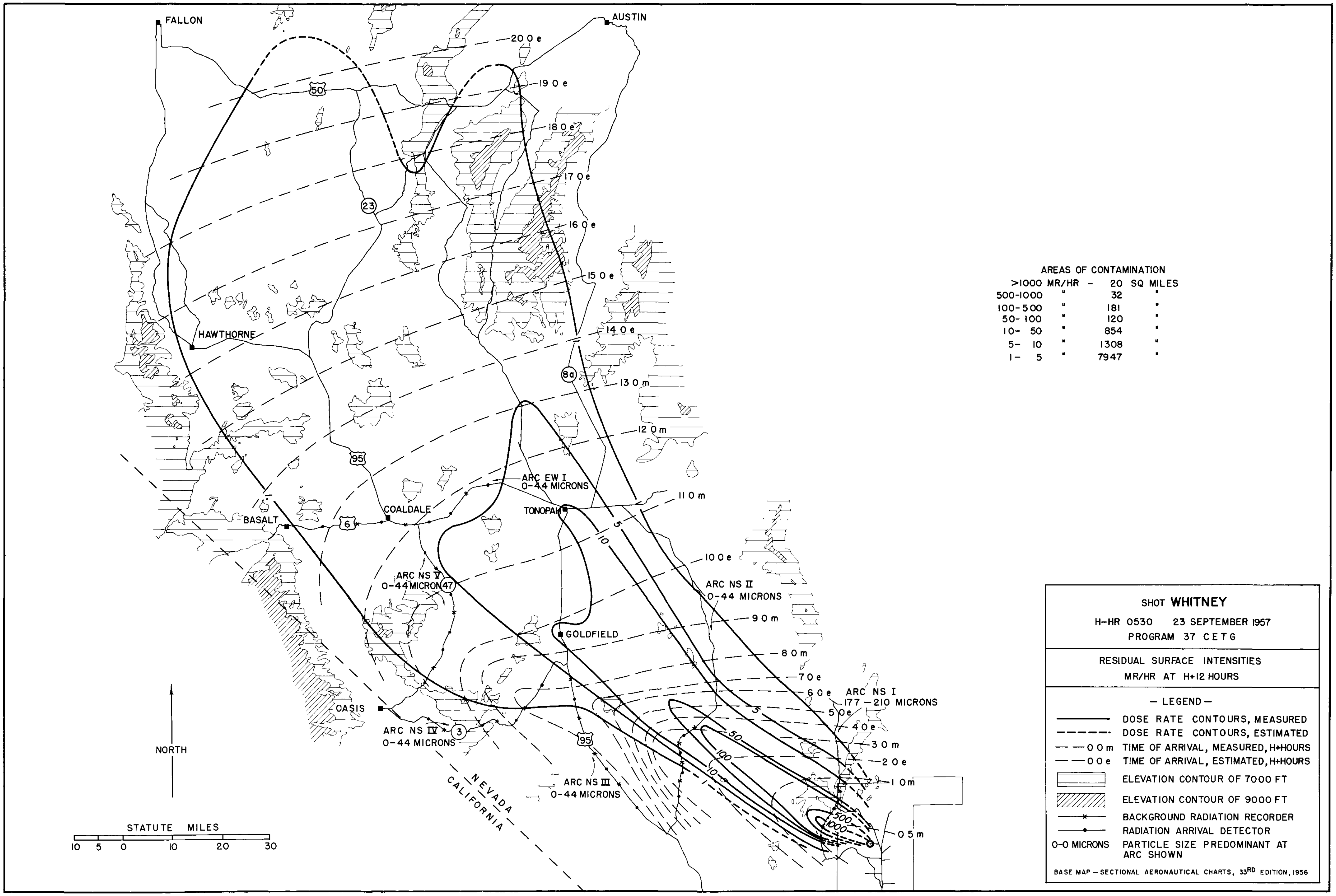

FIGURE 2.12 Whitney Fallout Pattern

2.3.2 Fallout Arrival Time and Duration

A rise of 2 mr/hr above background was arbitrarily chosen as giving the time of fallout arrival. Arrival times, both measured and estimated, are entered on the fallout pattern maps.

While the duration of fallout at individual locations is a function of a number of variables, e.g., initial particle size spectrum, particle size distribution within the cloud, vertical cloud shear, cloud height, a general relationship of fallout duration as a function of initial time-of-arrival was observed from recording gamma-radiation monitors (PRAM; see Appendix A for description). This relationship is illustrated in Figure 2.13 where data derived from six tower and three balloon mounted shots are presented. The regression curve indicates that the interval between initial and maximum activity increased from approximately 25 minutes at an initial fallout time of H + 1 hour to approximately 5 hours at fallout time of H + 12 hours. The number of observations employed in this study lends credence to the 1.4 constant especially in the time range H + 1 to H + 8 hours.

Examples of radiation intensity curves resulting from short and very long fallout duration are illustrated in Figure 2.14. Both curves were obtained at locations approximately 50 miles from ground zero but under quite different conditions of cloud velocity and shear. The long duration curve demonstrates discontinuity in fallout which is probably associated with deposition from different cloud strata. The declining portions of the curves do not reflect additional detectable fallout levels after reaching the maximum intensity in either case. No quantitative data were obtained on the continuance of the fallout process after the peak in intensity. A few recorder traces indicate, however, that the time period between the peak intensity and the end of the fallout process might be greater than the period between initial fallout and peak intensity. Similar data from the Teapot Series (Reference 1) indicate that anomalies observed during that study were not due to a redistribution of the original fallout material.

Analysis of the time-intensity data from the gamma-recording monitors aided in the determination of both the gamma decay rate and gamma dose (Chapter 4).

2.3.3 Ratio of Beta Activity Per Unit Area to Dose Rate

Gamma dose readings were obtained at time of recovery (H + 24 to 30 hours) of the stations. The ratio of beta activity per sq ft to dose rate (μc/sq ft:mr/hr) at H + 12 hours was determined from available data. The ratios served to augment and evaluate dose rate or activity per unit area values, particularly when previous fallout contamination was suspected. Table 2.3 shows the average ratio for each arc across the fallout patterns from ten shots at different distances from ground zero.

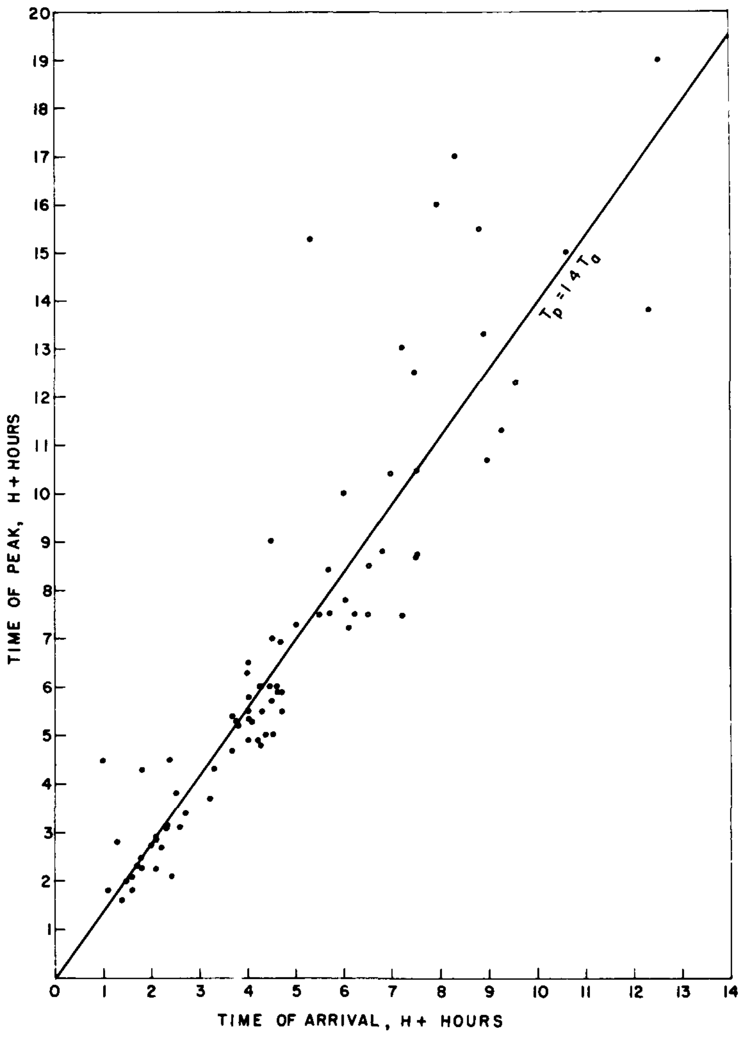

FIGURE 2. 13 Relationship of Time of Peak Activity as a Function of Time-of-Arrival of Fallout or Radiation.

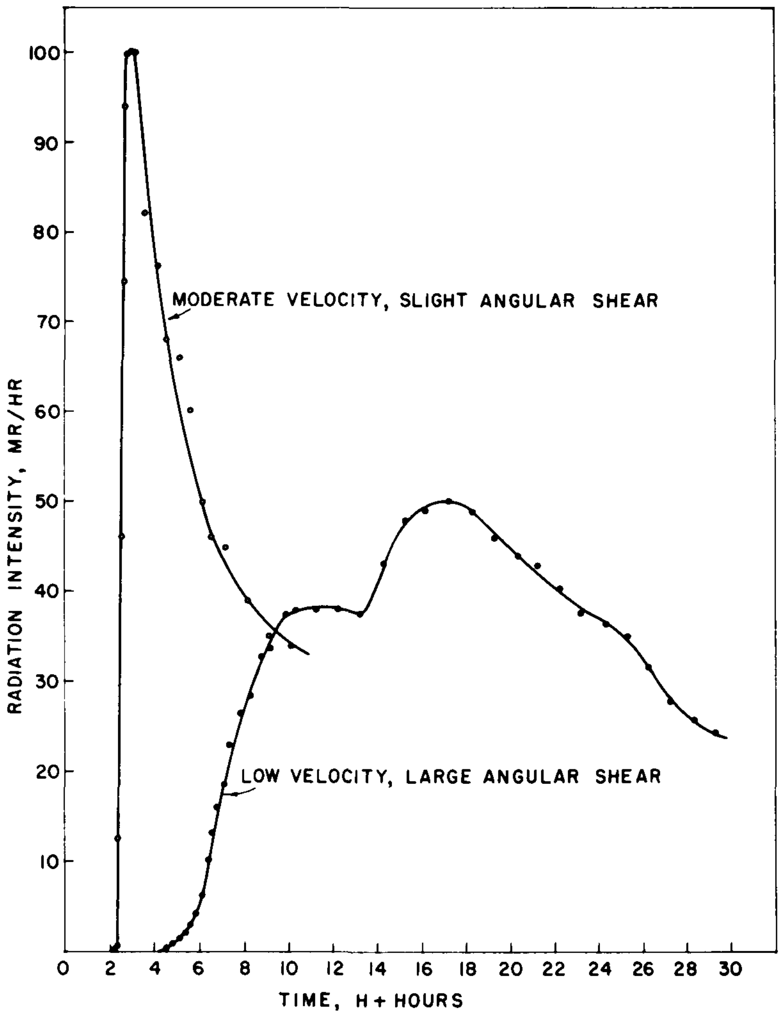

FIGURE 2. 14 Relationship of Fallout Duration as a Function of Time-of-Arrival Radiation.

TABLE 2 3 Ratio of Beta Activity per sq ft to Dose Rate

Shot	Location	Average Distance from G Z , Miles	Number of Stations	Beta μc/sq ft mr/hr, H + 12 hr
Boltzmann	Arc I	35	15	7 34 ± 5 36
	Arc II	48	16	11 67 ± 3 61
	Arc III	78	12	9 57 ± 4 28
	Average		43	9 58 ± 4 75
Priscilla	Arc I	18	20	1 86 ± 0 80
	Arc II	55	9	4 03 ± 0 69
	Arc III	69	24	1 77 ± 0 38
	Arc IV	129	13	2 89 ± 0 58
	Arc V	154	6	5 74 ± 0 92
	Arc VI	188	5	2 32 ± 0 61
	Average		77	2 59 ± 1 33
Hood	Arc I	14	8	0 51 ± 0 97
	Arc II	35	3	2 66 ± 1 24
	Arc III	71	5	1 56 ± 0 53
	Arc IV	104	3	2 59 ± 0 78
	Arc V	115	4	3 09 ± 1 98
	Arc VI	160	6	2 87 ± 0 73
	Arc VII	220	2	2 94 ± 0 02
	Arc VIII	230	2	4 13 ± 0 73
	Arc IX	280	4	1 31 ± 0 60
	Average		37	2 07 ± 0 41
Diablo	Arc I	15	4	13 03 ± 1 94
	Arc II	20	6	8 87 ± 3 09
	Arc III	40	28	8 45 ± 2 86
	Arc IV	62	14	11 02 ± 4 57
	Average		52	9 54 ± 3 62
Shasta	Arc NC I	18	19	14 45 ± 3 89
	Arc N I	32	15	10 92 ± 2 28
	Arc N II	44	38	10 80 ± 5 12
	Arc N III	76	10	15 64 ± 5 53
	Average		82	12 26 ± 4 85
Smoky	Arc I	10	12	8 69 ± 2 43
	Arc II	26	20	14 16 ± 6 18
	Arc III	50	19	10 11 ± 3 75
	Arc IV	70	32	12 05 ± 4 86
	Arc V	100	20	12 47 ± 3 41
	Arc VII	155	19	9 10 ± 2 34
	Arc VIII	200	5	9 08 ± 2 60
	Average		127	11 28 ± 4 51
Galileo	Arc NS I	16	36	7 64 ± 4 10
	Arc NS II	48	5	6 29 ± 1 31
	Arc EW I	45	37	14 79 ± 5 98
	Arc EW II	52	39	8 39 ± 3 26
	Average		117	10 09 ± 5 50
Fizeau	Arc NS I	30	8	5 40 ± 3 65
	Arc NS II	95	24	8 43 ± 2 77
	Arc EW I	50	14	9 23 ± 2 19
	Arc EW II	60	16	10 68 ± 3 87
	Arc EW III	95	13	9 26 ± 1 80
	Average		75	8 88 ± 3 19
Newton	Arc I	18	13	1 43 ± 0 96
	Arc II	55	20	1 48 ± 0 56
	Arc V	210	18	2 26 ± 0 83
	Average		51	1 74 ± 0 85
Whitney	Arc NS I	10	12	11 72 ± 6 23
	Arc NS II	43	13	10 66 ± 2 03
	Arc NS III	60	8	11 21 ± 2 57
	Arc NS IV	75	11	13 17 ± 3 01
	Arc NS V	96	20	16 26 ± 4 62
	Arc EW I	110	19	12 65 ± 4 67
	Average		83	13 00 ± 4 61

There is no apparent correlation between these ratios and time-of-arrival, distance from ground zero, or mean particle size. Balloon mounted detonations, however, appear to yield lower values, ratios of 1.5 to 2.5, than do tower mounted shot ratios of 8.9 to 13.0. This is at variance with data presented in Chapter 4 which indicate that laboratory determined beta to gamma ratios from granular collector samples were generally greater for balloon mounted shots than for tower mounted shots. The significance of these differences is obscure.

2.4 DISCUSSION

2.4.1 Fallout Deposition in the NTS Environs from Tower and Balloon Shots

Interpretation of fallout levels with respect to yield and height of detonation of tower mounted devices is somewhat obscured by the differences in shielding materials and their masses with the cab and the tower mass. Table 2.4 lists the approximate weight of towers and cabs used for the detonations documented by this Program. Balloon detonation close-in fallout was consistently less than tower fallout due to (1) height of burst and, therefore, the degree of fireball interception of the ground surface and (2) lack of a massive support structure. For tower mounted shots, the low level of radiation from Shot Fizeau was consistent with relatively low yield and tower-cab mass. However, the fallout radiation level for Shot Boltzmann of similar yield to Shot Fizeau was high. The total cab and metal shielding mass for both shots was approximately the same. The difference was probably due to the addition of 12.5 tons of silica sand in the Boltzmann cab and the effective height of detonation was 425ft because of the earth bunker immediately beneath the Boltzmann cab. With the exception of Shot Boltzmann, the higher fallout levels were associated with the heavily lead shielded cabs and the heavier towers (Diablo, Shasta, Smoky, and Whitney). A somewhat lower fallout level was associated with concrete shielding in the cab of Shot Galileo even though the tower weight was similar.

TABLE 2.4 Approximate Weights of Shot Towers and Cabs.

Shot	Tower Weight, Tons	Cab and Shielding, Tons
Boltzmann	< 25,000	< 50
Fizeau	< 25,000	< 50
Smoky	35,000 to 70,000	> 100
Galileo	25,000 to 50,000	> 100
Diablo	> 50,000	> 100
Shasta	> 50,000	> 100
Whitney	> 50,000	> 100

It has been reported (Reference 2) that available data from previous tower mounted shots at NTS are not adequate to determine the quantitative effects of the amount of shielding incorporated in fallout debris on fallout levels but that heavier towers do contribute to increases in fallout deposition.

Observations of the remains of towers and shielding material after detonation at several ground zeros indicate that large masses of material are not vaporized. Observation of the residue of the Smoky tower indicated that a very significant portion of that tower remained including the upper 200 feet of steel. Another example similar to Shot Smoky was Shot Apple II, Teapot Series. Even though the total yield of Shot Apple II was about 32 kt, the floor of the cab and the main tower support columns remained intact. The results of the Shot Fizeau tower melt studies (Reference 3) show that about 85 percent of tower material was accounted for after the detonation and that only the upper 50 feet of tower was vaporized. No melting occurred beyond 175 feet from the top of the tower although the fireball theoretically engulfed more than 400 feet of the tower.

These observations indicate that before a realistic approach can be made in formulating reliable prediction models, information should be obtained as to how much material is actually consumed in the formation of fallout particles.

2.5 SUMMARY

1. Dose rates and time of arrival of fallout or radiation resulting from Shots Boltzmann, Wilson, Priscilla, Hood, Diablo, Shasta, Smoky, Galileo, Fizeau, Newton, and Whitney were measured and are reported in terms of isodose-rate and isofallout-time contour maps.

2. Radiation hot spots were observed in fallout patterns of both tower and balloon mounted shots. These are probably caused by the atmospheric turbulence present over the mountain ridges.

3. A relationship between time of fallout arrival (T_a) to time of peak activity (T_P) was derived, $T_P = 1.4\ T_a$.

4. Ratios of beta activity (μc/sq ft) to dose rate (mr/hr) at H + 12 hours ranged from 8.9 to 13.0 for tower mounted shots and 1.5 to 2.5 for balloon mounted shots. No explanation is offered for the differences.

5. The levels of fallout from tower mounted shots were greatly influenced by mass and nature of tower and cab materials.

REFERENCES

1. L. Baurmash and others, "Distribution and Characterization of Fallout and Airborne Activity from 10 to 160 Miles from Ground Zero, Spring 1955", Project 37.2 (CETO), Operation Teapot, WT-1178, November 1958, Atomic Energy Project, School of Medicine, University of California, Los Angeles, California, Unclassified.

2. J. W. Reed; "Fallout Yield Prediction for Tower Shots"; Report No. SCTM 108-58 (51), March 1958; Sandia Corporation, Albuquerque, New Mexico; Classification, Secret.

3. W. K. Dolen and A. D. Thornborough; "Fizeau Tower Melt Studies as Related to Fallout Prediction"; Report No. SC-4185, April 1958; Sandia Corporation, Albuquerque, New Mexico; Classification, Secret.

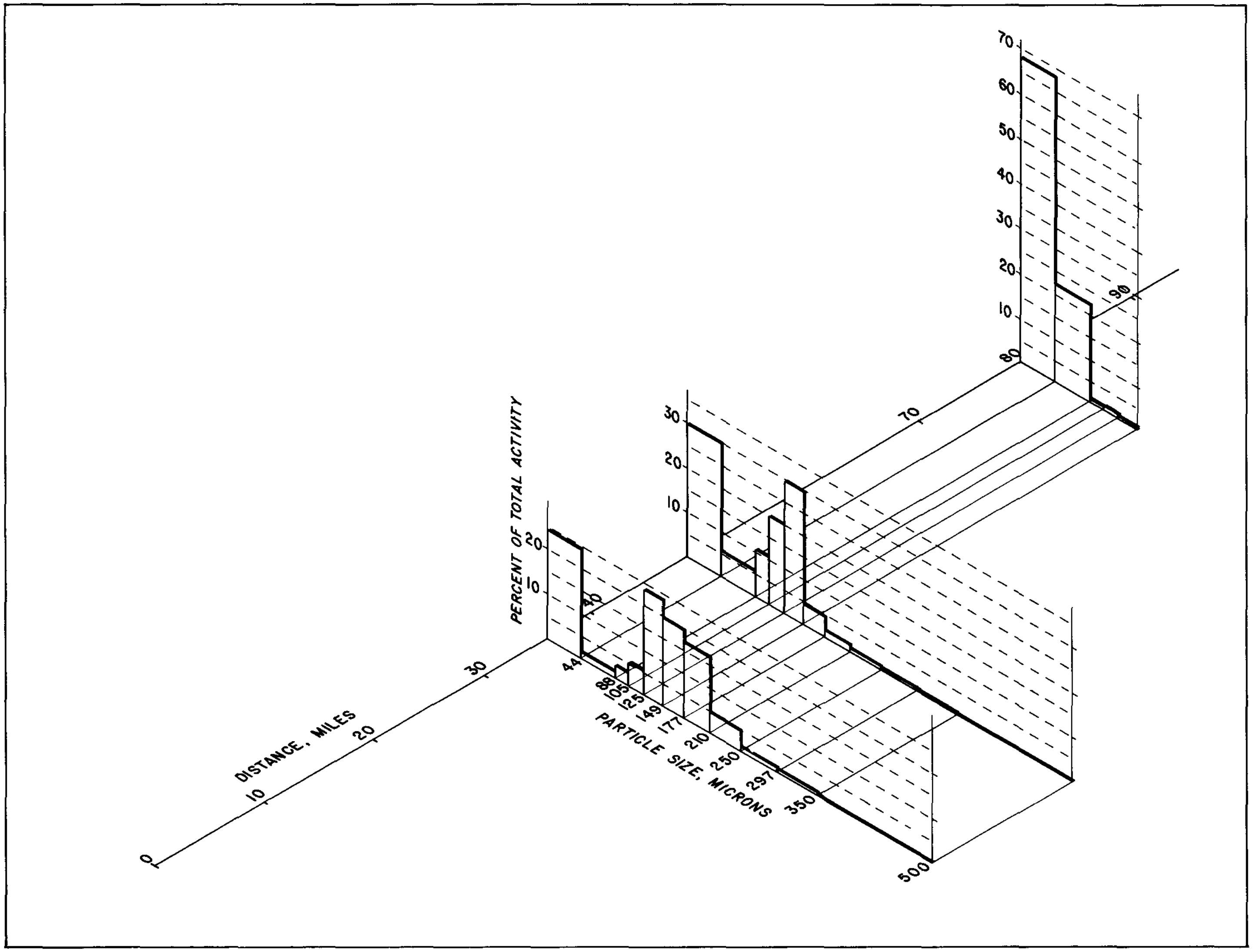

FIGURE 3.8 Total Particle Size Distribution of Fallout Material from Shot Boltzmann at Three Distances from Ground Zero.

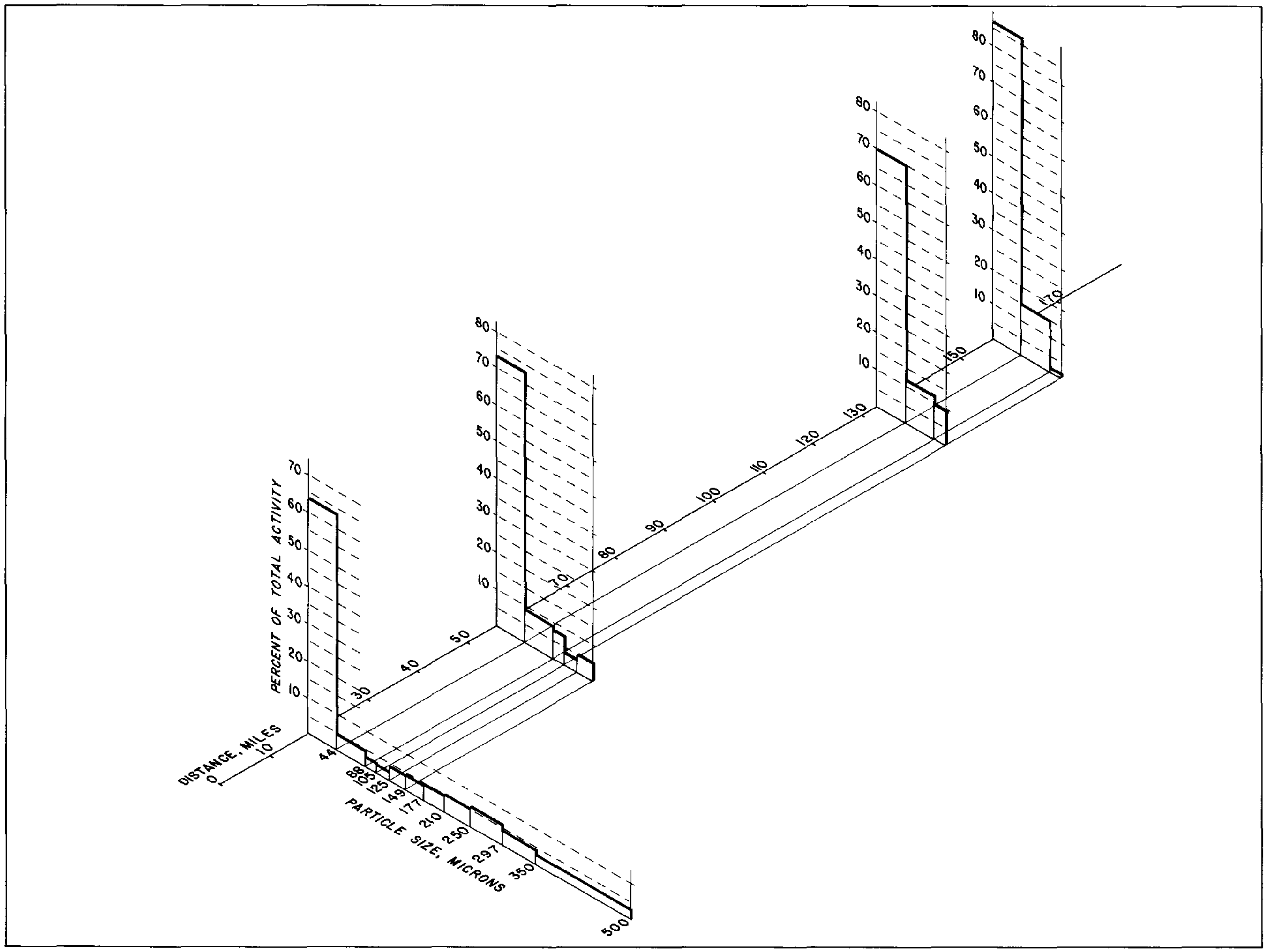

FIGURE 3.9 Total Particle Size Distribution of Fallout Material from Shot Priscilla at Four Distances from Ground Zero.

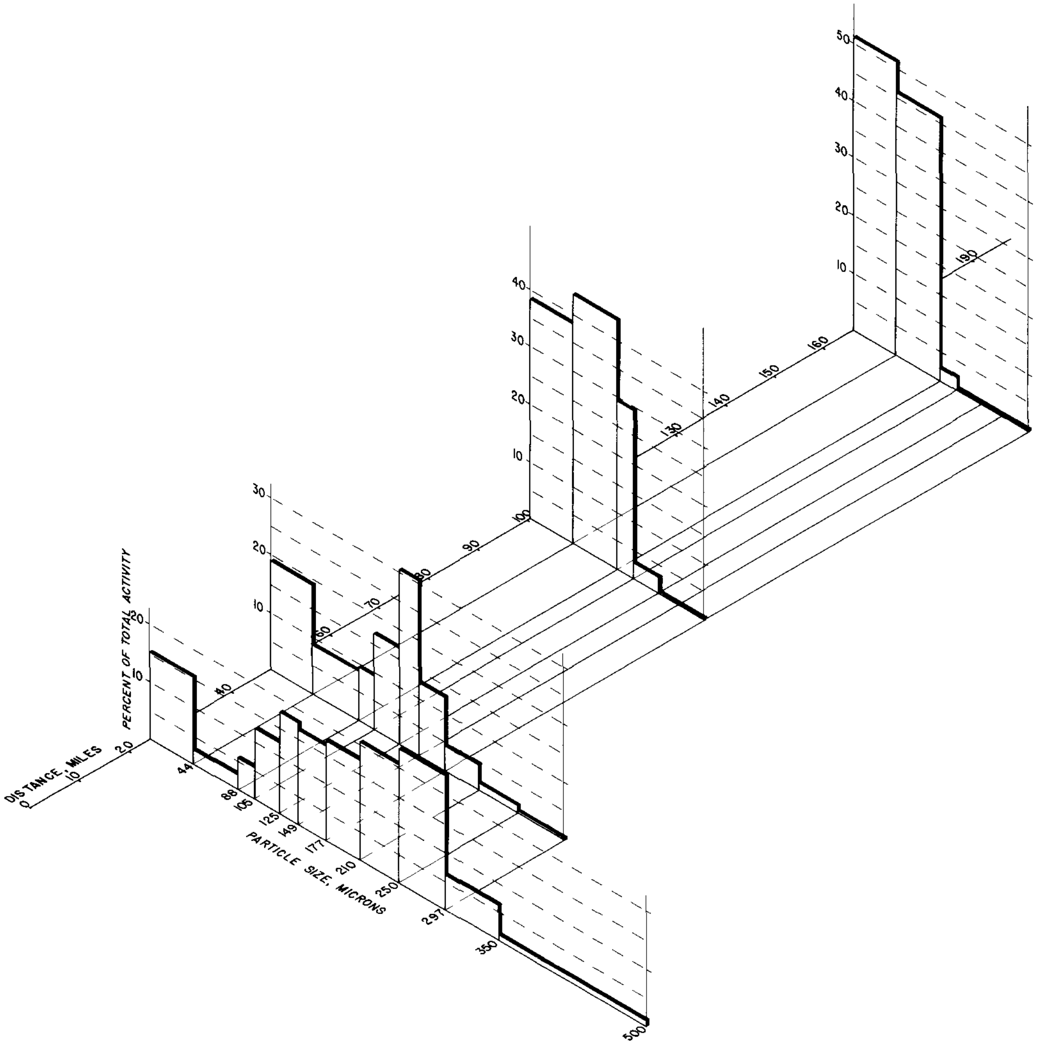

FIGURE 3.10 Total Particle Size Distribution of Fallout Material from Shot Smoky at Four Distances from Ground Zero.

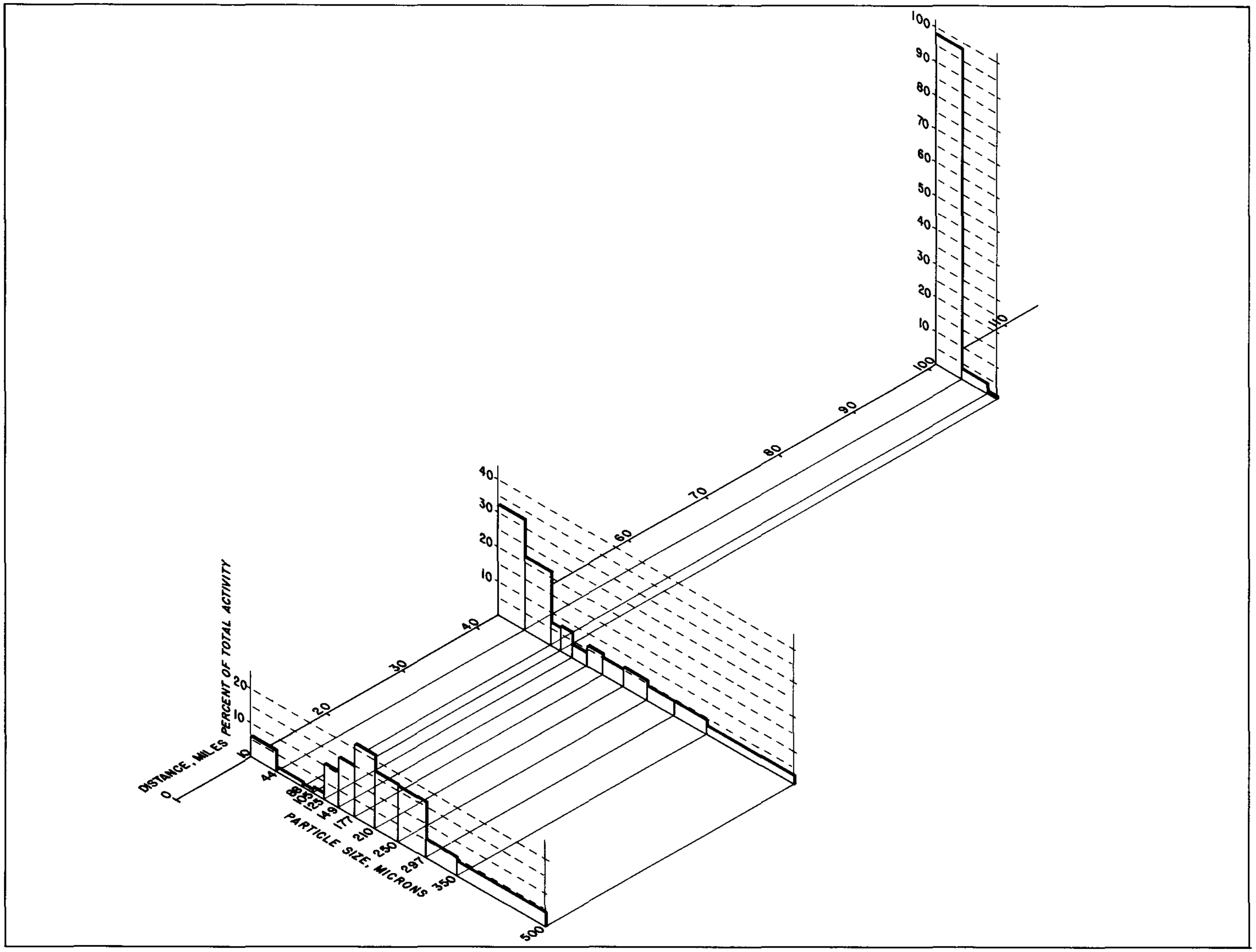

FIGURE 3.11 Total Particle Size Distribution of Fallout Material from Shot Whitney at Three Distances from Ground Zero.

graphically integrating the integrated arc radioactivity values of individual particle size ranges along the fallout midline as described in Chapter 2. The percentage contributions of the fallout fractions of various particle sizes, from Shots Boltzmann, Priscilla, and Smoky derived in this manner are tabulated in Table 3.1. The two tower shots had similar particle size distributions with approximately seventy percent of the fallout activity associated with particle sizes greater than 44 microns. The balloon Shot Priscilla had only approximately thirty percent of its fallout activity associated with such sizes.

TABLE 3.1 Particle Size Range Contribution to Fallout Deposited

Size Fraction, Microns	Pct of Total Beta Radioactivity, H + 12 hr		
	Boltzmann	Priscilla	Smoky
> 250	0.4	Nil	5.5
210 - 250	1.4	Nil	4.0
177 - 210	6.9	Nil	5.3
149 - 177	18.4	Nil	8.8
125 - 149	24.9	1.5	16.5
105 - 125	8.0	1.1	10.6
88 - 105	4.3	6.5	8.0
44 - 88	2.7	11.4	17.8
< 44	33.2	73.6	23.6

3.3.4 Particle Size Distributions Across Fallout Pattern Arcs

Examples of the distribution of individual particle size fractions across fallout pattern arcs appear in Figures 3.12 and 3.13 where particle size percentages across the closest Boltzmann (35 miles from ground zero) and Priscilla (18 miles from ground zero) arcs are presented. The total activity distributions across each arc are also presented for purposes of comparison.

The Boltzmann arc and, to a lesser extent, that of Priscilla demonstrate that the maximum percentage contributions of the various particle-size ranges occur at different locations in the traverse across the arc. Such distributions probably reflect the contributions of discrete elevation layers with the fallout cloud. The widespread distribution of less than 44 micron material suggests greater diffusion of smaller particle sizes within the cloud, relative to the larger size fractions.

Both Boltzmann and Priscilla arcs indicate that the location of maximum radiation intensity, at least in close-in areas, may be characterized by a variety of particle sizes probably originating from various strata within the cloud rather than a disproportionately large deposition of a given particle size range originating from a narrow cloud stratum. The lateral extremities of fallout pattern arcs in general were characterized by high percentages of less than 44 micron material; balloon shot arcs, in contrast to

Laboratory measurements of photon emission rates were not initiated sufficiently early for comparison with field dose-rate measurements with the exception of Shot Shasta after H + 10 hours and Smoky after H + 8 hours. The composite laboratory gamma decay curves are superimposed on field dose-rate curves over the appropriate time intervals in Figure 4. 1. The two Shasta curves diverge over the H + 10 to H + 16 hours common time period while the two Smoky curves demonstrate good agreement over the H + 8 to H + 27 hours common time period. While the data are too sparse for firm conclusions, the Smoky curves suggest that dose-rate decline as measured by the ion-chanber of the PRAM may be approximated by laboratory measurements of photon emission decline at least over certain early time periods.

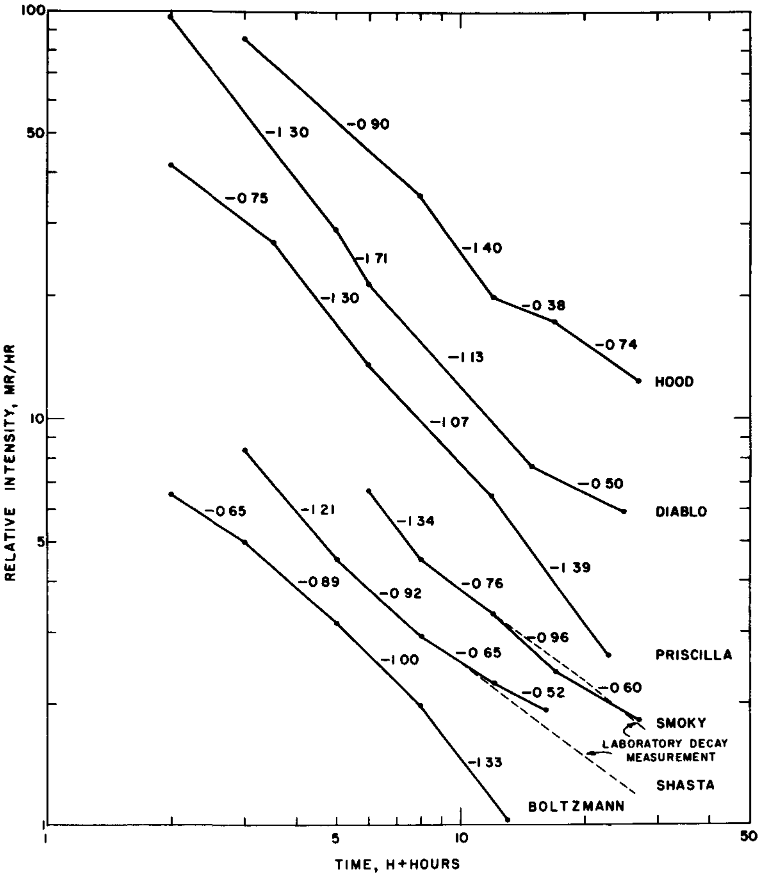

FIGURE 4.1 Mean Gamma Dose-rate Decay of Fallout Produced by Tower and Balloon Mounted Shots Measured in the Patterns by Portable Radiation Recorders.

4 3.1 2 Decay of Different Particle Size Fractions

The results of beta and gamma decay measurements of samples of different particle size ranges collected at the same or nearly the same fallout time are presented in Figures 4.2 (Boltzmann), 4.3 (Priscilla), 4. 4 (Smoky), and 4. 5 (Whitney).

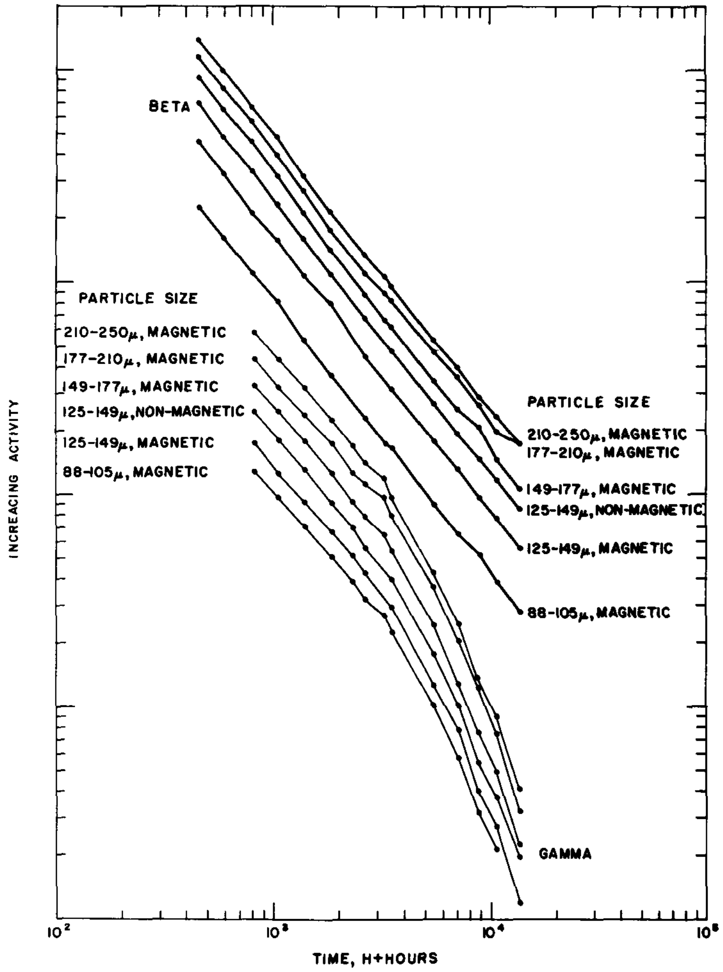

FIGURE 4.2 Beta and Gamma Decay Curves of Boltzmann Fallout of Different Particle Size and Magnetic Properties. (Samples from Stations Having Fallout Time-of-Arrival from 1.4 to 2.7 hours).

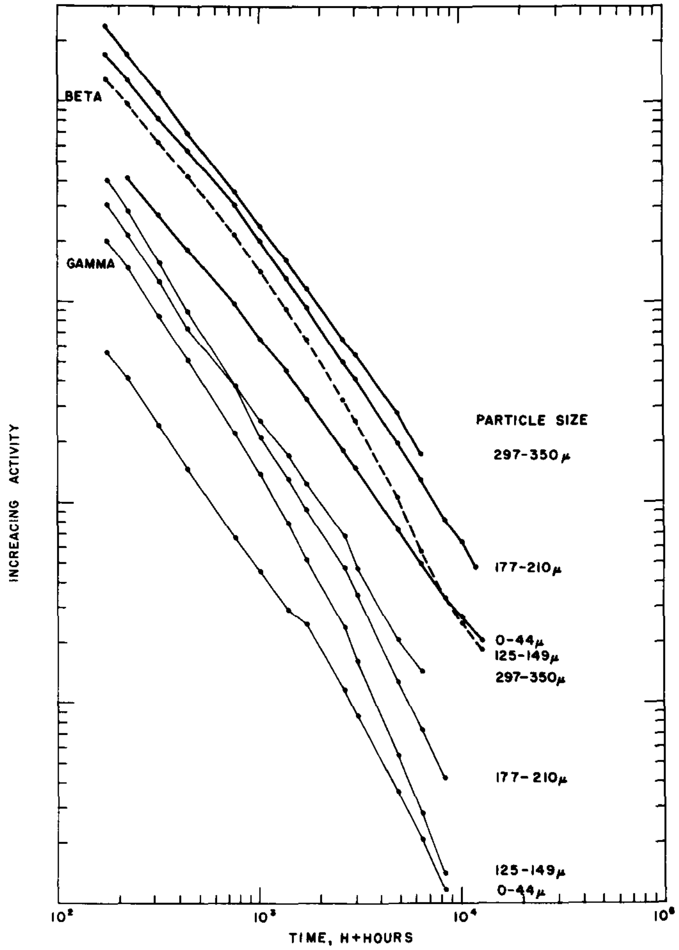

FIGURE 4.3 Beta and Gamma Decay Curves of Priscilla Fallout Material of Four Particle Size Fractions. (Samples from a Station Having Fallout Time-of-Arrival of 2.4 Hours).

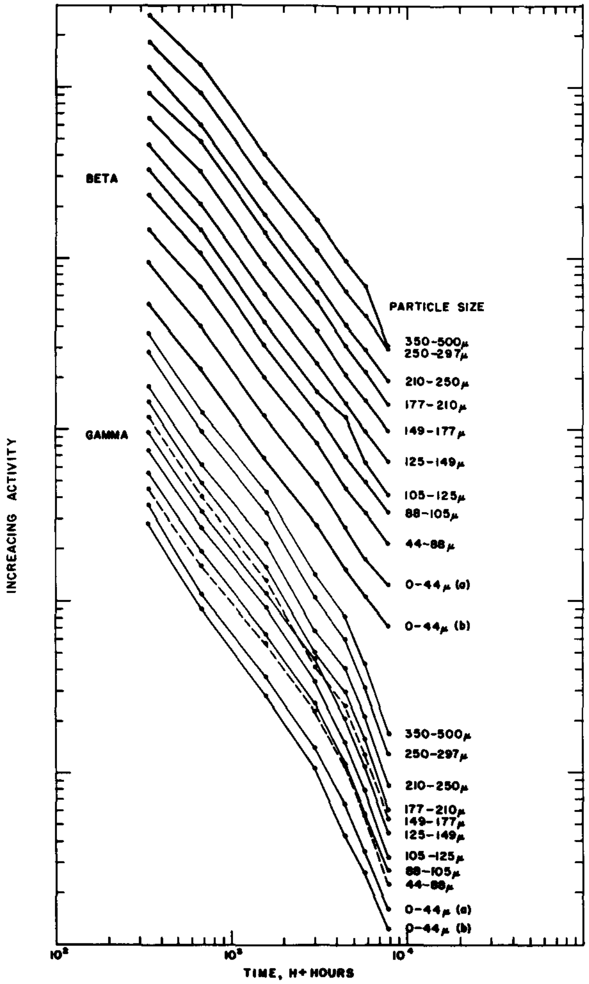

FIGURE 4.4 Beta and Gamma Decay Curves of Smoky Fallout of Eight Particle Size Fractions. (Samples from Station Having Fallout Time-of-Arrival from 0.4 to 1.3 Hours).

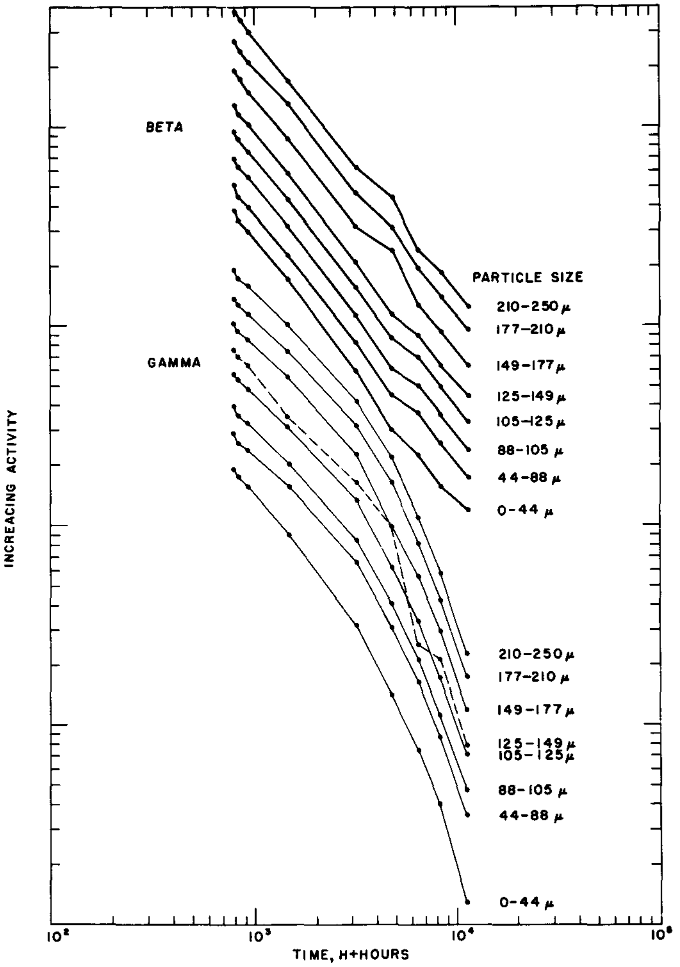

FIGURE 4.5 Beta and Gamma Decay Curves of Whitney Fallout of Different Particle Size Fractions. (Samples from Station Having Fallout Time-of-Arrival of 3 Hours).

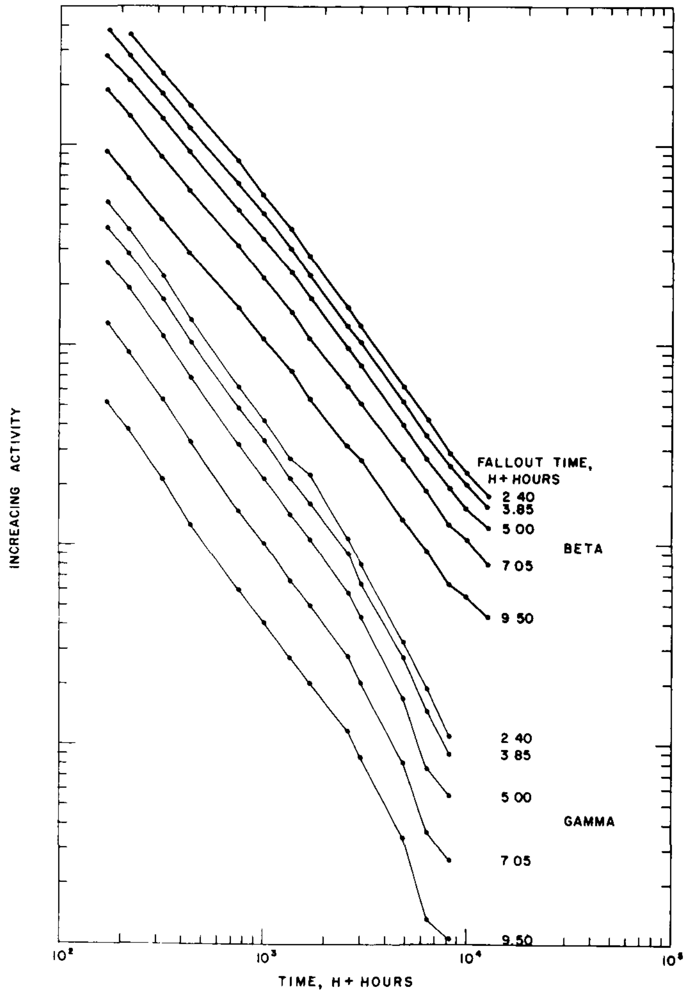

FIGURE 4.7 Comparison of Beta and Gamma Decay curves of < 44 Micron Size Fraction of Priscilla Fallout from Stations at Five Different Times-of-Arrival.

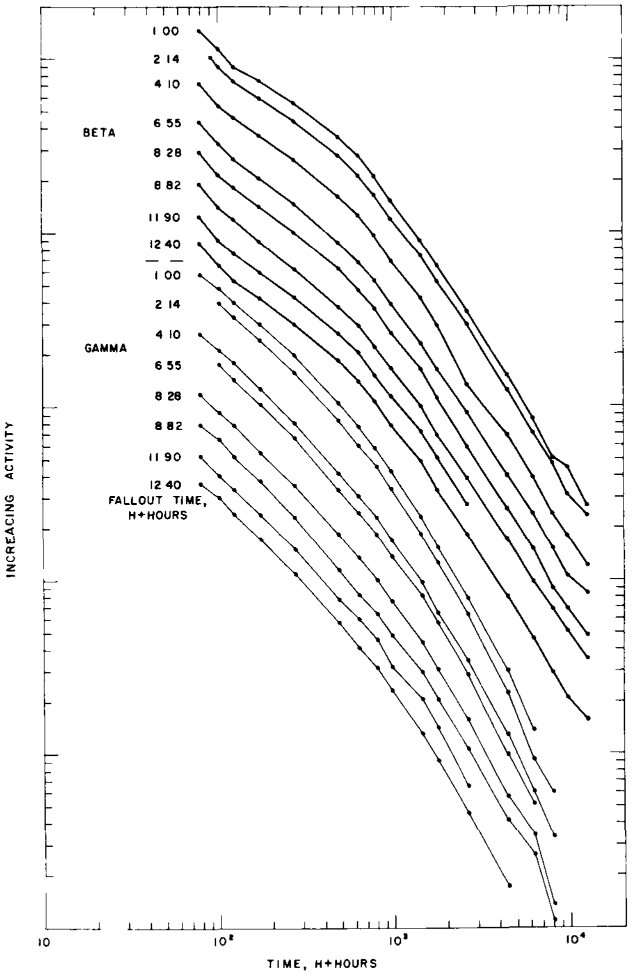

FIGURE 4.8 Beta and Gamma Decay Curves of < 44 Micron Size Fractions of Hood Fallout from Stations at Eight Different Times-of-Arrival.

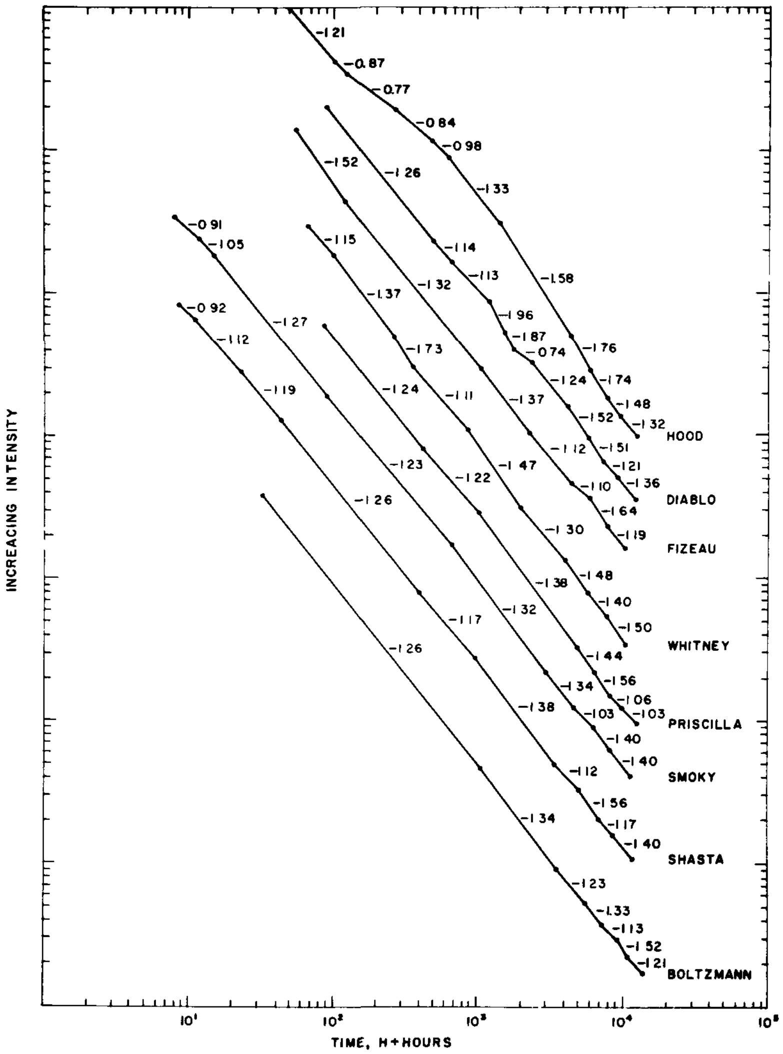

FIGURE 4. 9 Beta Decay Curves of Fallout from Eight Shots.

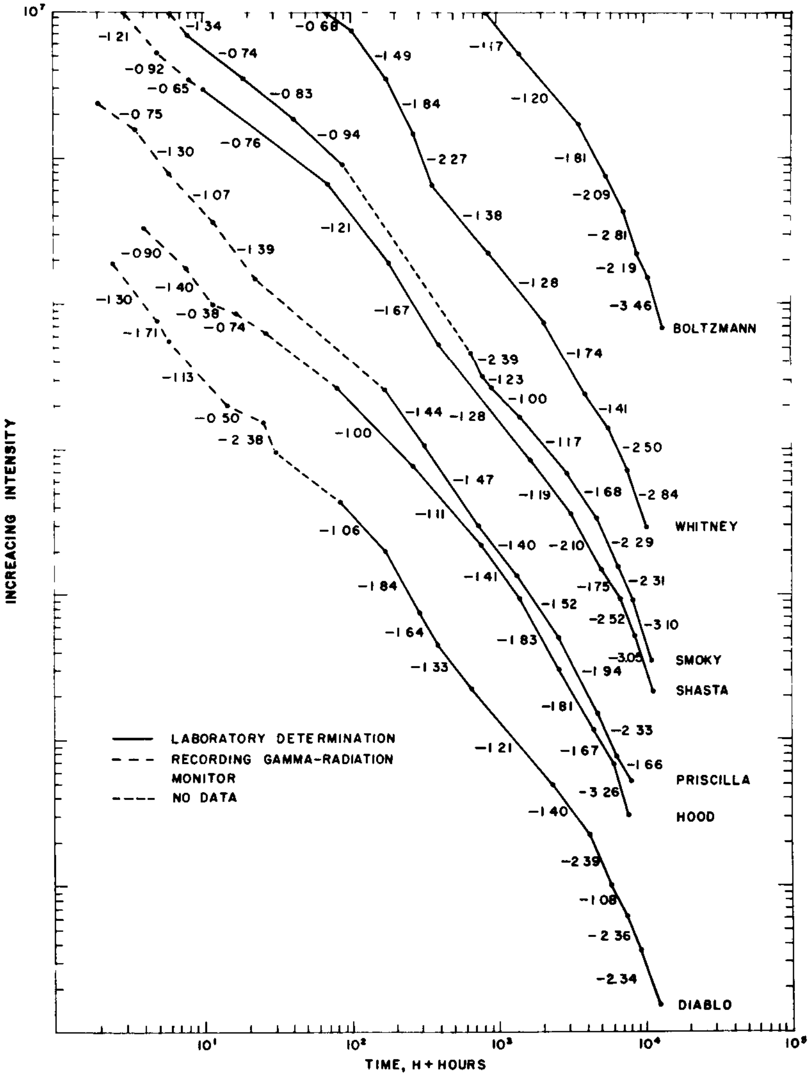

FIGURE 4. 10 Gamma Decay Curves of Fallout from Seven Shots.

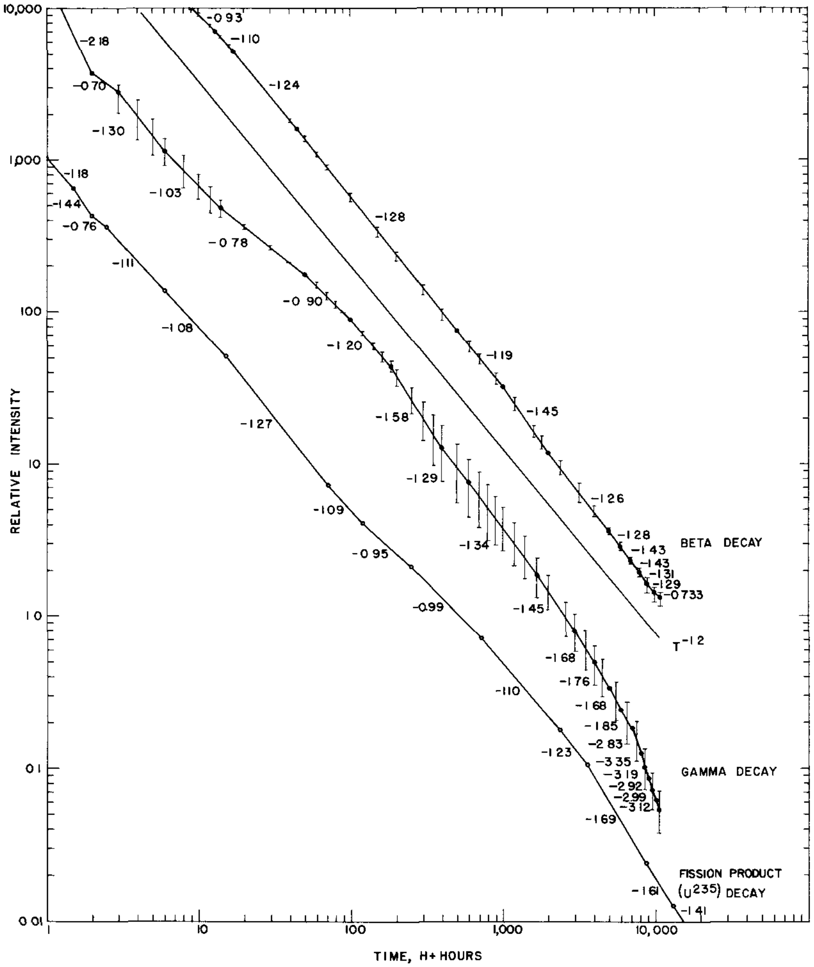

FIGURE 4.11 Plumbbob Composite Beta and Gamma Decay Curves.

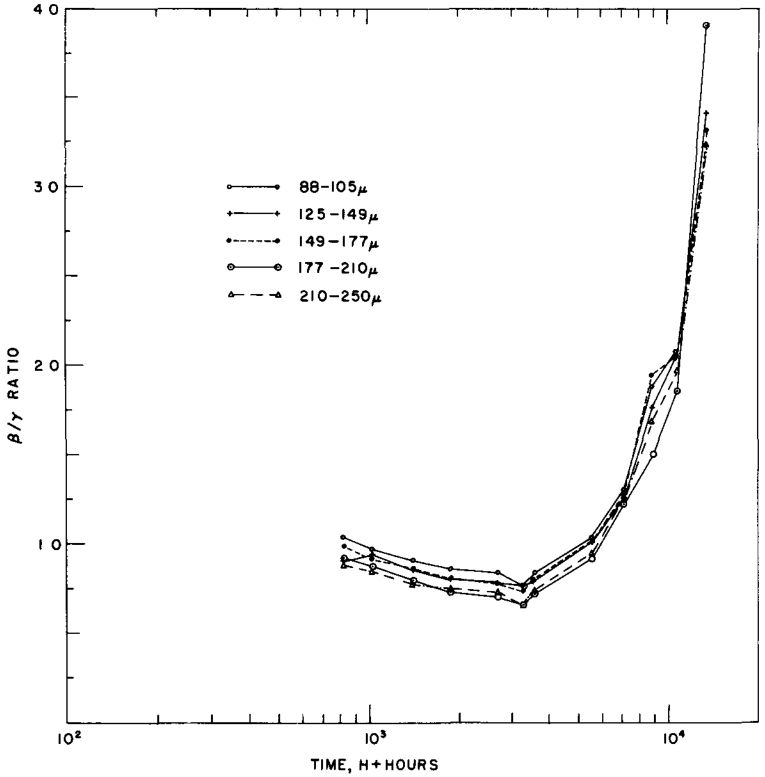

FIGURE 4.12 Comparison of Beta-to-Gamma Ratio Versus Time of Five Particle Size Fractions from Boltzmann Fallout.

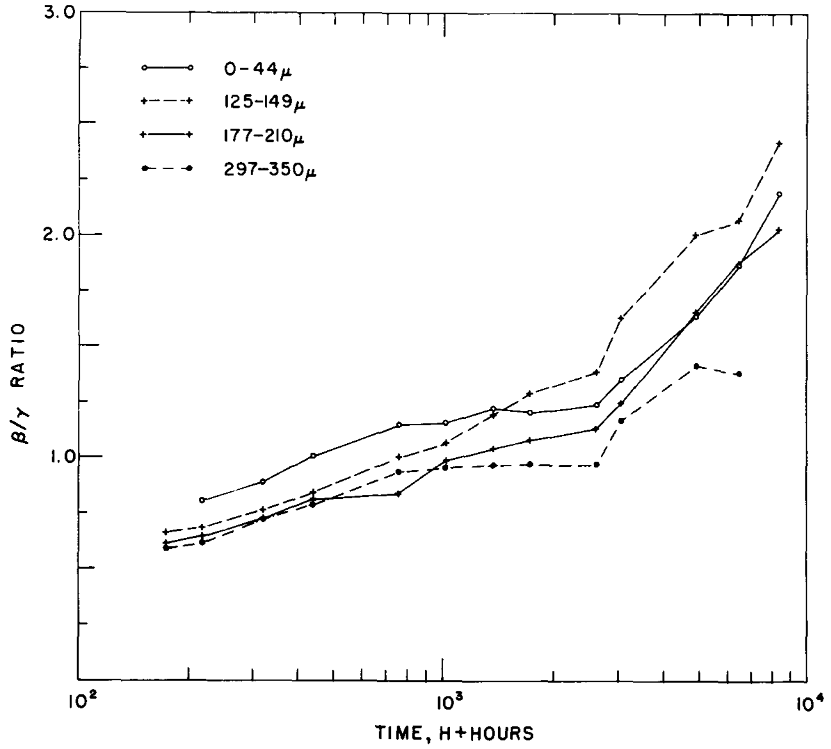

FIGURE 4.13 Comparison of Beta-to-Gamma Ratio Versus Time of Four Particle Size Fractions from Priscilla Fallout.

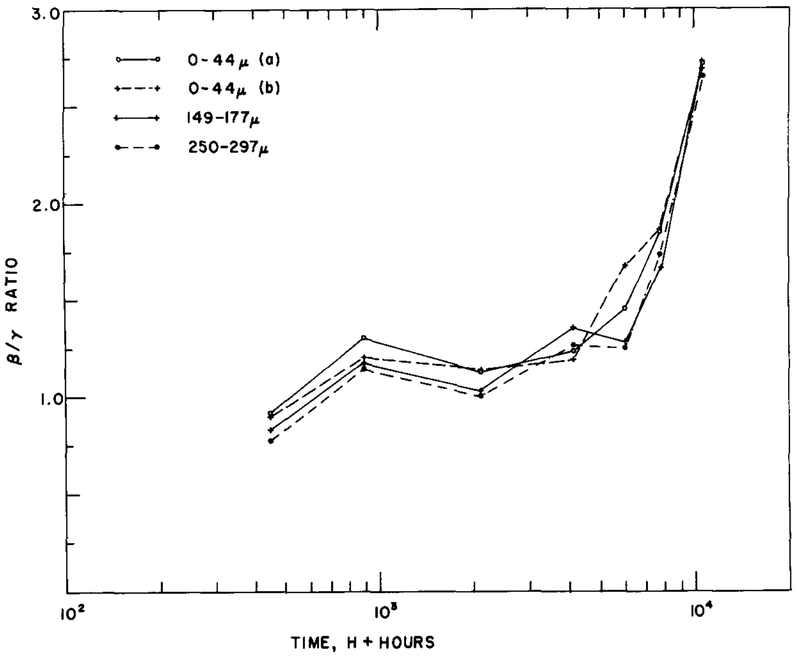

FIGURE 4.14 Comparison of Beta-to-Gamma Ratio Versus Time of Four Particle Size Fractions from Whitney Fallout.

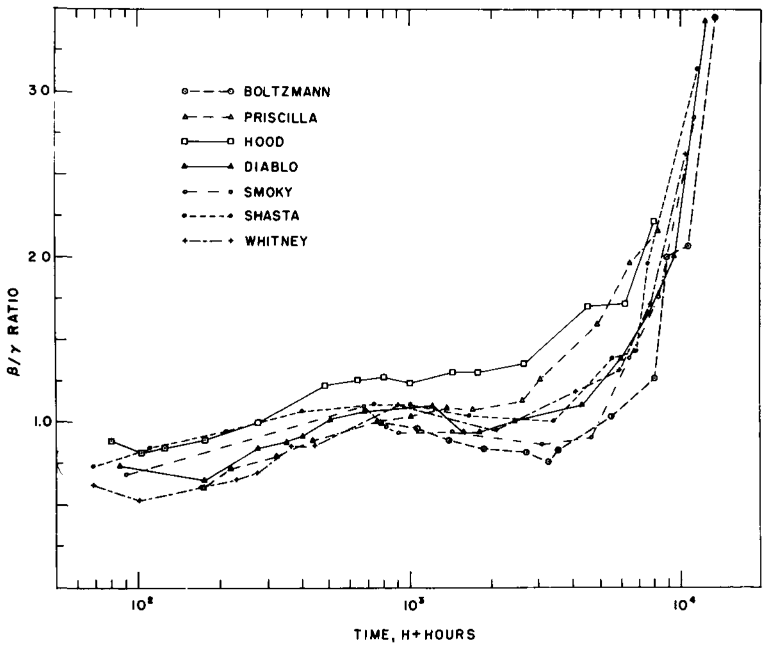

FIGURE 4.15 Comparison of Mean Beta-to-Gamma Ratio Versus Time from Five Tower and Two Balloon Mounted Shots.

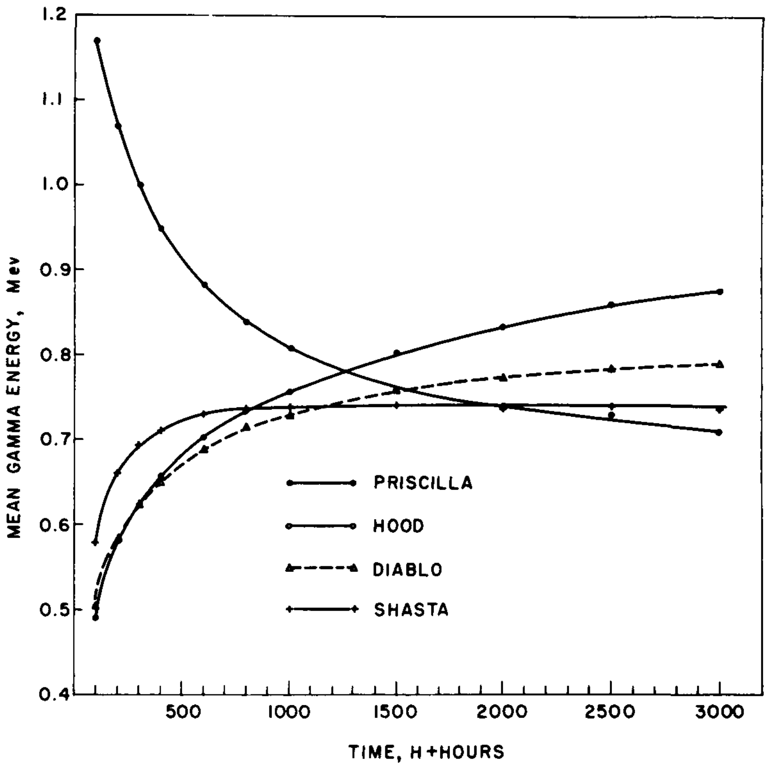

FIGURE 4.16 Mean Gamma Energy of Fallout Samples from Two Tower and Two Balloon Mounted Shots Versus Time After Shot.

contribution of iron from soil materials to the magnetic fraction of fallout apparently was minimal according to measurements made on fallout debris from Shot Priscilla. Its fireball was reported to have not quite intersected the soil surface. Also, it is apparent from these results that this method of analysis will not provide data that permit estimates of how much tower material was vaporized and incorporated in fallout debris.

TABLE 5.1. Beta Activity Magnetically Separated from Fallout Material

	Particle Size Range, Microns	Magnetic Fraction, Pct of Total Beta Activity
Tower Mounted		
Boltzmann	44-300	77.0 ± 4.2
	<44	11.9 ± 5.0
Shasta	44-210	56.1 ± 17.0
	<44	9.2 ± 6.7
Diablo	44-125	80.2 ± 7.2
	<44	6.4 ± 2.8
Smoky	88-250	83.6 ± 8.7
	44-88	80.7 ± 8.0
	<44	46.3 ± 5.5
Balloon Mounted		
Priscilla	<500	<0.2
Hood	<44	<0.1

5.3.2 Solubility

The data concerning the solubility of fallout material derived from Shots Boltzmann, Priscilla, Hood, Diablo, Shasta, and Smoky are given in Appendix E, Table E.2.

5.3.2.1 Solubility Rates

The results of successive one hour water extractions of Priscilla and the magnetic fraction of Diablo fallout size fractions appear in Figure 5.1. The shapes of the Priscilla curves indicate that the cumulative solubility approached its maximum after the fourth extraction The total solubility of fallout debris obtained after the fourth extraction ranged from 45 to 90 percent depending upon the particle size, of those obtained with a single one hour extraction Successive extractions were least effective in removing additional radioactivity from smaller particles, or, in other words the initial extraction removed a greater percentage of the total extractable radioactivity of small particles than of larger particles

The corresponding curves for successive one hour water extractions of Diablo fallout size fractions are more variable in shape, which was probably a result of the low solubility percentages involved (less than 0 6 percent of the total beta activity after the fourth extraction) Cummulative total solubility of fallout debris obtained with the fourth extraction ranged from 20 to 96 percent of those obtained with the single extraction, a range which is not greatly different from those observed with Priscilla samples.

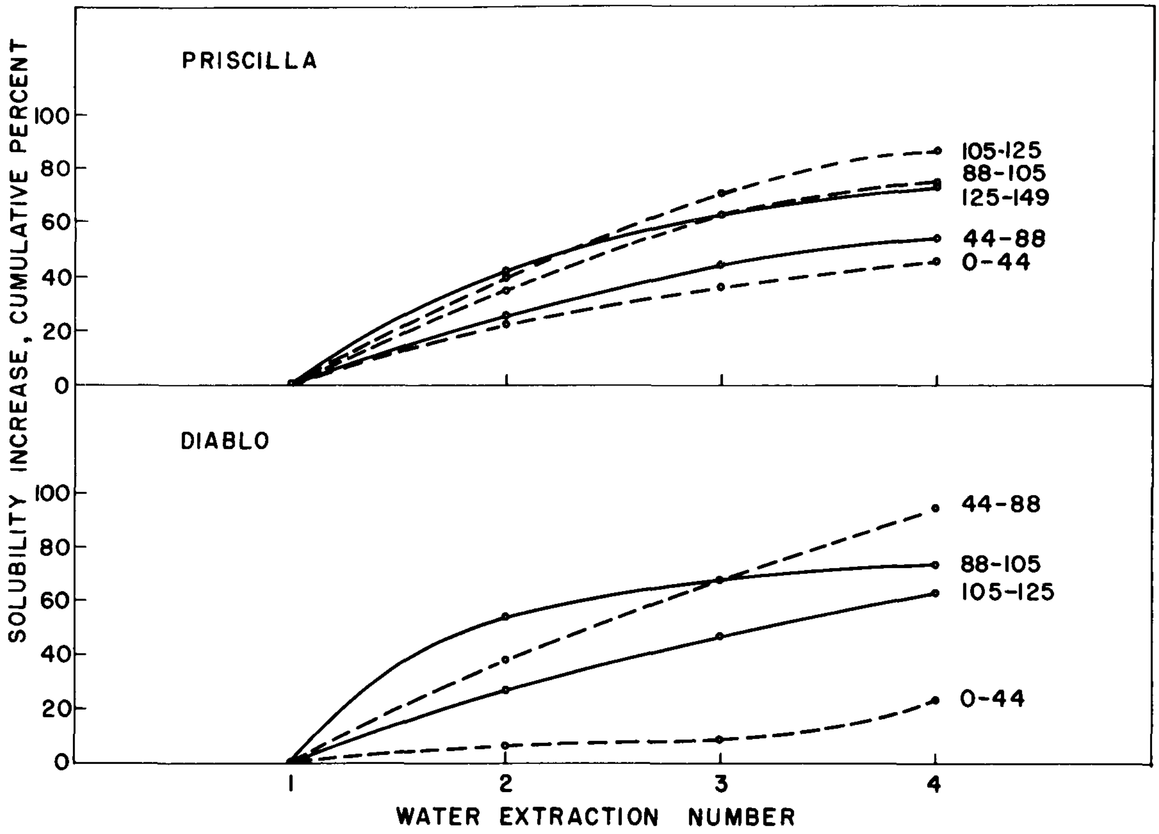

Figure 5.1 Cumulative Increase in Water Solubility of Selected Priscilla and Diablo Fallout Samples as a Function of the Number of Extractions.

The results of successive 0.1 N HCl one hour extractions of Priscilla and Diablo fallout size fractions are presented in Figure 5.2. The shapes of the Priscilla curves indicate that the cumulative solubility was more complete with the fourth acid extraction than with the fourth water extraction. The cumulative solubility of fallout debris obtained after the fourth extraction of Priscilla particles ranged from 10 to 22 percent of those obtained with a single extraction.

The acid-extraction curves of Diablo fallout materials are similar to the water-extraction curves in that the cumulative solubility of fallout debris ranged from 48 to 90 percent of those obtained with a single extraction. The shapes of the curves suggest that, in some cases, continued extraction would have yielded solubility in excess of 100 percent of those obtained with a single extraction. Trends of the effect of particle size on extractability are not apparent.

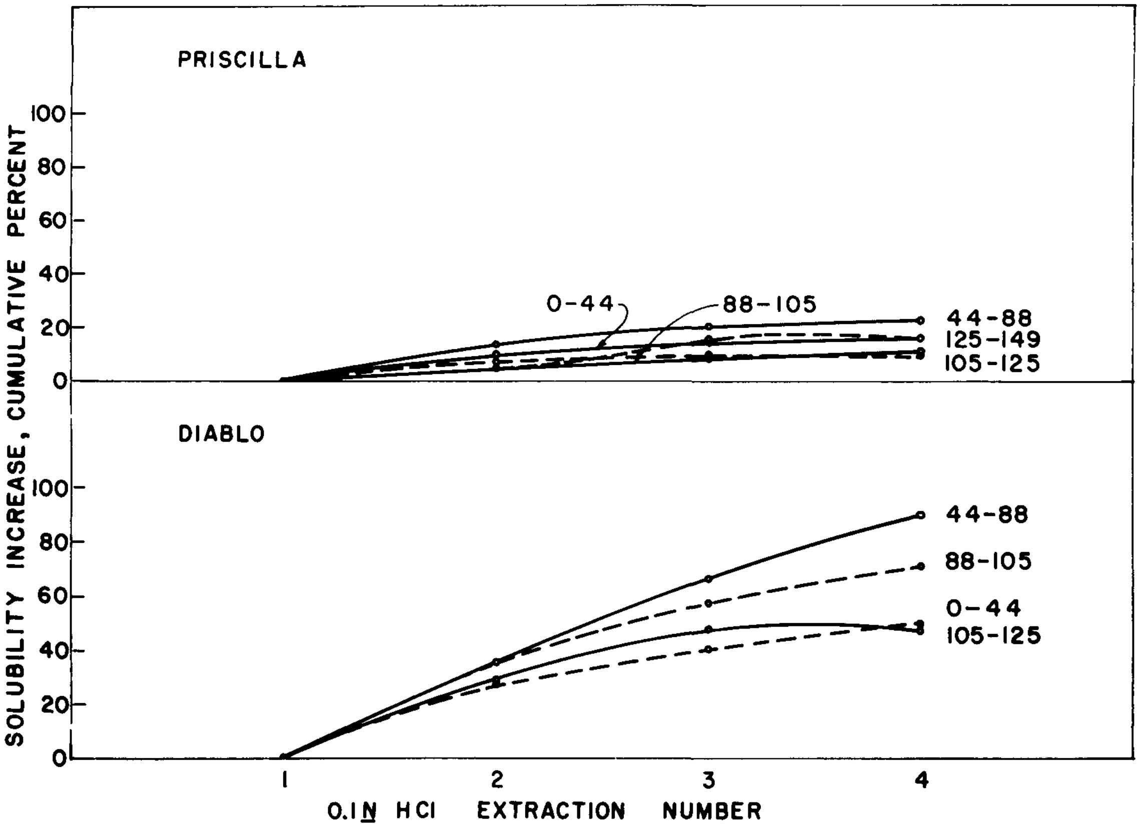

Figure 5.2 Cumulative Increase in HCl solubility of Selected Priscilla and Diablo Fallout Samples as a Function of the Number of Extractions.

5.3.2.2 Solubility of Magnetic versus Nonmagnetic Fractions

Measurements of solubility percentages of magnetic and nonmagnetic fractions of Shasta, Diablo, and Smoky fallout are summarized in Table 5.2. The data indicate that nonmagnetic fallout was 3 to 10 times more soluble in water and 1.3 to 3 times more soluble in 0.1 N HCl than was magnetic fallout.

TABLE 5.2 Solubility of Magnetic and Nonmagnetic Fallout from Tower Mounted Shots

		Solubility Pct of Beta Activity			
		Magnetic		Nonmagnetic	
Shot	Particle Size Range, Microns	H_2O	0.1 N HCl	H_2O	0.1 N HCl
Shasta	44-210	0.08 ± 0.05	3.0 ± 0.9	0.4 ± 0.1	6.7 ± 1.0
	< 44	0.03 ± 0.1	6.9 ± 0.2	1.8 ± 0.2	22.6 ± 3.1
Diablo	44-125	0.2 ± 0.1	3.0 ± 0.7	1.1 ± 0.4	8.2 ± 1.8
	< 44	0.5 ± 0.1	7.1 ± 1.5	1.7 ± 0.6	14.6 ± 2.5
Smoky	88-250	0.2 ± 0.05	19.2 ± 1.6	1.2 ± 0.4	25.7 ± 4.2
	44- 88	0.3 ± 0.05	24.4 ± 5.3	3.3 ± 0.7	43.1 ± 5.0
	< 44	1.0 ± 0.02	29.9 ± 2.9	2.8 ± 0.5	41.8 ± 3.0

5 3. 2. 3 Solubility of Tower and Balloon supported Shot Fallout

The net solubility percentages of different size fractions of fallout from Shots Priscilla, Hood, Boltzmann, Shasta, Diablo, and Smoky, after accounting for the different solubilities of magnetic and nonmagnetic components, are summarized in Table 5 3.

TABLE 5.3 Solubility of Fallout from Tower and Balloon Mounted Shots

Shot	Particle Size Fractions, Microns	Solubility, Pct of Beta Activity H_2O	Solubility, Pct of Beta Activity 0.1 N HCl
Balloon mounted			
Priscilla	297-500	31.3 ±1.2	99.2 ± 3.8
	<297	14 2 ±3.0	65.9 ± 4.5
Hood	< 44	14.5 ±2.3	61.8 ± 4.4
Tower mounted			
Boltzmann[a]	44-300	0.4 ±0.2	5.0 ± 1.2
	< 44	1.2 ±0.4	35.1 ± 8.1
Shasta	44-210	0.2 ±0.1	4.6 ± 0.8
	< 44	1.7 ±0 2	21.1 ± 3.1
Diablo	44-125	0.4 ±0.2	4.0 ± 0.9
	< 44	1.6 ±0.6	14.0 ± 2.4
Smoky	88-250	0.4 ±0.2	20.3 ± 2.0
	44- 88	0.9 ±0.2	28.0 ± 5.3
	< 44	2.0 ±0.4	36.3 ± 3.0

[a] Based on magnetic fallout only.

The data indicate the following observations·

(1) The solubility of tower shot fallout tended to increase with decreasing particle size while the opposite was true of balloon shot fallout

(2) The solubility of tower shot fallout in water was 2 percent or less, depending upon the particle size, the water solubility of balloon shot fallout was approximately 14 percent for the less than 44 micron size fraction, the predominant size

(3) The solubility of tower shot fallout in 0. 1 N HCl was approximately 5 percent for particle sizes greater than 44 microns with the exception of the Smoky fallout which averaged 24 percent solubility in acid. The acid solubility of less than 44 micron fraction tower shot fallout was more variable and ranged between 14 and 36 percent. The acid solubility of balloon shot fallout was of the order of 65 percent for its predominant particle size, less than 44 micron fraction.

5.3.3 Analysis of Fallout Samples for Seven Radionuclides

Samples of different particle sizes derived from the tower mounted Shots Boltzmann, Diablo, Shasta, and Smoky and the Priscilla balloon shot were analyzed for radionuclides of barium, cerium, cesium, ruthenium, strontium, yttrium, and zirconium. The results are reported in terms of percentage of total beta activity at D + 30 days.

Values for specific radioelements were extrapolated from date of analysis to D + 30 days on the basis of experimentally determined decay values. Based upon the experimental decay curves and published values of decay rates, Ba^{140}, Cs^{136}, Sr^{89}, Y^{91}, and Zr^{95} were determined to represent approximately 100 percent of the respective radioelement percentages at D + 30 days. The experimental decay curves of separated cerium and ruthenium indicated that mixtures of these radionuclides were involved in both cases.

Similarities in radioelement percentages were generally observed for particle sizes greater than 88 microns in diameter for individual shots. Consequently, the primary data tabulated in Appendix D have been summarized in succeeding sections in terms of the less than 5 (where analyzed), less than 44, 44-88, and greater than 88 micron size fractions.

5.3.3.1 Radionuclide Analyses of Fallout from Four Tower Shots and Priscilla

The results of radionuclide analyses of tower shot (Boltzmann, Diablo, Shasta, and Smoky) fallout samples are presented in Table 5.4. Fractionation trends with respect to particle size were frequently not certain due to the magnitudes of standard deviation values. However, based on mean values, the data indicate the following observations:

(1) All shots except Boltzmann demonstrated increasing Ba^{140} percentages with decreasing particle size. The average Ba^{140} percentages of the less than 44 micron and the less than 5 micron size fractions were larger than those of the greater than 88 micron material by as much as 22 percent (Smoky) and 50 percent (Smoky, Shasta), respectively.

(2) The average Ce^{141}+$Ce\text{-}Pr^{144}$ percentages tended to decrease with decreasing particle size; Ce^{141}+$Ce\text{-}Pr^{144}$ percentages of the less than 44 micron fraction were as much as 20 percent (Boltzmann, Smoky) less than those of greater than 88 micron fraction.

(3) The Cs^{136} percentages were of the order of 0.2 percent, but extremely low values precluded further analysis.

(4) Radioruthenium values demonstrated the greatest percentage differences among the several tower shots: the Boltzmann $Ru^{103,106}$ percentages were approximately three times greater than those of corresponding particle sizes of the other shots. The $Ru^{103,106}$ percentages tended to increase with decreasing particle size; the less than 44 micron percentages were 50 to 130 percent more than those of the greater than 88 micron material (Smoky, Diablo, Shasta).

(5) $Strontium^{89,90}$ percentages were of the same order of magnitude as those of $Ru^{103,106}$ and demonstrated similar fractionation in favor of the smaller particle sizes. The less than 44 micron fraction percentages were approximately 85 percent more than those of greater than 88 micron material. The $Sr^{89,90}$ percentages of the less than 5 micron fraction were approximately 15 percent more than those of the less than 44 micron fraction of which it is a part.

TABLE 5.4 Radionuclide Content of Fallout Material According to Particle Size Fractions

NS, not significant at time of analysis

	Boltzmann	Diablo	Shasta	Smoky	Priscilla
Particle size, microns	88-149	88-350	88-500	88-1000	88-500
No. of samples used for mean	3	11-12	38-54	37-43	12-14
Radionuclide, Pct of sample beta activity, D + 30 days					
Ba^{140}	15.5 ± 1.8	12.9 ± 1.1	13.0 ± 2.7	11.7 ± 2.6	17.7 + 1.8
$\mathrm{Ce}^{141} + \mathrm{Ce\text{-}Pr}^{144}$	20.9 ± 1.0	17.2 ± 2.8	15.9 ± 2.5	19.4 ± 3.1	16.5 ± 1.9
Cs^{136}	0.24 ± 0.05	0.15 + 0.03	NS	NS	0.08 ± 0.01
$\mathrm{Ru}^{103,106}$	5.2 ± 3.2	1.5 ± 0.2	1.2 ± 0.4	1.3 + 0.5	7.2 ± 3.3
$\mathrm{Sr}^{89,90}$	1.7 0.47	1.3 ± 0.2	1.3 ± 0.4	1.3 ± 0.4	2.8 + 0.3
Y^{91}	9.9 ± 1.1	9.9 ± 1.3	9.6 ± 1.3	10.3 + 1.0	14.7 ± 2.1
Zr^{95}	8.7 ± 1.6	9.0 ± 1.8	7.4 ± 1.2	7.6 ± 0.7	3.8 + 1.3
Pct of total beta activity (Σ)	62	52	49	52	63
Particle size, microns	44-88	44-88	44-88	44-88	44-88
No. of samples used for mean	1	4	10-13	6	5
Radionuclide, Pct of sample beta activity, D + 30 days					
Ba^{140}	14.5	13.1 ± 1.1	12.6 ± 1.3	11.8 ± 1.0	17.3 ± 1.8
$\mathrm{Ce}^{141} + \mathrm{Ce\text{-}Pr}^{144}$	17.7	18.6 ± 5.1	16.9 ± 1.8	18.9 + 4.0	13.1 ± 1.5
Cs^{136}	0.24	0.16 ± 0.04	NS	NS	0.05 ± 0.03
$\mathrm{Ru}^{103,106}$	3.4	1.6 ± 0.3	1.5 ± 0.2	1.3 ± 0.3	9.4 ± 2.7
$\mathrm{Sr}^{89,90}$	1.6	1.5 ± 0.2	1.2 ± 0.2	1.5 ± 0.3	3.8 ± 1.2
Y^{91}	9.1	10.6 ± 1.4	9.2 ± 1.1	10.7 ± 0.8	13.7 ± 4.5
Zr^{95}	9.1	9.1 ± 2.2	7.4 ± 1.0	6.7 + 1.0	3.8 ± 0.6
Pct of total beta activity (Σ)	56	55	49	51	61
Particle size, microns	<44	<44	<44	<44	<44
No. of samples used for mean	3	4	11-15	6	6
Radionuclide, Pct of sample beta activity, D + 30 days					
Ba^{140}	15.1 ± 0.5	14.6 ± 0.8	14.9 ± 1.5	14.3 ± 1.1	18.6 ± 1.9
$\mathrm{Ce}^{141} + \mathrm{Ce\text{-}Pr}^{144}$	16.8 ± 1.4	17.2 ± 2.4	14.9 ± 1.9	16.2 + 1.0	13.4 ± 2.4
Cs^{136}	0.23 ± 0.03	0.16 ± 0.01	NS	NS	0.11 ± 0.03
$\mathrm{Ru}^{103,106}$	6.7 ± 1.5	2.8 ± 0.3	2.8 ± 0.5	2.0 ± 0.3	11.0 ± 1.7
$\mathrm{Sr}^{89,90}$	2.8 ± 1.0	2.4 ± 0.2	2.4 ± 0.5	2.7 ± 0.3	6.4 ± 0.6
Y^{91}	10.3 ± 0.7	11.5 ± 0.6	11.0 ± 1.0	13.1 ± 1.6	13.5 ± 2.3
Zr^{95}	8.0 ± 0.2	7.9 ± 0.9	6.4 ± 0.9	6.3 ± 0.8	4.2 ± 0.4
Pct of total beta activity (Σ)	60	56	52	55	67
Particle size, microns	5	<5	<5	<5	<5
No. of samples used for mean	0	0	4-6	4-6	0
Radionuclide, Pct of sample beta activity, D + 30 days					
Ba^{140}	--	--	19.8	17.3 ± 5.0	--
$\mathrm{Ce}^{141} + \mathrm{Ce\text{-}Pr}^{144}$	--	--	14.1 ± 2.9	16.5 ± 2.7	--
Cs^{136}	--	--	NS	NS	--
$\mathrm{Ru}^{103,106}$	--	--	2.4 ± 0.9	1.5 ± 0.2	--
$\mathrm{Sr}^{89,90}$	--	--	2.8 ± 0.4	3.1 ± 0.3	-
Y^{91}	--	--	10.6 ± 2.3	11.8 ± 2.6	--
Zr^{95}	--	--	6.6 ± 0.3	6.4 ± 0.5	--
Pct of total beta activity (Σ)	--	--	56	57	--

(6) The Y^{91} percentages increased with decreasing particle size in all cases but to quite different degrees. The Sr^{89,90} percentages of the less than 44 micron fraction were more than those of the greater than 88 micron fraction by 4 to 27 percent.

(7) The Zr^{95} percentages decreased with decreasing particle size; the percentages of the less than 44 micron size fraction, 10 to 15 percent, were lower than those of the greater than 88 micron fallout material.

Radionuclide percentages from the balloon mounted Shot Priscilla are also presented in Table 5.4.

The Priscilla radionuclide percentages of Ba^{140}, Ru^{103,106}, Sr^{89}, and Ce^{141}+ Ce-Pr^{144} indicated the same trends of fractionation with respect to particle size as those described above for tower shots. The Ba^{140}, Ru^{103,106}, and Sr^{89} percentages of the less than 44 micron size fraction were 5, 53, and 129 percent, respectively, more than those of the greater than 88 micron fraction. The Ce^{141}+ Ce-Pr^{144} percent of the less than 44 micron fraction was 23 percent lower than that of the largest size group. The Y^{91} and Zr^{95} demonstrated slight fractionation trends opposite to those of tower shots.

Selected particle size fractions, previously analyzed for Sr^{89,90} (total radiostrontium), from various locations within the Diablo, Shasta, and Smoky fallout patterns were analyzed for Sr^{90} content approximately one year following the conclusion of the Plumbbob Test Series. The results of these analyses appear in Table 5.5 in terms of Sr^{90} percentages of total radiostrontium and total beta activity at D + 30 days.

TABLE 5.5 Percentages of Total Radiostrontium and of Total Beta Activity at D + 30 Days.

Size Fraction, Microns	No of Sr^{90} Samples	Pct Sr^{90} of Total Radiostrontium	Pct of Total Beta Activity	
			Total Sr Activity[a]	Sr^{90}
Shot Diablo				
88-500	13	2.7 ±0.55	1.3 ±0.16	0.035
44- 88	4	1.7 ±0.35	1.5 ±0.20	0.026
< 44	8	2.0 ±0.61	2.4 ±0.20	0.048
Shot Shasta				
88-500	6	3.4 ±1.15	1.3 ±0.35	0.044
44- 88	7	3.1 ±0.67	1.2 ±0.23	0.037
< 44	10	2.0 ±0.49	2.4 ±0.50	0.048
Shot Smoky				
88-210	4	2.6 ± 0.85	1.3 ±0.36	0.034
44- 88	5	3.1 ± 1.3	1.5 ±0.27	0.047
< 44	6	3.4 ± 1.6	2.7 ±0.32	0.092
< 5	5	3.5 ±1.6	3.1 +0.27	0.11

[a] Mean values from Table 5.4

Fractionation of Sr^{90} with respect to particle size was not detectable with the possible exception of Smoky samples where mean Sr^{90} percentages of total beta activity increased as particle size decreased. Strontium ^{90} percentages of total radiostrontium, however, are associated with relatively high standard deviation values; and fractionation trends with respect to particle size are more reliably indicated for total radiostrontium, which was primarily Sr^{89} at D + 30 days.

5.3.3.2 Tower versus Balloon Shot Radionuclide Percentages

Similar percentage values for specific radionuclides among the same size fractions of the different tower shots permit the determination of mean percentage values descriptive of tower shots in general. These values, derived from the data appearing in Table 5.4 are presented in Figure 5.3 in conjunction with the radionuclide percentages of Priscilla fallout samples.

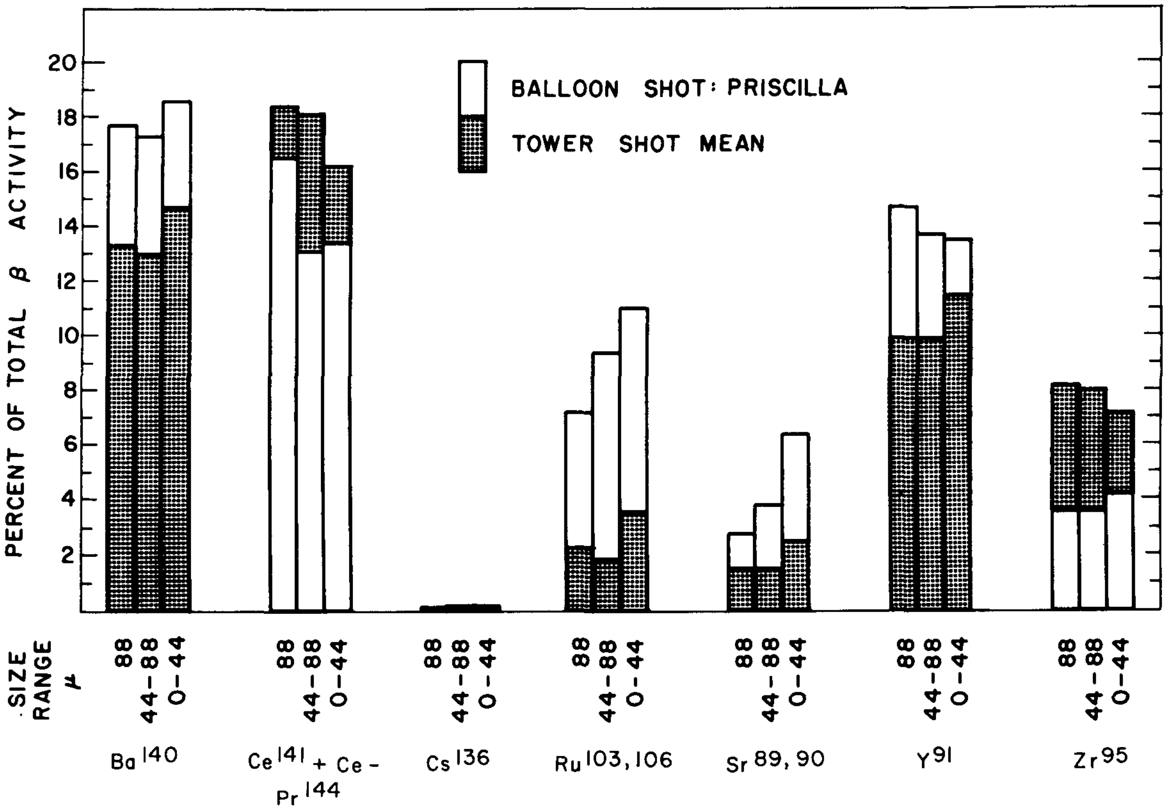

Figure 5.3 Comparison of Radionuclide Percentages of Different Particle Size Fractions of Tower and Balloon Shot Fallout.

The comparison of mean tower shot percentages to those of Shot Priscilla indicates that for corresponding size fractions: Priscilla radionuclide percentages were approximately 30 percent higher for Ba^{140}; 11 to 38 percent higher for Ce^{141}+Ce-Pr^{144}; 300

to 400 percent higher for Ru^{103,106}; 250 percent higher for Sr^{89}; 20 to 50 percent higher for Y^{91}; and 50 percent lower for Zr^{95} than the corresponding percentages of tower shots.

5.3.4 Physical Characteristics

The shape of all fallout particles observed tended to be spherical with frequent protrusions. Examples of particles larger than 88 microns in diameter from Shots Hood, Priscilla, Diablo, and Shasta appear in Figure 5.4. Examples of particles less than 44 microns in diameter from the Boltzmann shot appear in Figure 5.5 in conjunction with ground zero soil material of the same size fraction. Spherical particles as small as several microns in diameter were detectable in contrast to the predominantly angular particles of ground zero soil.

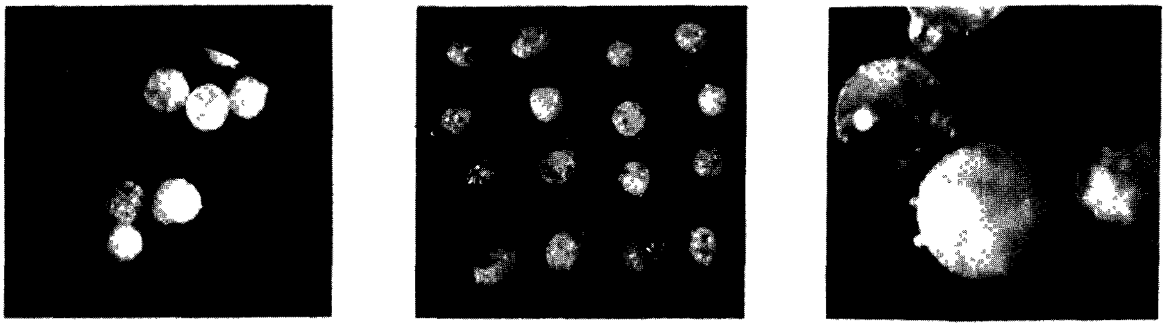

BALLOON (HOOD), 350-500 u TRANSLUSCENT

BALLOON (HOOD), 350-500 u TRANSLUSCENT

BALLOON (PRISCILLA), 350-500 u TRANSLUSCENT

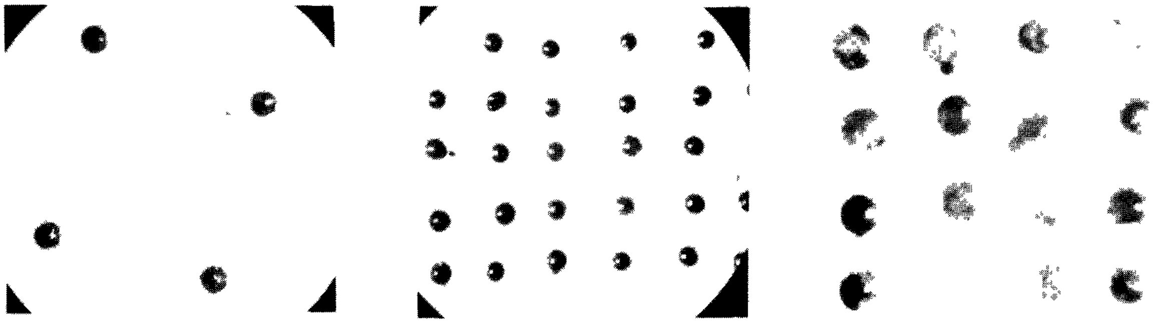

TOWER (DIABLO), 105-125 u OPAQUE

TOWER (SHASTA), 88-105 u OPAQUE

TOWER (SHASTA), 105-125 u TRANSLUSCENT

Figure 5.4 Examples of Translucent and Opaque Fallout Particles from Tower and Balloon Shots.

Particles orginating from Shots Diablo and Shasta demonstrated two general appearance groups; those which were opaque and those which were transparent or translucent (Figure 5.4). Opaque particles varied in color from black to dark red with smooth, highly vitreous to rough, lusterless surfaces. Transparent and translucent particles were generally colorless with smooth, vitreous surfaces. These particles generally contained large numbers of internal bubbles.

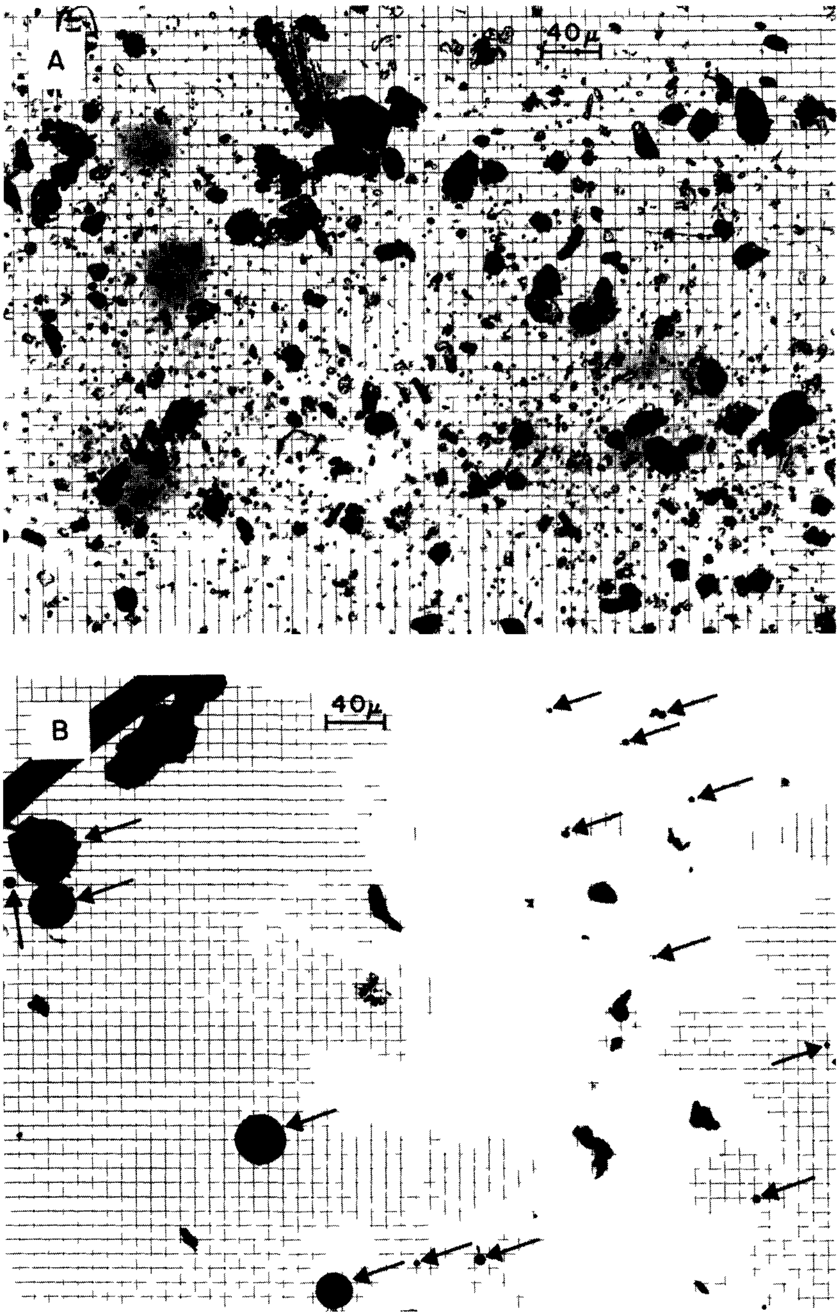

Figure 5.5 Particles less than 44 microns in Boltzmann surface ground zero soil (A) and Boltzmann fallout samples (B) from about 80 miles from ground zero. One grid unit equivalent to ten microns. (Photographs by LRL).

The distribution of the various types of opaque as well as transparent particles was determined for a Diablo fallout area by classifying all particles in successive microscope fields. The results appear in Table 5.6. Opaque particles comprised 70 percent or more of the total number of radioactive particles. The predominance of opaque particles in tower shot fallout materials in general was estimated by a less precise inspection of samples from other tower shots.

TABLE 5.6 Particle Distribution According to Appearance and Size

Particles collected at GC Station 14.2 miles from ground zero, 5.8 miles east of midline, Shot Diablo

Particle Appearance	Particle Size Range, microns										
	1000-500	500-350	350-297	297-250	250-210	210-177	177-149	149-125	125-105	105-88	88-44
	Pct of Number of Particles Observed per Size Range										
Opaque											
black, rough	31.1	62.1	67.4	48.6	44.3	38.2	58.3	42.0	44.1	62.6	42.0
black, smooth	23.4	0.0	17.4	14.9	9.8	16.7	15.3	11.5	12.5	10.5	21.7
dark red	33.8	32.2	13.0	33.8	31.2	23.5	19.4	16.0	26.5	23.4	26.1
SUBTOTAL	88.3	94.3	97.8	97.3	85.3	78.4	93.0	69.5	83.1	96.5	89.8
Transparent	1.3	3.4	0.0	0.0	9.8	6.9	1.4	13.5	9.3	0.6	5.8
Other	10.4	2.3	2.2	2.7	4.9	14.7	5.6	17.0	7.6	2.9	4.4

In contrast to tower shot fallout, inspection of fallout materials derived from the balloon mounted Shots Priscilla and Hood indicated that transparent or translucent particles comprised virtually 100 percent of the particles present (Figure 5.4). The particles were generally characterized by internal gas bubbles.

5.3.5 Specific Activity per Particle

The different types of opaque particles and transparent particles collected at different locations within the Diablo and Shasta fallout patterns were isolated and analyzed for beta radioactivity. The particles were analyzed in groups and values of the mean activity per particle were determined. The mean values, thus obtained, were variable; and no consistent relationships were observed among the different types of opaque particles or with respect to fallout time-of-arrival. However, differences were detected between the opaque particles as a group and the transparent particles. Table 5.7 summarizes the results of analysis of the two types of particles as a function of particle size for particles produced by Shots Diablo and Shasta. The mean values presented are weighted on the basis of the number of particles per particle group.

The values of the mean radioactivity per particle of opaque Diablo particles do not demonstrate a definitive reduction with particle size, with the possible exception of the 44-88 micron size fraction. Particle sizes from 2000 to 88 microns averaged 1.06 microcuries per particle at H + 12 hours and the 44-88 micron size range averaged 0.31 microcuries per particle at H + 12 hours. Transparent particles averaged 0.19 microcuries per particle or approximately 20 percent of the particle activities of opaque particles.

Opaque Shasta particles in the size range of 250 to 44 microns averaged 0.49 µc per particle at H + 12 hours. Transparent particles averaged 0.17 µc per particle or approximately 35 percent of the particle activities of opaque particles.

TABLE 5.7 Radioactivity Per Particle of Different Particle Size Fractions

Size Fraction Microns	Total No. of Particles	No. of Particle Groups	Beta µc/particle, H + 12 hours Range	Mean
Shot Diablo: Opaque Particles				
2000-1000	40	4	0.527-0.994	0.832
1000- 500	29	3	1.056-1.372	1.18
500- 350	20	2	0.846-1.018	0.932
350- 297	16	3	0.736-1.469	1.301
297- 250	23	3	0.850-1.629	1.292
250- 210	22	3	1.029-1.091	1.064
210 177	28	3	0.891-1.013	0.943
177- 149	23	5	0.319-1.170	0.786
149- 125	49	9	0.155-1.062	0.695
125- 105	77	14	0.086-2.941	1.18
105- 88	72	8	0.623-2.228	1.43
88- 44	58	6	0.122-0.613	0.306
Shot Diablo: Transparent Particles				
2000-1000	8	1	0.258	0.258
1000- 500	1	1	--	0.051
250- 210	2	1	0.143	0.143
210- 177	3	1	0.0163	0.016
177- 149	1	1	--	0.232
149- 125	13	2	0.0505-0.233	0.205
125- 105	20	2	0.140 -0.567	0.354
105- 88	2	1	0.382	0.382
88- 44	11	1	0.0452	0.045
Shot Shasta: Opaque Particles				
250-210	12	1	--	0.370
210-177	26	4	0.230-1.69	0.506
177-149	52	2	0.560-0.579	0.570
149-125	55	3	0.335-0.549	0.483
125-105	129	7	0.260-1.45	0.517
105- 88	617	14	0.313-0.965	0.585
88- 44	4751	24	0.163-0.706	0.400
Shot Shasta: Transparent Particles				
149-125	63	1	--	0.176
125-105	34	3	0.101-0.304	0.243
105- 88	213	5	0.112-0.244	0.176
88- 44	526	7	0.075-0.146	0.099

5.4 DISCUSSION

5.4.1 Comparison of Deposition of Soluble Radionuclides by Shots Priscilla and Smoky

The net effect of differential fallout levels, degree of solubility, and radionuclide percentages of tower and balloon shot fallout upon potential biological availability at different fallout times may be estimated on the basis of values reported in previous sections of this chapter.

Shots Smoky and Priscilla are most appropriate for comparison of the two types of detonation since they were detonated at the same height and had similar yields. The comparison can be further simplified by considering only the less than 44 micron size fraction on the basis that this particle size is the most widely distributed and potentially the most important with respect to biological accumulation.

In the case of equal radioactivity levels of the less than 44 micron Smoky and Priscilla fallout, approximations of the relative amounts of radionuclides of barium, cerium, ruthenium, strontium, yttrium, and zirconium, as of D + 30 days, in the original, acid-soluble and water-soluble forms may be obtained by multiplying the solubility percentages of Table 5.3 by the radionuclide percentages of Table 5.4. This treatment of these data assumes minimal radioelement fractionation among the initial or untreated fallout and water and acid extracts. The results are illustrated in Figure 5.6. The calculated values indicate that acid-soluble radionuclides derived from the Priscilla less than 44 micron fallout exceed those from Smoky by factors ranging from slightly in excess of 1 to approximately 10. Water-soluble radioelements derived from Priscilla fallout exceed those from Smoky by factors ranging from approximately 5 to 40.

Where equal radioactivity levels of the less than 44 micron fallout are considered, the greater amounts of soluble radionuclides derived from Priscilla fallout in comparison to those from Smoky, are opposed by higher fallout levels from Shot Smoky at different fallout times. The integrated total and the less than 44 micron fallout levels presented for the two shots in Figure 3.14 are compared in Figure 5.7 in terms of ratios of Smoky and Priscilla fallout as a function of fallout time. The levels of fallout of all sizes from Shot Smoky exceeded those from Shot Priscilla by factors in excess of 20 for fallout times-of-arrival up to 15 hours; the levels of less than 44 micron fallout from Shot Smoky exceeded those from Shot Priscilla by factors of approximately 8 to 13.

Based on the ratios appearing in Figures 5.6 and 5.7, the relative levels of the various radionuclides in the initial or untreated form, and in the acid- and water-soluble forms derived from the less than 44 micron Smoky and Priscilla fallout can be estimated for the various fallout times. Examples of such calculations appear in Figures 5.8 and 5.9 for Ba^{140} and Sr^{89}, respectively. The amounts of total Ba^{140} and Sr^{89}, and acid-soluble Ba^{140} and Sr^{89} to a less degree, derived from Smoky less than 44 micron fallout considerably exceed those from Shot Priscilla over the 1 to 15 hour fallout time period. However, the amounts of water-soluble Ba^{140} derived from Shot Smoky only slightly

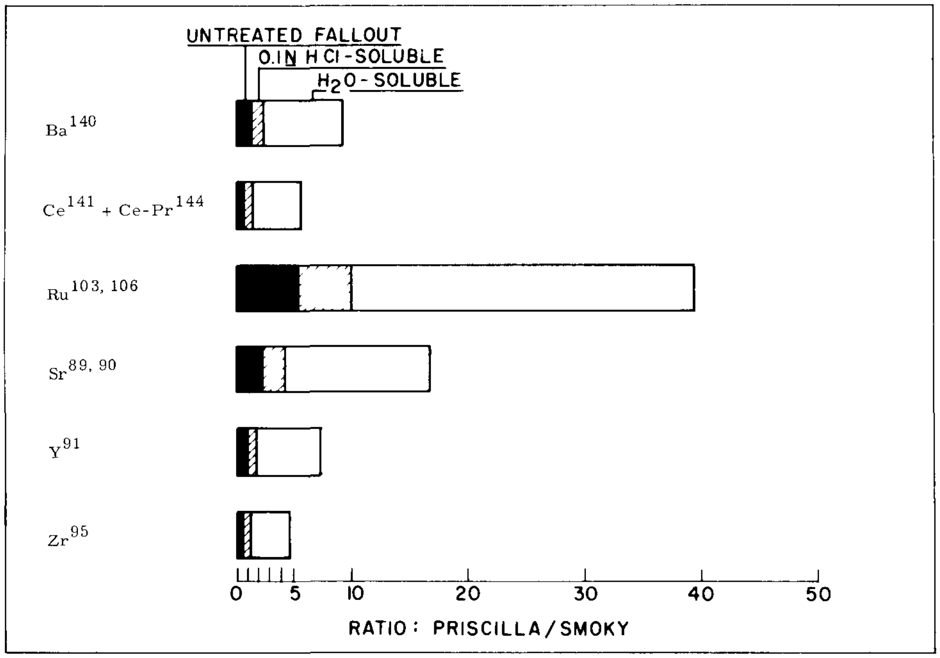

Figure 5.6 Priscilla-to-Smoky Radionuclide Ratios (D + 30 days) in Untreated, Acid-Soluble, and Water-Soluble Fractions of Less Than 44 Micron Diameter Fallout Particles.

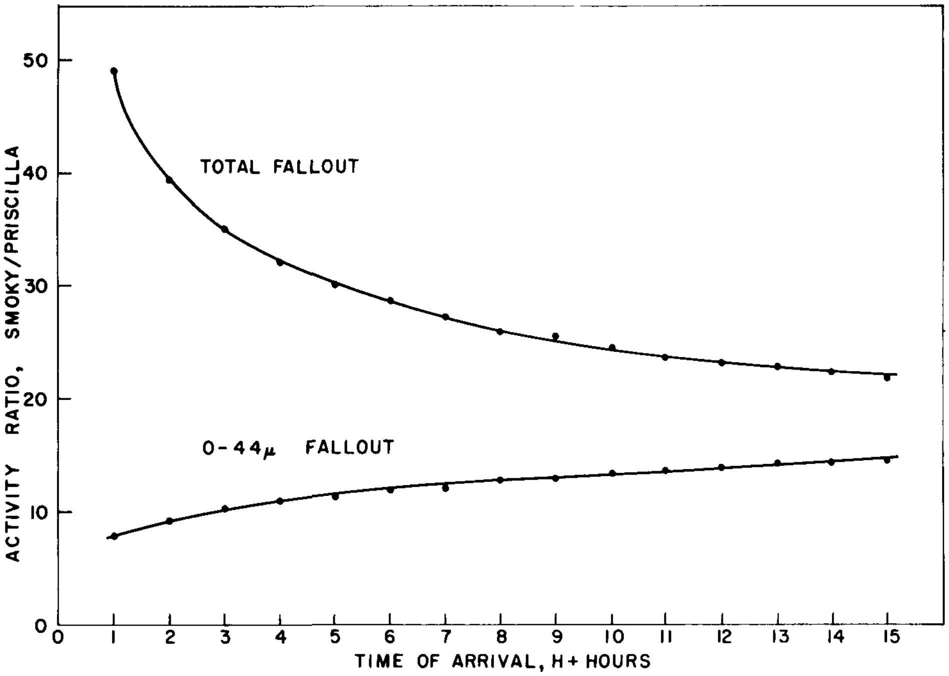

Figure 5.7 Smoky-to-Priscilla Activity Ratios Versus Various Fallout Times-of-Arrival.

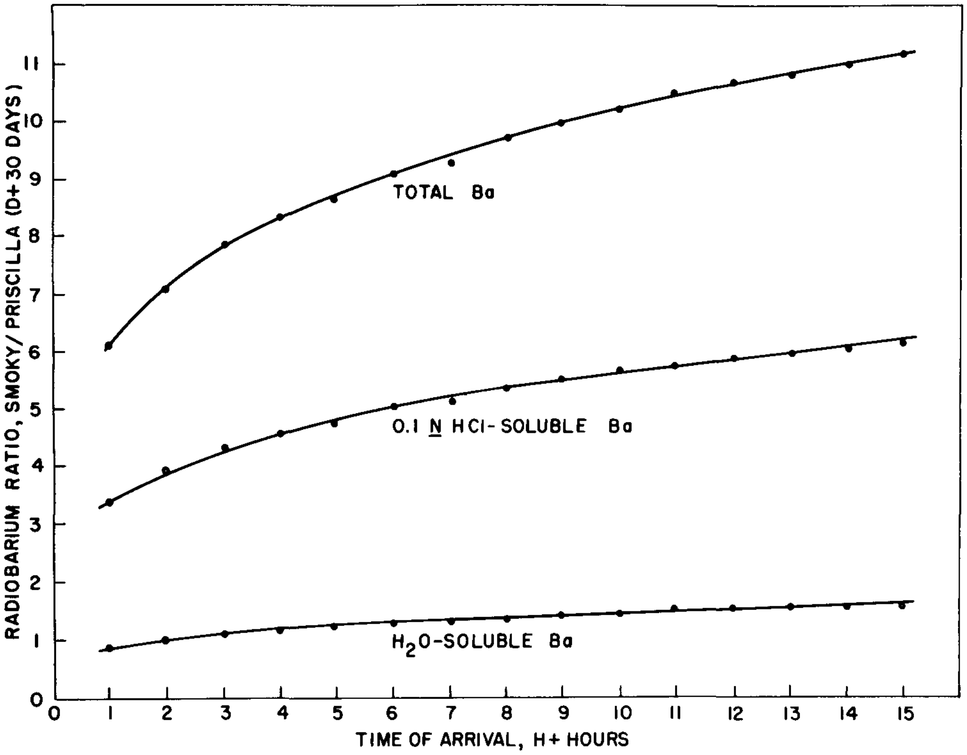

Figure 5.8 Calculated Smoky-to-Priscilla Total, Acid-Soluble, and Water-Soluble Less Than 44 Micron Fallout Ba^{140} Ratios at Various Times-of-Arrival.

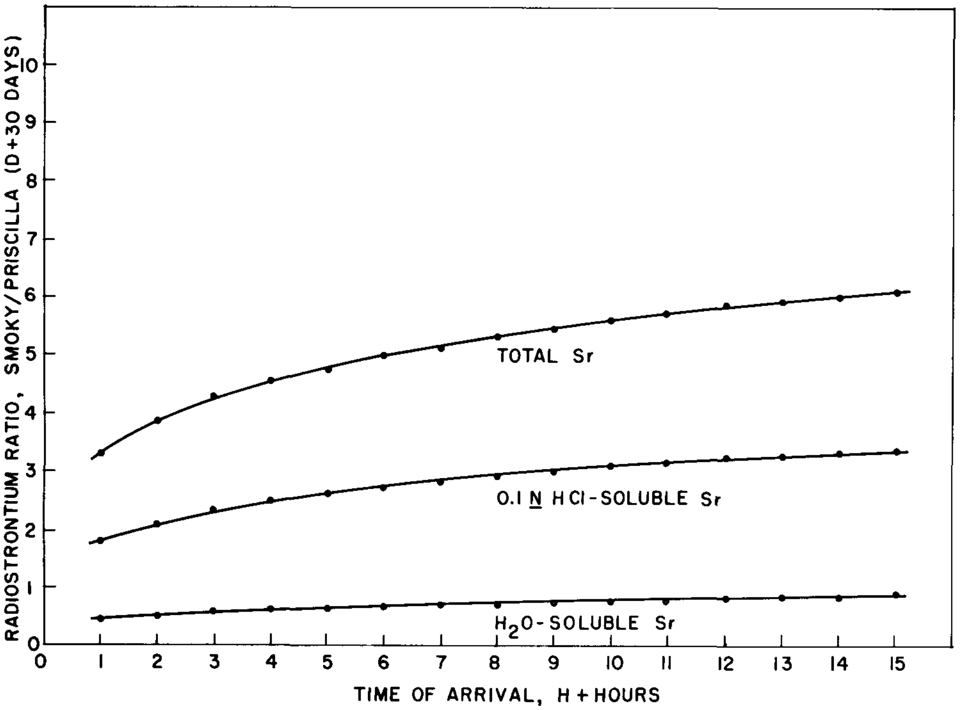

Figure 5.9 Calculated Smoky-to-Priscilla Total, Acid-Soluble, and Water-Soluble Less Than 44 Micron Fallout Sr^{89} Ratios at Various Times-of-Arrival.

exceed those from Shot Priscilla, and more water-soluble Sr^{89} occurs over the 15 hour fallout period due to Shot Priscilla than to Shot Smoky.

The above examples support the assumption that total fallout radioactivity levels may be poor indicators of potential biological accumulation of fission products derived from fallout debris depending upon the applicability of water and 0.1N HCl extractions as indices of biological availability. If such indices are applicable, low radiation levels of balloon shot fallout may result in equivalent or greater biological uptake than the higher levels of tower shot fallout.

5.4.2 Close-in Deposition of Sr^{89} and Sr^{90} by Plumbbob Shots

On the basis of data reported elsewhere in this report, the amounts of Sr^{89} and Sr^{90} deposited in close-in fallout (one mile from ground zero to the distance at which fallout arrived at H + 12 hours) in relation to those amounts available for deposition at greater distances may be estimated for several Plumbbob detonations.

The calculations for each shot were based on (1) total fallout levels from one mile from ground zero to H + 12 hour fallout time in terms of (mr/hr) (mi^2) at H + 12 hours; (2) mean μc/sq ft : mr/hr ratios at H + 12 hours (Chapter 2); (3) mean Sr^{89} percentages of total beta activity of different particle size fractions at D + 30 days (Figure 5.3) weighted according to the distribution of greater and less than 44 micron size fractions in tower shots and the Priscilla balloon shot (Chapter 3); (4) mean Sr^{90} percentages of total beta activity assuming no particle size fractionation (Table 5.5); (5) Sr^{89} and beta activity extrapolations from D + 30 days to H + 12 hours on the basis of 53 day half-life and the composite Plumbbob beta decay curve (Figure 4.11), respectively; (6) production of one gram or 2.77×10^4 curies of Sr^{89} per kt, and (7) production of 1.14 grams or 146 curies of Sr^{90} per kt (U^{235}) (References 1 and 2).

The relative amounts of Sr^{89} and Sr^{90} deposited within the limits of one mile from ground zero and H + 12 hour fallout time appear in Table 5.8. Tower mounted shots deposited maximums of two percent of the total Sr^{89} and seven percent of the total Sr^{90} theoretically assumed to be produced; balloon mounted shots deposited a maximum of 0.1 percent of the total Sr^{89} produced. Consequently, in excess of 90 percent of the $Sr^{89,90}$ produced by the tower and balloon mounted shots for which measurements were made was associated with fallout occurring at fallout times greater than H + 12 hours.

TABLE 5.8 Estimated Sr^{89} and Sr^{90} Deposition from one Mile from Ground Zero to Fallout Arrival Time of H + 12 Hours

Shot	Yield, kt	H + 12 hours Distance, Miles	Pct Deposited	
			Sr^{89}	Sr^{90}
Tower mounted Shots				
Fizeau	11	160	0.4	1.6
Galileo	11	83	0.8	2.8
Boltzmann	12	213	1.8	6.3
Shasta	17	150	2.1	7.2
Diablo	17	146	1.2	4.3
Whitney	19	87	1.6	5.7
Smoky	44	238	1.7	6.0
Balloon mounted Shots				
Wilson	10	92	0.04	--
Newton	12	200	0.004	--
Priscilla	37	260	0.13	--
Hood	74	365	0.008	--

5.5 SUMMARY

(1) Balloon mounted shot fallout was essentially non magnetic. In contrast, tower mounted shot particle sizes larger than 44 microns were 56 to 84 percent magnetic; particles less than 44 microns were of the order of 10 percent magnetic with the exception of Shot Smoky where the magnetic fraction was 46.3 percent.

(2) Successive one-hour exposures to 10 ml of water indicated that the total water-soluble radioactivities removed by four extractions of the Priscilla and Diablo fallout were 45 to 90 and 20 to 96 percent larger, respectively, than those removed by single extractions. Four successive extractions of Priscilla and Diablo fallout each with 10 ml of 0.1 N NCl produced total acid-soluble radioactivities which were 10 to 22 and 48 to 90 percent larger, respectively, than those obtained by single extractions.

Based on single extractions: (a) Tower mounted shot nonmagnetic fallout was 3 to 10 times more soluble in water and 1.3 to 3 times more soluble in 0.1 N HCl than magnetic fallout; (b) solubility of tower mounted shot fallout in water or acid increased with decreasing particle size, and the reverse was true of balloon mounted shot fallout; (c) the water solubility of tower mounted shot fallout was 2 percent of the total beta radioactivity or less and that of balloon mounted shot fallout was 14 percent for the predominant less than 44 micron particle size; (d) the 0.1 N HCl solubility of tower mounted shot fallout was 5 percent for sizes greater than 44 microns (except for 24 percent of Smoky fallout) and 14 to 36 percent for less than 44 micron particle size; the 0.1 N HCl solubility of balloon mounted shot fallout was 65 percent of the total beta radioactivity for less than 44 micron particle sizes.

(3) Radiochemical analysis of tower and balloon mounted shot fallout materials indicated that, as of D + 30 days, $Ru^{103,106}$ and Sr^{89} percentages of total beta radioactivity tended to increase with decreasing particle sizes, and Ce^{141}+ $Ce\text{-}Pr^{144}$ percentages tended to decrease. Fractionation trends with respect to particle size were less definitive for Ba^{140}, Y^{91}, Zr^{95} and Sr^{90}.

Priscilla radionuclide percentages were approximately 30 percent higher for Ba^{140}, 11 to 38 percent higher for Ce^{141}+$Ce\text{-}Pr^{144}$, 300 to 400 percent higher for $Ru^{103,106}$, 250 percent higher for Sr^{89}, 20 to 50 percent higher for Y^{91}, and 50 percent lower for Zr^{95} than mean tower mounted shot percentages of corresponding size fractions.

(4) Tower mounted shot fallout particles were predominantly opaque with small percentages of transparent or transluscent particles. Balloon fallout particles were transparent or transluscent. Opaque particles for Shot Diablo averaged 1.06 microcuries per particle at H + 12 hours for sizes from 2000 to 88 microns in diameter and 0.31 microcuries per particle for 44 to 88 micron particles. Transparent Diablo particles averaged 0.19 microcurie per particle. Opaque 250 to 44 micron Shasta particles averaged 0.49 microcurie per particle at H + 12 hours, and transparent particles averaged 0.17 microcurie per particle.

(5) A comparison of Shots Smoky and Priscilla, utilizing integrated levels of activity associated with less than 44 micron fallout, the percent of soluble activity, and percent of radionuclides, indicated that over the 1 to 15 hour fallout time period the amounts of water-soluble Ba^{140} and Sr^{89} deposited by the two shots were similar despite relatively large differences in the deposited activity of less than 44 micron fractions.

(6) Within the limits of one mile from ground zero and H + 12 hours fallout time, tower shots deposited maximums of two percent of the total Sr^{89} and seven percent of the total Sr^{90} produced; balloon shots deposited a maximum of 0.1 percent of the total Sr^{89} produced.

REFERENCES

1. Chief, AFSWP, Washington, D. C.; Letter to: Commander, Field Command, AFSWP, Albuquerque, New Mexico; AFSWP-978, Subject: "Evaluation of Radioactive Fallout", 15 September 1955; Secret Restricted data.

2. E. A. Martell; "The Chicago Sunshine Method; Absolute Assay of $Strontium^{90}$ in Biological Materials, Soils, Waters, and Air Filters"; May 1956; The Enrico Fermi Institute for Nuclear Studies, University of Chicago; Chicago, Illinois; Unclassified.

TABLE 7.1 Time of Fallout and Radioactive Levels in Areas Sampled by Project 37.1

Dose rate at time of fallout is calculated from monitoring values. Fallout time-of-arrival values were measured or estimated from trajectory analysis. ~ , approximate or estimated.

Sta. No.	Miles from Ground Zero	Miles from midline	Estimated time of arrival, H + hr	Dose rate, mr/hr		Pct <44 micron fraction deposited	Beta Activity in <44 μ fraction, μc/sq ft (H + 12 hr)
				time of fallout	H + 12 hr		
Shot Boltzmann (D day: 28 May)							
1	36	0.0	1.4	2030	140	20	246
2	48	0.0	2.1	430	66	30	330
3	78	0.5 W	3.7	310	78	76	675
4	79	1.0 W	3.7	410	105	75	670
5	91	0.0	5.4	290	~120	--	--
Shot Priscilla (D day: 24 June)							
I	68	0.0	4.5	70	22.5	80	26
8	84	12.0 N	6.7	5	~2.5	--	--
III	129	1.0 N	7.1	9	4.7	85	7.8
IV	155	2.0 N	9.5	1.3	~1.0	82	6.6
V	197	4.0 N	9.5	2.5	~2.0	78	4.9
Shot Diablo (D day: 15 July)							
10	10	0.0	2.5	8880	~1500	--	--
11	13	~2.0 S	2.9	3680	~700	--	--
12	20	~1.0 S	3.8	690	180	~20	~190
13	40	0.5 S	5.1	180	70	50	210
14	60	0.0	6.5	95	50	--	--
Shot Shasta (D day: 18 August)							
15	10.5	5.0 W	0.5	500	NS	--	--
16	14.6	1.3 W	0.7	5940	100	13	240
17	14.8	1.0 W	0.7	9320	177	13	347
18	15.3	0.3 W	0.8	11240	236	13	455
19	16.9	0.7 E	1.0	6780	217	12	418
21	31	4.5 E	2.0	680	~100	--	--
24	44	3.0 E	3.3	390	86	70	535
25	44	0.5 E	3.0	615	120	43	589
26	44	0.3 W	2.9	570	107	40	480
27	44	0.8 W	2.9	590	110	39	421
28	44	1.1 W	2.9	600	111	39	420
30	76	3.9 W	4.9	14	5	--	--
31	76	0.2 W	5.3	90	37	--	--
32	76	0.4 E	5.4	62	26	--	--
33	75	0.2 E	5.5	45	~20	--	--
34	74	3.5 E	5.6	30	14	--	--
35	172	0.0	13.0	4	~4	--	--
Shot Smoky (D day: 31 August)							
36	48	0.0	3.2	1200	250	16	1310
VI	99	0.0	4.5	170	55	38	260
VII	136	0.2 S	4.8	77	27	--	--
41	159	0.7 N	5.6	55	~24	48	100
49	282	1.5 N	19.0	2	~4	--	--

TABLE 7.2 Average Total Activity in Tissues of Native Animals, (Boltzmann Fallout Pattern)

See Table 7.1 for station information of fallout contamination. Tot/Rep, total No. of animals used for measurement/ No. of sample replications used for average activity value.

Sta. No.	Miles from GZ	No. in Sample Tot/Rep	Average nc/gm of Tissue at Time of Collection (D + 16 days)							
			Skin	GI Content	Lung	Thyroid	Liver	Kidney	Muscle	Bone
Jackrabbits (Lepus)										
3	78	1/1	25.5	4.71	0.053	545	0.355	0.169	0.039	0.252
5	91	1[a]/1	29.1	9.57	0.062	277	0.709	0.171	0.495	18.1
Kangaroo Rat (Dipodomys)										
1	36	2/1	5.69	0.527	0.043	126	0.103	0.061	0.081	1.18
3	78	5/1	22.4	4.32	0.117	769	0.538	0.327	0.268	5.00
4	79	4/1	8.89	3.56	0.078	98.6	0.591	0.218	0.218	4.98
5	91	5/1	21.8	1.32	0.069	284	0.115	0.083	0.156	0.974
Deer Mouse (Permoyscus)										
1	36	1/1	7.94	0.325	nil	334	nil	nil	0.028	nil
2	48	7/1	7.58	1.03	0.045	494	0.125	0.077	0.128	1.50
3	78	19/2	22.0	1.80	0.047	548	0.104	0.081	0.178	2.26
4	79	4/1	25.9	1.84	nil	287	0.021	nil	0.113	0.747
5	91	2/1	17.1	2.34	0.072	684	0.285	0.178	0.548	2.95
Pocket Mouse (Perognathus)										
1	36	1/1	13.0	0.531	0.026	327	0.087	0.053	0.084	0.764
2	48	1/1	10.5	0.078	nil	472	0.083	nil	0.188	0.460
3	78	6/1	46.5	1.34	--	209	0.125	--	0.118	0.596

[a] Juvenile (See Figure 7.3)

TABLE 7.3 Concentration of Radionuclides in Bone of Kangaroo Rats, (Boltzmann Fallout Pattern)

MFP, beta activity values corrected for tissue beta background activity. Radionuclide values may contain trace amounts from previous fallout. All values corrected to time of collection. D + 16 days. Sampling locations along midline of pattern.

Sta. No.[a]	Miles from GZ	No. in Sample	Average dis/min/gm of Tissue MFP	Ba^{140}	$Sr^{89,90}$	Pct of MFP Activity
1	36	2	2,630	600	230	32
3	78	5	11,090	2,230	1,300	32
4	79	4	11,055	2,010	1,510	32
5	91	5	2,160	280	350	29

[a] See Table 7.1 for Station Radioactivity Levels.

TABLE 7.4 Average Beta Activity in Tissues of Jackrabbits, (Priscilla Fallout Pattern)

See Table 7.1 for station information of fallout contamination. NS, not significant.

Time of Collection, D + day	Dose Rate, mr/hr	No. Sampled	Average nc/gm of Tissue at Time of Collection							
			Skin	Cecum	Lung	Thyroid	Liver	Kidney	Muscle	Bone
Station I (68 miles from GZ)										
3	0.64	1	7.95	9.97	0.148	377	6.59	0.638	0.071	0.206
7	--	2	4.38	8.20	0.111	64.1	0.468	0.105	0.014	1.16
9	0.17	4	1.85	2.22	0.052	109	0.312	0.057	0.011	0.214
13	0.10	4	2.53	2.33	0.054	61.6	0.149	0.034	0.013	1.22
20	0.04	3	1.15	1.10	0.039	14.0	0.069	0.030	0.003	1.38
Station III (129 miles from GZ)										
3	0.26	4	7.39	3.97	0.387	234	2.25	0.182	0.042	1.46
4	--	1	11.3	2.94	0.353	17.1	1.29	0.220	0.048	1.30
5	0.12	2	8.10	1.11	0.056	14.8	0.687	0.148	0.011	0.984
9	<0.05	3	1.77	0.988	0.020	52.4	0.264	0.011	0.023	1.19
13	nil	12	0.273	0.130	NS	10.1	0.011	0.004	0.001	0.321
20	nil	12	0.273	0.130	0.003	10.1	0.011	0.004	0.001	0.321
Station V (197 miles from GZ)										
3	<0.05	1	4.46	1.58	0.022	87.7	2.97	0.233	0.006	0.050
4	--	1	4.68	3.84	0.069	232	3.25	0.203	0.025	0.038
6	--	1	0.677	1.73	0.021	73.2	0.213	0.074	0.020	0.087
10	nil	1	0.924	0.251	0.005	6.89	0.058	0.004	0.004	nil
13	nil	3	0.275	0.239	0.004	11.5	0.016	0.003	0.002	0.142
14	nil	1	0.498	0.275	0.001	11.6	0.032	0.012	0.002	0.475
20	nil	3	0.071	0.152	0.003	6.85	0.020	0.003	nil	0.422

TABLE 7.5 Concentration of Radionuclides in Bone of Jackrabbits, (Priscilla Fallout Pattern)

Total beta activity (MFP) values corrected for tissue background beta activity. Some radionuclides may contain trace amounts from previous fallout. See Table 7.1 for station radioactivity levels. NS, not significant.

	Sta I			Sta 8	Sta III	Sta V	
Miles from GZ	68			84	129	197	
Time of Collection, D + days	3	7	13	4	3	3	6
BONE, dis/min/gm of tissue[a]							
MFP	570	5030	3850[b]	2440	6330[b]	220	2020
Ba^{140}	95	980	960	340	1020	44	520
Ce^{141} + $Ce\text{-}Pr^{144}$	--	NS	300	290	NS	NS	NS
$Cs^{136,137}$	--	--	NS	--	--	--	--
$Ru^{103,106}$	--	--	--	--	--	--	--
$Sr^{89,90}$	27	470	340	140	290	7	150
Y^{91}	--	320	66	37	8	3	20
Zr^{95}	--	14	2	NS	NS	NS	5
Pct Radionuclide Activity Accounted for	21	36	44	33	21	24	34

[a] dis/min/gm tissue corrected to time of collection.

[b] Results are average of tissues from two animals; all other values based on one animal per sample.

TABLE 7.6 Average Beta Activity in Tissues of Kangaroo Rats, (Priscilla Fallout Pattern)

See Table 7.1 for station information of fallout contamination. Tot/Rep, total number of animals used for measurement per number of sample replications used for average activity value. ND, activity not detected.

Time of Collection, D + Day	Dose Rate, mr/hr	No. in Sample, Tot/Rep	Average nc/gm of Tissue at Time of Collection							
			Skin	GI Content	Lung	Thyroid	Liver	Kidney	Muscle	Bone
Station I (68 mi from GZ)										
3	0.64	17/4	17.5	3.43	0.075	404	0.696	0.237	0.060	0.559
5	0.37	29/6	7.46	1.99	0.043	83.6	0.442	0.176	0.034	0.477
9	0.17	13/3	9.89	1.05	0.048	153	0.117	0.103	0.024	0.287
13	0.10	23/5	4.62	0.587	0.024	59.5	0.057	0.017	0.046	0.480
20	0.04	26/5	1.63	0.183	0.009	13.1	0.008	0.011	0.012	0.153
Station III (129 mi from GZ)										
3	0.26	16/3	6.47	0.726	0.031	96.7	0.566	0.233	0.020	0.086
5	0.12	7/2	2.96	0.312	0.008	187	0.112	0.054	0.009	0.033
9	0.05	8/1	2.31	0.150	0.010	39.1	0.071	0.020	0.006	0.077
13	0.03	5/1	0.894	0.058	0.002	18.4	0.011	0.001	0.001	0.008
20	ND	1/1	0.370	0.001	0.003	12.4	0.009	0.003	nil	0.005

TABLE 7.7 Beta Activity in Tissue of Native Animals, (Diablo Fallout Pattern)

See Table 7.1 for station information of fallout contamination. Tot/Rep, total number of animals used for measurement per number of sample replications used for average activity value.

Sta. No.	Miles from GZ	No. in Sample Tot/Rep(b)	Average nc/gm of Tissue at Time of Collection (D + 5 days)							
			Skin	GI Content	Lung	Thyroid	Liver	Kidney	Muscle	Bone
Jackrabbit (Lepus)										
11	13	1/1	165	90.6	1.02	788	6.61	0.49	0.56	12.3
12	20	1/1	197	38.1	1.93	396	7.08	0.59	0.18	5.54
14	60	2/2	47.1	48.5	0.32	245	1.70	0.41	0.56	0.56
Kangaroo Rat (Dipodomys)										
10	10	9/2	362	60.1	1.31	1,126	10.9	2.19	1.78	7.64
11	13	20/4	101	20.6	0.19	456	2.44	0.38	0.46	1.87
12	20	16/3	130	26.6	0.46	232	3.48	0.61	0.57	1.77
13	40	34/7	40/6	11.3	0.13	124	1.00	1.85	0.18	0.54
14	60	2/2	32/6	13.8	0.58	77.7	0.44	1.18	0.59	1.91
Deer Mouse (Peromyscus)										
10	10	58/6	1647	160	2.24	2,472	14.9	4.46	8.15	11.3
12	20	12/2	293	40.4	0.81	10,017	18.5	4.89	3.88	9.28
14	60	23/8	40.5	10.5	0.53	71.1	3.0	1.01	0.76	1.43

TABLE 7.8 Concentration of Radionuclides in Tissues of Native Animals, (Diablo Fallout Pattern)

Total beta activity (MFP) values corrected for tissue background beta activity. Some radionuclides may contain trace amounts from previous fallout. See Table 7.1 for station radioactivity levels. Dis/min/gm values corrected to time of collection, D + days.

	Kangaroo Rat		Woodrat		Deer Mouse	
Station No/miles from GZ	10/10		10/10		10/10	
Kind of Tissue	Bone	Muscle	Bone	Muscle	Bone	Muscle
No. of Animals in Sample	2	2	2	2	58	58
Activity, dis/min/gm of tissue						
MFP	13,420	4,060	55,800	8,510	30,930	22,180
Ba^{140}	2,650	405	14,680	1,310	7,220	2,270
$Ce^{141}+Ce\text{-}Pr^{144}$	320	--	490	160	1,550	875
$Cs^{136,137}$	--	21	9	74	7	86
$Ru^{103,106}$	--	24	270	53	150	96
$Sr^{89,90}$	600	32	2,000	140	1,150	180
Y^{91}	260	68	450	74	440	400
Zr^{95}	23	75	7	6	95	--
Pct Radionuclide Activity Accounted for	29	15	31	21	34	18

	Kangaroo Rat		Jackrabbit	
Station No/miles from GZ	12/20		12/20	
Kind of Tissue	Bone	Muscle	Bone	Muscle
No. of Animals in Sample	None	15	1	1
Activity, dis/min/gm of tissue				
MFP	--	1,575	19,080	380
Ba^{140}	--	200	4,150	250
$Ce^{141}+Ce\text{-}Pr^{144}$	--	112	19	33
$Cs^{136,137}$	--	19	--	11
$Ru^{103,106}$	--	18	35	6
$Sr^{89,90}$	--	15	650	25
Y^{91}	--	38	110	15
Zr^{95}	--	6	--	6
Pct Radionuclide Activity Accounted for	--	26	26	91

TABLE 7.9 Beta Activity in Tissues of Jackrabbits, (Shasta Fallout Pattern)

See Table 7.1 for station information of fallout contamination.

Sta. No.	Time of Collection, D + day	Miles from GZ	Miles from Midline	No. Sampled	Average nc/gm of Tissue at Time of Collection							
					Skin	Cecum	Lung	Thyroid	Liver[a]	Kidney[a]	Muscle	Bone
21	D-day	31	4.5 E	1	1244	239	0.796	--	0.530	0.259	0.579	1.69
25		44	0.5 E	2	2590	437	0.989	--	0.680	0.692	1.20	0.794
28		44	1.1 W	1	750	734	1.17	--	--	0.377	2.32	2.82
15	D + day	10.5	5.0 W	1	245	158	0.210	7,877	384	0.199	0.792	
16		14.6	0.3 W	2	357	150	0.215	--	0.504	0.153	1.60	1.10
18		15.3	0.3 W	1	584	327	0.519	--	0.800	0.271	0.432	1.22
19		16.9	0.7 E	2	490	223	0.289	4,567	0.573	0.168	0.932	2.27
27		44	0.8 W	1	903	383	0.348	--	0.99	0.390	0.661	3.55
28		44	1.1 W	2	540	239	0.342	--	0.66	0.276	0.193	2.11
31		76	0.2 W	2	156	187	0.418	--	2.07	0.561	1.50	2.00
33		75	0.2 E	1	53.3	79.7	0.134	1,367	0.580	0.322	3.50	0.426
34		74	3.5 E	2	155	137	1.08	2,287	1.94	0.634	3.39	3.01
17	D + 2	14.8	1.0 W	1	185	122	0.124	--	0.181	0.166	3.19	0.376
19		16.9	0.7 E	2	140	53.1	0.141	1,257	0.322	0.118	5.04	1.97
24		44	3.0 E	1	161	127	0.235	1,421	2.47	0.459	1.48	2.58
25		44	0.5 E	1	144	144	0.525	4,751	2.52	0.306	2.79	3.91
26		44	0.3 W	2	463	202	0.504	12,846	1.45	1.02	2.44	6.48
28		44	1.1 W	2	310	157	1.12	--	2.12	1.80	2.27	6.72
30		76	3.9 W	2	8.86	4.87	0.091	458	0.124	0.060	0.056	0.237
31		76	0.2 W	1	29.7	25.7	0.515	--	0.351	0.635	0.072	0.252
32		76	0.4 E	2	127	69.4	0.250	--	2.26	0.478	0.193	2.11
35		172	0	7	23.5	54.5	0.400	2,809	147	7.81	0.610	3.02

[a] Decay correction made on basis of site of collection rather than shot average (Table 7.16).

TABLE 7.10 Concentration of Radionuclides in Tissues of Jackrabbits, (Shasta Fallout Pattern)

Total beta activity (MFP) values corrected for tissue beta background activity. Radionuclide values may contain trace amounts from previous fallout. Radionuclides are Ba^{140}, Ce^{141} + $Ce\text{-}Pr^{144}$, $Cs^{136,137}$, $Ru^{103,106}$, $Sr^{89,90}$, Y^{91}, Zr^{95}. See Table 7.1 for station radioactivity levels. NS, not significant. Sample locations along midline of pattern.

Sta. No.	Miles from GZ	No. In Sample	Average dis/min/gm of Tissue at Time of Collection, D+2 days								Pct Radionuclide Activity Accounted For
			MFP	Ba	Ce	Cs	Ru	Sr	Y	Zr	
Bone											
19	16.9	2	3,140	519	22	2	15	200	48	--	26
26	44	3	5,200	910	74	9	23	186	59	10	24
31	76	2	4,430	842	22	4	17	174	56	7	25
35	172	3	6,170	848	25	10	22	134	45	6	18
Muscle											
19	16.9	2	3,970	107	27	3	3	9	14	--	4
26	44	3	6,020	178	34	6	5	19	23	8	5
31	76	3	4,800	142	28	5	7	10	18	12	5
35	172	3	1,550	126	26	4	4	10	14	8	13
Liver											
19	16.9	2	970	1	--	NS	NS	NS	--	--	NS
26	44	4	5,020	10	2	NS	NS	NS	2	NS	NS
31	76	3	3,660	2	NS	1	--	NS	NS	NS	NS
Lung											
19	16.9	2	380	12	--	2	NS	2	--	--	4
31	76	1	110	9	--	--	--	1	--	--	9

TABLE 7.11 Comparison of Beta Activity in Tissues of Native Animals, (Shasta Fallout Pattern)

See Table 7.1 for station information of fallout contamination. Tot/Rep, total number of animals used for measurement per number of sample replications used for average activity value.

Sta. No.	Miles from GZ	No. in Sample Tot/Rep	Average nc/gm of Tissue at Time of Collection (D + 2 days)							
			Skin	GI Contents	Lung	Thyroid	Liver	Kidney	Muscle	Bone
Jackrabbit (Lepus)										
31	76	1/1	29.7	25.7	0.515	--	0.351	0.635	0.072	0.252
35	172	7/7	23.5	54.5	0.400	2809	147	7.81	0.610	3.02
Kangaroo Rat (Dipodomys)										
31	76	21/4	36.3	7.52	0.020	507	0.158	0.046	0.203	0.519
35	172	108/21	9.55	7.62	0.078	1369	18.5	2.12	0.057	0.244
Mice (2 Species)										
31	76	3/1	51.3	5.45	0.051	1093	0.295	0.178	0.163	1.06
35	172	36/3	38.4	3.74	0.126	1393	15.0	2.24	0.121	0.422

TABLE 7.12 I^{131} and I^{133} in Thyroid of Jackrabbits, (Shasta Fallout Pattern)

See Table 7.1 for station radioactivity levels. Measurements made by single channel spectrometer using a 2 inch NaI crystal.

Sta. No.	Miles from GZ	Time of Collection H + hr	No. of Animals Sampled	Pct at H + 72 hrs			Ratio I^{133}/I^{131}	
				I^{131}	I^{133}	Activity Accounted for	Observed at H + 72 hrs	At Time of Collection
21	31	17	1	33	51	84	1.6	7.0
26	44	18	3	23	63	86	2.7	12
19	17	42	3	20	67	87	3.3	8.0
26	14	42	3	17	65	82	3.8	8.7
31	76	41	3	17	66	83	3.9	9.1

TABLE 7.13 Beta Activity in Tissues of Jackrabbits and Kangaroo Rats, (Smoky Fallout Pattern)

See Table 7.1 for station information of fallout contamination. Tot/Rep, total number of animals used for measurement per number of sample replications used for average activity value. ND, activity not detected.

Time of Collection, D + days	Dose Rate, mr/hr	No. in Sample Tot/Rep	Average nc/gm of Tissue at Time of Collection							
			Skin	Cecum	Lung	Thyroid	Liver	Kidney	Muscle	Bone
Jackrabbits (Lepus)										
Station VI (99 miles from GZ)										
3	9.5	1/1	100	21.4	0.986	280	2.45	0.142	0.151	0.258
12	ND	1/1	9.73	3.48	0.335	7.50	0.309	0.143	0.050	0.897
13	2.00	3/3	18.6	7.27	0.201	134	0.430	0.176	0.073	1.42
20	1.24	1/1	12.6	5.60	0.071	70.9	nil	0.113	4.11	1.06
Station VII (136 miles from GZ)										
3	2.91	4/4	39.3	13.2	0.451	497	6.95	1.02	0.330	0.952
5	1.79	5/5	35.1	9.39	0.252	138	2.13	0.662	0.249	1.14
9	1.10	4/4	10.8	2.69	0.190	89.5	0.488	0.141	0.129	1.50
13	0.70	1/1	12.2	3.63	nil	52.7	0.259	nil	0.035	0.755
20	0.48	5/5	3.57	0.982	nil	18.8	nil	nil	0.044	0.671
Kangaroo Rats (Dipodomys)										
Station VI (99 miles from GZ)										
3	9.5	25/5	77.0	9.42	0.113	216	2.47	0.836	0.390	0.520
5	6.18	33/7	26.2	8.29	0.149	124	1.77	0.657	0.213	0.430
9	4.88	25/5	11.1	2.32	0.056	31.1	0.235	0.157	0.063	0.247
13	2.00	44/9	10.6	1.93	0.074	29.3	0.189	0.142	0.118	0.372
20	1.24	46/9	6.01	1.32	0.057	29.2	nil	nil	0.051	0.234
Station VII (136 miles from GZ)										
3	2.91	25/5	18.8	1.09	0.065	186	0.665	0.301	0.229	0.470
5	1.79	39/8	24.2	2.23	0.070	86.2	0.434	0.172	0.089	0.484
9	1.10	55/11	6.88	0.725	0.039	53.6	nil	nil	0.039	0.361
13	0.70	58/12	6.41	0.603	0.041	25.7	nil	nil	0.043	0.391
20	0.48	30/6	1.87	0.198	nil	18.1	nil	nil	0.096	0.242

TABLE 7.14 Concentration of Radionuclides in Tissues of Jackrabbits, (Smoky Fallout Pattern)

Total beta activity (MFP) values corrected for tissue beta background activity. Radionuclide values may contain trace amounts from previous fallout. Radionuclides are Ba^{140}, Ce^{141}+Ce-Pr^{144}, $Cs^{136,137}$, $Ru^{103,106}$, $Sr^{89,90}$, Y^{91}, Zr^{95}. See Table 7.1 for station radioactivity levels. NS, not significant. Sample locations along midline of pattern.

Sta. No.	Miles from GZ	No. in Sample	Average dis/min/gm of Tissue at Time of Collection (D + 20 days)								Pct Radionuclide Activity Accounted for
			MFP	Ba	Ce	Cs	Ru	Sr	Y	Zr	
Bone											
36	48	1	20,420	6470	22	2	18	1700	125	4	41
VI	99	1	2,350	810	6	2	8	260	29	2	48
VII	136	3	1,810	610	4	2	4	200	34	--	47
41	159	1	1,280	390	3	11	6	80	25	NS	40
49	282	2	1,330	520	5	nil	NS	120	28	--	51
Muscle											
36	48	2	668	210	21	25	9	56	31	9	54
VI	99	1	90	19	2	19	1	5	2	NS	54
VII	136	2	170	18	8	--	2	3	2	2	20
41	159	1	64	12	3	--	1	3	6	NS	41
49	282	1	36	10	NS	--	NS	2	NS	--	37
Liver											
36	48	3	740	3	2	10	--	--	NS	--	nil
VI[a]	99	1	280	4	2	--	--	NS	3	--	nil
VII[a]	136	3	58	NS	NS	NS	--	--	NS	--	nil
49[a]	282	3	30	--	--	--	NS	NS	--	--	nil
Lung											
36	48	2	830	59	64	21	--	6	--	--	18
VI[a]	99	1	160	24	20	--	--	2	11	--	37
VII[a]	136	2	494	7	5	--	--	--	3	--	30
49[a]	282	3	38	3	4	--	--	NS	--	--	21

---

[a] Questionable data due to low activity in sample aliquots.

TABLE 7.15 Changing Concentrations of Radionuclides in Tissues of Jackrabbits, (Smoky Fallout Pattern)

Total beta activity (MFP) values corrected for tissue beta background radioactivity. Radionuclides are Ba^{140}, Ce^{141}+Ce-Pr^{144}, Cs^{137}, $Ru^{103,106}$, $Sr^{89,90}$, Y^{91}, Zr^{95}. See Table 7.1 for location and fallout characteristics of this Station VII.

Time of Collection, D + Days	Dose Rate, mr/hr	Number of Animals	Forage[a], nc/gm	Average dis/min/gm of Tissue at Time of Collection								Pct Radionuclide Activity Accounted For
				MFP	Ba	Ce	Cs	Ru	Sr	Y	Zr	
Bone												
3	2.91	3	18.1	1900	507	7	6	2	96	10[b]	--	34[b]
5	1.79	2	9.5	3350	717	6	5	13	181	59[b]	--	29[b]
9	1.10	3	6.4	3670	748	10	7	7	222	38[b]	--	28[b]
20	0.48	3	2.1	1810	615	4	2	4	198	33[b]	--	47[b]
Muscle												
3	2.91	3	18.1	840	37	8	3	0.8[b]	4	5	2	7
5	1.79	2	9.5	930	159	21	4	6	8	13	7	23
9	1.10	2	6.4	350	35	12	4	4	5	15	6	23
20	0.48	2	2.1	170	18	8	--	2	3	2	2	20

[a] Dried Sage (Artemesia tridentata) believed to be primary forage of jackrabbits in this area. (Figures 7.8 and 7.9).

[b] Values only approximate.

TABLE 7.20 Accumulation of Beta Activity (MFP) from Fallout Material in Bone from Kangaroo Rats and Jackrabbits with Respect to Distance from Ground Zero and Fallout Time of Arrival.

	Distance from GZ, miles	Fallout Time of Arrival, H + hours	Beta Activity, nc/gm of Tissue
Kangaroo Rats			
Shot Boltzmann (Time of Collection, D + 16 days)			
	36	1.4	1.18
	78	3.7	5.00
	79	3.7	4.98
	91	5.4	0.974
Shot Priscilla (Time of Collection, D + 13 days)			
	68	4.5	0.480
	129	7.1	0.008
Shot Diablo (Time of Collection, D + 5 days)			
	10	2.5	7.64
	13	2.9	1.87
	20	3.8	1.77
	40	5.1	0.54
	60	6.5	1.91
Shot Shasta (Time of Collection, D + 2 days)			
	76	5.3	0.519
	172	13.0	0.244
Shot Smoky (Time of Collection, D + 3 days)			
	99	4.5	0.520
	136	4.8	0.470
Jackrabbits			
Shot Priscilla (Time of Collection, D + 13 days)			
	68	4.5	1.22
	129	7.1	0.321
	197	9.5	0.142
Shot Diablo (Time of Collection, D + 5 days)			
	13	2.9	12.3
	20	3.8	5.54
	60	6.5	0.56
Shot Shasta (Time of Collection, D + 2 days)			
	16.9	1.0	1.97
	44	2.9	6.48
	76	5.4	2.11
	172	13.0	3.02

For comparative purposes, total Sr^{90} was measured in a duplicate set of soil cores following a carbonate fusion; Sr^{90} values obtained by this procedure were generally much higher than those obtained by leaching the soils with 6 N HCl. Consequently, the carbonate fusion method was used for determining the total Sr^{90} in soils during this study. The data are presented in Figure 8.1

8.2.2 Chemical Properties of NTS Fallout in Soil

The 6 N HCl solubility of Sr^{90} in soil varied from 13 to 100 percent of the amount of Sr^{90} found by the carbonate fusion method (Table 8.4). The solubility of Sr^{90} in fallout debris is considered to be an important factor in determining the biological availability of the Sr^{90} to plants, to domestic animals, and to man.

TABLE 8.4 Soil Sr^{90}, Acid-Soluble Sr^{90}, and Infinite Gamma Dose at Various Distances from GZ

Soil samples are 0 to 6 inches deep. Collection locations are defined in Table 8.2. Infinite dose are taken from Table 8.1. Extractions with 6 N HCl and Sr^{90} analyses by USAEC Health and Safety Laboratory, New York Operations Office.

Collection Location	Infinite Dose, roentgens	Distance from GZ, miles	Total Sr^{90}, mc/mi^2	Sr^{90} Soluble in 6 N HCl, pct
Tempiute, Nev.	5.9	45	218	19
St. George, Utah	3.7	135	111	22
Mesquite, Nev.	2.0	115	39.1	13
Alamo, Nev.	1.3	55	30.8	50
Lund, Nev.	1.2	130	64.4	47
Caliente, Nev.	0.7	95	22.9	63
Cedar City, Utah	0.6	170	62.4	58
Overton, Nev.	0.4	95	22	44
Beaver, Utah	0.3	205	28.8	102

Data related to the solubility of Sr^{90}, shown in Figure 8.1, Tables 8.1 and 8.2, are summarized in Table 8.4. Linear relationships were not indicated for the variables tabulated. There was an inverse relationship between fallout gamma dose (in roentgens) and the acid solubility of Sr^{90} in that the least-soluble fallout material was at locations at which the radiation dose was greatest and that the most-soluble Sr^{90} was at the location with the lowest fallout intensity. At locations having fallout of intermediate acid solubility, there was little correlation between solubility and either the total Sr^{90} deposited or the fallout intensity.

Soil properties were not significant in affecting the acid-solubility of Sr^{90}. Laboratory studies indicate the recovery of Sr^{85} from "spiked" samples ranged from 87 to 99 percent with 6 N HCl; and, with 1 N ammonium acetate (NH_4OAc), the recovery was between 77 and 90 percent (Table 8.5).